THEORY OF EMISSION PROCESSES

D.S. Delion [1,2]
[1] *National Institute of Physics and Nuclear Engineering, 407 Atomiştilor, Bucharest-Măgurele, România*
[2] *Academy of Romanian Scientists, 54 Splaiul Independenţei, Bucharest, România*
(Dated: January 10, 2008)

C O N T E N T S

I. INTRODUCTION

A. Binding energy

Daily experience tells us that by adding two objects, each of them wighting one kilogram, one obtains exactly two kilograms. But in this case the mathematical obvious relation $1+1=2$ is actually an approximation, and this amazing fact was revealed in the beginning of the XX-th century by Albert Einstein in his well known relation, connecting the energy and mass $E=mc^2$, where c is the speed of the light in vacuum. Indeed, electromagnetic forces between atoms have the order of magnitude 1 electron volt (eV), while the mass of the lightest atom (hydrogen) is about 1 GeV= 10^9 eV. In this way practically the mass is concentrated in the nucleus. Its dimension of about 1 fermi (fm) = 10^{-15} m is by five orders of magnitude smaller than the whole atom, i.e. 1 Ångström (Å). This means that the matter we feel is actually almost "empty" and the basic constituents (atoms) are weekly bound in comparison with their mass. Thus, the usual addition rule of masses holds with a high precision at the atomic level.

The situation completely changes by "weighting" for instance a deuteron, built from one proton and one neutron. Its mass M_dc^2 is smaller than the sum of the constituents $M_pc^2+M_nc^2$, because the magnitude of the strong force, binding the two nucleons, is comparable with their masses, i.e. 1 MeV= 10^6 eV.

A basic concept of the nuclear physics is that of the binding energy, defined as the difference between the mass of the nucleus and the masses of its constituents, i.e. Z protons and N neutrons

$$B(Z,N)=Mc^2-ZM_pc^2-NM_nc^2\ . \tag{1.1}$$

This quantity is a negative number and it defines the amount of energy binding together the nucleons inside the nucleus. The range of nuclear forces between nucleons is comparable with their size, i.e. about 1 fm, and therefore only neighboring nucleons interact with each other. Moreover, at distances larger than 0.2 fm the interaction is attractive, while for shorter distances it becomes repulsive. Thus, the binding energy per nucleon is aproximately constant, $B(Z,N)/A\approx 8$ MeV and this property reflects the saturation property of nuclear forces, i.e the nucleus behaves like a liquid drop.

Actually the binding energy per nucleon has minimuma, with larger negative values, along a valley called stability valley. Due to the electrostatic repulsion between protons the binding energy per nucleon becomes less negative by increasing the mass number. In order to compensate the effect of the Coulomb repulsion the number of neutrons increases faster than that of protons and therefore the stability line Z(N) lies below the first bisectrice. Actually the nuclei with $Z>92$ (transuranic nuclei) are unstable and were synthetized artificially.

The surface $B(Z,N)/A$ has another remarcable property. It has local minima along the stability valley for some proton (neutron) numbers, called magic numbers with Z (N) = 2, 8, 20, 28, 50, 82, 126. Double magic nuclei like ${}^{4}_{2}\mathrm{He}_2$, ${}^{16}_{8}\mathrm{O}_6$, ${}^{40}_{20}\mathrm{Ca}_{20}$, ${}^{56}_{28}\mathrm{Fe}_{28}$, ${}^{132}_{50}\mathrm{Sn}_{82}$, ${}^{208}_{82}\mathrm{Pb}_{126}$ are the most stable nuclei in nature (we used the notation ${}^{A}_{Z}\mathrm{X}_N$). This property is explained by the so-called shell model of the nucleus, where a given nucleon moves in the field created by all other nucleons. The nucleons are fermions and their spin $s=\frac{1}{2}$ strongly interact with the angular momentum l by a spin-orbit force. A single particle state in this selfconsistent mean field is labeled by the isospin index $\tau=p,n$ (for protons or neutrons), energy level ϵ, angular momentum l, total spin j and its projection m, i.e.

$$a^{\dagger}_{\tau\epsilon ljm}|0\rangle\rightarrow\psi_{\tau\epsilon ljm}(\mathbf{r},\mathbf{s})\ , \tag{1.2}$$

where $\mathbf{r}$ denotes the spatial and $\mathbf{s}$ the spin coordinate. The above notation means that the operator $a^{\dagger}$ acts on the vacuum state $|0\rangle$ in order to create a single particle state. The conjugate operator $a_{\tau\epsilon ljm}$ annihilates this state.

Due to these two properties the single particle levels, created in this selfconsistent potential, are grouped in regions separated by larger gaps, corresponding to the above mentioned magic numbers. In the first approximation protons and neutron fill these levels. Two nucleons cannot occupy the same single particle state and this property is described mathematically by the antisymmetric charecter of a two-particle state, i.e.

$$a^{\dagger}_{j_1m_1}a^{\dagger}_{j_2m_2}|0\rangle\rightarrow\frac{1}{\sqrt{2}}\left[\psi_{j_1m_1}(\mathbf{r}_1,\mathbf{s}_1)\psi_{j_2m_2}(\mathbf{r}_2,\mathbf{s}_2)-\psi_{j_2m_2}(\mathbf{r}_1,\mathbf{s}_1)\psi_{j_1m_1}(\mathbf{r}_2,\mathbf{s}_2)\right]\ , \tag{1.3}$$

where we used the short-hand notation $(\tau\epsilon lj)\rightarrow j$. On each level with given quantum numbers (ϵ,l,j) one finds two nucleons of the same kind with opposite spin projections $(m,-m)$. These nucleons interact with each other via residual two-body forces, the most important one being pairing interaction. In this way a nuclear state becomes a coherent superposition of several pair states

$$a^{\dagger}_{jm}a^{\dagger}_{j-m}|0\rangle\rightarrow\frac{1}{\sqrt{2}}\left[\psi_{jm}(\mathbf{r}_1,\mathbf{s}_1)\psi_{j-m}(\mathbf{r}_2,\mathbf{s}_2)-\psi_{j-m}(\mathbf{r}_1,\mathbf{s}_1)\psi_{jm}(\mathbf{r}_2,\mathbf{s}_2)\right]\ , \tag{1.4}$$

and the nucleons loose their individuality.

The nuclei out of the stability valley are in general unstable versus the splitting process into two or more fragments. To be more specific the decay process is allowed as soon as the final configuration is energetically more favourable (i.e. more bound) than the initial one. For transitions between ground states this means that the binding energy of the initial nucleus is lower (more positive) than for the final configuration. Therefore the so-called Q-value of the splitting process into 1,2,... components is positive, i.e.

$$Q = B_i - B_1 - B_2 - ... > 0 \ . \tag{1.5}$$

B. Strong emission processes

The instability of nuclei is called radioactivity. Nuclear physics was born with the discovery of the natural spontaneous radioactivity of Uranium by H. Becquerel in 1896. The new discovered radiations were called in 1899 by E. Rutherford with the first Greek letters, namely α, β and γ rays. Soon it was recognized that the α-radioactivity consists in emission of charged particles from atomic nuclei, β^- particles were identified with electrons, while γ rays with the electromagnetic radiation of much higher frequency than the usual light. Physicists realized that α-decay involves a new type of short range force called strong interaction, while β-decay is connected with the so-called weak interaction.

In 1928 G. Gamow proposed a simple explanation for the exponential dependence of half-lives in α-decays upon Q-values, evidenced experimentally by the Geiger-Nuttall law [1]. Gamow conceived the α-particle as a small ball (although composed of six particles, namely four protons and two electrons) moving in the mother nucleus which, through bouncing upon the nuclear surface, eventually penetrates quantum mechanically the surrounding Coulomb barrier.

Only after the discovery of the neutron in 1932 by J. Chadwick nuclear physicists found out that α-particles are very bound clusters, made from two protons and two neutrons. By denoting the parent nucleus by ${}^{A}_{Z}P_N$, where A is the mass number, Z proton number and N neutron number, this process can be written as follows

$${}^{A}_{Z}P_N \rightarrow {}^{A-4}_{Z-2}D_{N-2} + \alpha \ . \tag{1.6}$$

Here by D with the corresponding labels we denoted the daugher nucleus. Of course α-decay is allowed by the large binding energy of ${}^{4}_{2}$He. The nuclei connected by α-decays are situated on a line paralel with the first bisectric in the (N,Z) plane. This line is called α-line.

Several important theoretical achievements in the field of nuclear physics are directly onnected with the α-decay theory. We mention here the Breit-Wigner theory of nuclear resonances [2, 3], the R-matrix approach of reactions and emission processes [4–7], Feshbach theory of nuclear reactions [8], description of α-decays from deformed nuclei [9] and the shell-model estimate of the α-particle spectroscopic factor [10–12].

Nowdays nuclear physics uses α-decays to investigate nuclear structure. The so-called α-spectroscopy gives important experimental information concerning the nuclear structure of collective low-lying states. At present there are a lot of high precision data concerning α-decay intensities not only to ground but also to to excited states. On the other hand the α-decay chains are the only tool to investigate superheavy nuclei, which are very exotic systems, lying at the border of the nuclear stability.

In 1980, long time after the discovery of the α-decay, based on the large binding energy of ^{208}Pb, it was predicted the spontaneous emission of heavier clusters like ^{14}C, ^{24}Ne and ^{28}Mg [13]. This new kind of natural radioactivity was soon experimentally found [14]. Now there are found about 20 nuclei emitting heavy clusters and their half-lives are much larger in comparison with typical α-decay half-lives. The corresponding decay process can be written as

$${}^{A}_{Z}P_N \rightarrow {}^{A-a}_{Z-z}D_{N-n} + {}^{a}_{z}C_n \ . \tag{1.7}$$

The main characteristics is that the heavy fragment is close or coincides with some Pb isotope and this is the reason why this kind of decay is also called "magic radiactivity". It lies between α-decay and fission.

In the last years the study of the exotic very unstable nuclei became the central subject of the nuclear physics. Proton rich nuclei are such systems, which can be investigated exclusively by proton emission, by using radioactive beams. The first discovery of the proton emission was made in 1970 from ^{53}Co [15] and today are known about 50 proton emitters [16]. A very exotic decay, namely two proton emission, is supposed to exist for some nuclei, where this process is energetically allowed. It was predicted in 1960 [17], but only relative recently it was detected [18] in ^{45}Fe and ^{48}Ni [19]. These two processes can be represented as follows

$${}^{A}_{Z}P_N \rightarrow {}^{A-k}_{Z-k}D_N + kp \ , \quad k = 1, 2 \ . \tag{1.8}$$

On the other extreme the nuclear fission is an important and active field in studying neutron rich nuclei. They are born during binary or ternary fission processes. Nuclear fission accompanied by the emission of neutrons was discovered in 1939 by O. Hahn and F. Strassmann

$$ {}^{A}_{Z}P_N \rightarrow {}^{A_1}_{Z_1} D_{N_1} + {}^{A_2}_{Z_2} D_{N_2} + kn \ , \tag{1.9} $$

where

$$ Z_1 + Z_2 = Z \ , \quad N_1 + N_2 + kn = N \ . \tag{1.10} $$

Only in 1962 some fission experiments reported binary fission fragments with very large kinetic energy [20]. In this case the excitation energy of fragments shows that they are close to their ground states [21]. Therefore this process was called cold (neutronless, k=0) fission. We also mention the magic character of the cold fission, because one of fragments is close or coincides with some Sn isotope. The first direct observation of the cold binary fission of ^{252}Cf was reported at Oak Ridge National Laboratory in 1994 [22, 23]. On the other hand it is possible the so-called ternary fission

$$ {}^{A}_{Z}P_N \rightarrow {}^{A_1}_{Z_1} D_{N_1} + {}^{A_2}_{Z_2} D_{N_2} + {}^{a}_{z} C_n \ . \tag{1.11} $$

It is characterized by emission of two heavy fragments together with the equatorial emission of different light clusters, like α-particles, ^{10}Be, $^{12-14}$C, etc.

All these decay processes have a common feature: the emitted fragments are in their ground or low-lying states and this is the reason they are called cold emission processes. As we already mentiond, another characteristic is that they are triggered by the strong interaction.

C. Electro-weak emission processes

By performing a cut perpendicular to the first bisectrice in the (N,Z) plane (called also β-direction), connecting nuclei with a given mass number $A = Z + N$, one obtains for the binding energy a parabolic dependence. The nuclei along both sides of this parabola decay by β-decays until they rich the bottom. The β^--decay corresponds to neutron rich nuclei and consists in the emission of two leptons, namely an electron plus an antineutrino

$$ {}^{A}_{Z}P_N \rightarrow {}^{A}_{Z+1} D_{N-1} + e^- + \tilde{\nu} \ . \tag{1.12} $$

The energy spectrum of this process (Q-value) is continuous due to its three body character. On the other hand β^+-decay corresponds to the emission of a positron and a neutrino

$$ {}^{A}_{Z}P \rightarrow {}^{A}_{Z-1} D_{N+1} + e^+ + \nu \ . \tag{1.13} $$

It is related to another process called electron-capture decay from the lowest atomic s-orbital

$$ {}^{A}_{Z}P + e^- \rightarrow {}^{A}_{Z-1} D_{N+1} + \nu \ . \tag{1.14} $$

These decay processes are trigerred by the weak interaction. The two involved leptons are fermions with the spin $s = \frac{1}{2}$. In beta decays their final state can have total spin $S = 0$ or $S = 1$. In the electron capture the initial proton and electron can couple to $j \pm \frac{1}{2}$ and the final neutron and neutrino to $j \pm \frac{1}{2}$ or $j \mp \frac{1}{2}$. Thus, in all cases lepton spins can change the total nuclear angular momemntum J by 0 or 1. Beta decays with no angular momentum change are called Fermi transitions and those with an angular momentum change by one unit are called Gamow-Teller transitions.

There is also possible another process called double beta decay, involving the emission of two electrons and two antineutrinos

$$ {}^{A}_{Z}P_N \rightarrow {}^{A}_{Z+2} D_{N-2} + 2e^- + 2\tilde{\nu} \ . \tag{1.15} $$

This process occurs due to the fact that the pairing force renders the even-even nuclei more stable than odd-odd nuclei with brocken pairs. Thus, the single β-decay process becomes energetically forbidden and $2\nu\beta\beta$-decay is the only possible channel.

Due to the small value of the coupling constant the decay rate can be estimated perturbativelly, in a similar way to the γ-decay process, which is the emission of an electromagnetic radiation with a very large frequency, as a result of the transition from an excited to the ground state, i.e

$$ {}^{A}_{Z}X^* \rightarrow {}^{A}_{Z} X_N + \gamma \ . \tag{1.16} $$

$\beta^{(\pm)}$-decays are collective processes involving many single particle orbitals. Therefore, the corresponding transition operators can be written as a superposition of a neutron/proton annihilation and proton/neutron creation single particle operators (1.2), i.e.

$$\begin{aligned}\hat{\beta}^{(-)}_{\lambda} &= \Sigma_{if}\langle pf|T_{\lambda\mu}|ni\rangle a^{\dagger}_{pf}a_{ni} \\ \hat{\beta}^{(+)}_{\lambda} &= \Sigma_{if}\langle nf|T_{\lambda\mu}|pi\rangle a^{\dagger}_{nf}a_{pi}\ ,\end{aligned} \tag{1.17}$$

where i/f denotes the quantum numbers ϵljm of the intial/final state. The meaning of the above expression is simple: in each terms a neutron/proton initial state in annihilated and a proton/neutron final state is created. The coefficients are the β-decay matrix elements of the transition operator with the multipolarity $\lambda = 0, 1$. Fermi transition operator is obviously the unity $T_{00} = 1$, while Gammow-Teller decay is described by the Pauli matrix $T_{1\mu} = \sigma_{1\mu}$.

Electromagnetic transitions can be described in a similar way, but with one kind of single particle operators (protons)

$$\hat{\gamma}_{\lambda} = \Sigma_{if}\langle pf|T_{\lambda\mu}|pi\rangle a^{\dagger}_{pf}a_{pi}\ . \tag{1.18}$$

The electric transition operator is proportional with the spherical harmonics defined below $T_{\lambda\mu} = r^{\lambda}Y_{\lambda\mu}$.

These decays in which the lepton number is conserved, are described within the so-called standard model of electro-weak interaction formulated by Glashow [24], Weinberg [25] and Salam [26]. We mention here that it is possible another hypothetical double β-decay process, namely neutrino-less $0\nu\beta\beta$-decay

$${}^{A}_{Z}P_N \rightarrow {}^{A}_{Z+2}\ D_{N-2} + 2e^{-}\ , \tag{1.19}$$

within the so-called Grand Unification Theory, if neutrino is a Majorana particle, i.e. it coincides with antineutrino, and the lepton-number conservation is violated.

II. PHENOMENOLOGICAL DESCRIPTION

We will describe only strong emission processes. As we already mentioned α-decay is the first discovered emission triggered by strong forces. The importance of the interplay between the Coulomb barrier and the energy of the emitted particle (Q-value) on the α-decay was one of the most important discoveries in the early days of the nuclear physics, made by G. Gamow [1]. It explained the exponential dependence of half-lives upon the Q-value, evidenced experimentally by the Geiger-Nuttall law. The proposed physical picture was very simple, but contradicting the classical intuition, namely a preformed α-particle inside the nucleus penetrates quantum mechanically the repulsive Coulomb barrier.

In a phenomenological description one supposes that the dynamics of the decaying systems is fully described by a potential acting between the emitted fragments. It contains two main components, namely the nuclear attraction in the internal region, surounded by a Coulomb repulsion. Indeed, systematic calculations of half-lives for α-particle emitters have shown that experimental values are well described by using an equivalent local potential [27]. The attractive depth and the radius determines the energy and wave function of the decaying state, understood as a narrow resonance [3, 9].

In this first part we will review different approaches, all of them based on the phenomenological description of emission processes, involving ground or low-lying excited states in both parent and daughter nuclei. We will introduce the main tool to describe emission processes, namely Gamow resonances. Then we will describe the experimental material in terms of the Geiger-Nuttall law for different emission processes.

On the other hand it turns out that half lives of α-decays or heavy cluster emission processes, predicted by these potentials, are too short and this feature is a signature that such clusters do not exist as free components on the nuclear surface. The problem how the binary system system is born from the initial nucleus concerns the microscopic description of the decay process. The so-called spectroscopic amplitude, computed by the overlap between the initial and final configurations, can explain experimentally measured half lives. We will discuss this concept in the second part, devoted to microscopic approaches.

Most of nuclei decay by emitting a particle like proton, neutron, electron, positron or a composite cluster as deuteron, α-particle, Be, C, O, Mg, Ne, Si. Heavy nuclei can also fission into two fragments with comparable sizes. All these decays are called binary emission processes and can schematically be written as follows

$$P(J_iM_i) \rightarrow D_1(J_1M_1) + D_2(J_2M_2)\ , \tag{1.20}$$

where $J_i M_i$ is the initial spin and its projection. We suppose that other quantum numbers, like parity, are also embedded into this notation. The final spins J_k , $k = 1, 2$ satisfy the triangle rule

$$|J_1 - J_2| \leq J_i \leq J_1 + J_2 \ , \tag{1.21}$$

and the initial parity equals the product of fragment parities.

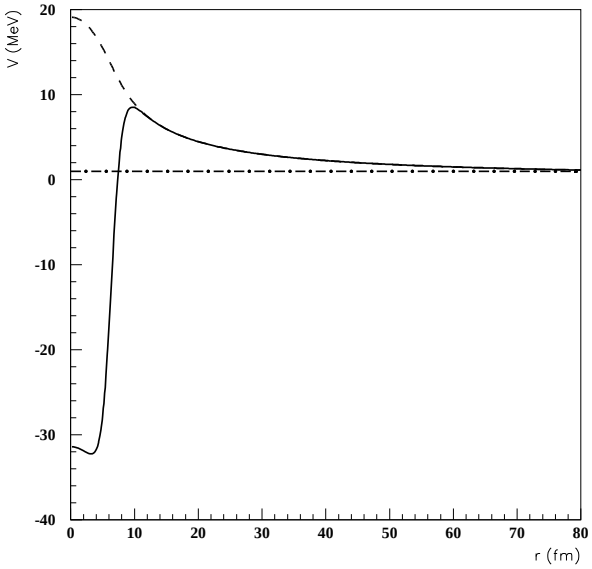

FIG. 1: *Spherical part of the nuclear plus Coulomb interaction (solid line) as a function of the radius in* ^{131}*Eu. The Coulomb part (dash line) and the proton Q-value (dot-dashed line) are also shown.*

As already we pointed out, our presentation concerns the description of decay processes induced only by the strong interaction. An important feature of these decays is connected with the large Coulomb barrier preventing the two fragments from moving apart. In the phenomenological description we suppose that this barrier is extended in the internal region, such that the dynamics of the two fragments is fully described by a potential defined for all distances. Such interaction is shown for the proton emission in figure 1, where it is given the spherical part of the Woods-Saxon potential, describing proton emission from ^{131}Eu. The energy of the system (dashed line) is smaller that the height of the barier, but the two fragments can penetrate it, due to the very small, but different from zero, wave function outside the barrier. We will show below that this property, characteric to the wave propagation, is described in terms of the so-called penetrability.

The main difficulty that one encounters when studying decay processes, not only from experimental point of view, but also theoretically is the instability of the initial nucleus. One may expect that these decay processes cannot be considered stationary and one has to use the time-dependent Schrödinger equation

$$i\hbar \frac{\partial \Phi(t, \mathbf{r})}{\partial t} = \mathbf{H}\Phi(t, \mathbf{r}) \ . \tag{1.22}$$

Anyway, due to large Coulomb barriers the probability of a cluster to escape from nucleus is very small and short lived states actually correspond to very narrow decay widths of such resonant states. For instance the shortest measurable half-life is at present $T = 10^{-12}$ sec for proton emission and the width is, according to the uncertainty relation, $\Gamma = 6.6 \times 10^{-10}$ MeV. Since the characteristic nuclear time is $T_N \approx 10^{-22}$ *sec* the nucleus lives a long time before decaying in this energy-time scale and, therefore, the decay process may be considered stationary.

The wave function in the region of a resonance, with the width Γ, lying at an energy $E^{(0)}$ can be factorized in terms of the energy depending Lorentzian distribution as [28]

$$\Phi(E, \mathbf{r}) = -\frac{\Gamma/2}{\pi\left[(E - E^{(0)})^2 + (\Gamma/2)^2\right]}\Psi(\mathbf{r}) = \frac{1}{2\pi i}\left[\frac{1}{E - (E^{(0)} - i\Gamma/2)} - \frac{1}{E - (E^{(0)} + i\Gamma/2)}\right]\Psi(\mathbf{r}) \ . \tag{1.23}$$

The corresponding evolution in time is given by the Cauchy theorem

$$\Phi(t,\mathbf{r}) = \int_{-\infty}^{\infty} \Phi(E,\mathbf{r}) e^{-iEt/\hbar} dE = \Psi(\mathbf{r}) e^{-iE_r t/\hbar} \ , \tag{1.24}$$

and therefore it has the form of a stationary state, but with a complex energy

$$E_r = E^{(0)} - \frac{i}{2}\Gamma \ . \tag{1.25}$$

as first proposed by Gamow in his paper explaining α-decay as a quantum penetration process, thus imposing the probabilistic interpretation of the quantum mechanics as well as theoretical nuclear physics [1].

Gamow put forward this idea, novel for his time and bold even today, that since the time dependence of the wavefunction, corresponding to the decaying resonance, should have the stationary form (1.24) the resonance energy could be considered complex with the form (1.25).

This idea proved to be of great significance in the study of all resonant processes. On the other hand one of its important consequences is that, by going to the complex energy plane, the theory becomes dubious and difficult, but it has the great feature of transforming a time dependent process into a stationary one [29].

A. Angular momentum representation

The general framework to describe emission processes is the stationary scattering theory. The main tool is the angular momentum representation of solutions. First we will give a simple version of the formalism for spherical nuclei emitting structureless fragments and then we will generalize it to deformed nuclei emitting fragments with a given structure.

Spherical boson emitters

First let us consider that the fragments are structureless bosons emitted from spherical nuclei. This is the case for instance in the α-decay, connecting ground states of even-even spherical nuclei. The stationary Schrödinger equation describing such a process is written as follows

$$\left[-\frac{\hbar^2}{2\mu}\Delta + V_0(r)\right] \Psi(\mathbf{r}) = E\Psi(\mathbf{r}) \ , \tag{1.26}$$

where μ denotes the reduced mass of the α-daughter system. The potential $V_0(r)$ between the α particle and daughter nucleus has two components: the short range nuclear part $V_N(r)$ and the Coulomb interaction $V_C(r)$. The wave function can be expanded in partial waves in terms of spherical harmonics

$$\Psi(\mathbf{r}) = \sum_l \frac{f_l(r)}{r} Y_{lm}(\hat{r}) \ , \tag{1.27}$$

where $\mathbf{r} = (r,\hat{r}) \equiv (r,\theta,\phi)$. The spherical harmonics are factorized as follows

$$Y_{ln}(\theta,\phi) = \Theta_{lm}(\theta)\Phi_m(\phi) \ , \quad \Phi_m(\phi) = \frac{e^{im\phi}}{\sqrt{2\pi}} \ , \tag{1.28}$$

where each component is orthonormal

$$\begin{aligned} \int_0^\pi \Theta^*_{lm}(\theta)\Theta_{l'm'}(\theta) sin\theta d\theta &= \delta_{ll'} \\ \int_0^{2\pi} \Phi^*_m(\phi)\Phi_{m'}(\phi) d\phi &= \delta_{mm'} \ . \end{aligned} \tag{1.29}$$

The Laplacian in spherical coordinates has the following form

$$\Delta = \frac{1}{r}\frac{\partial^2}{\partial r^2} r - \frac{\hat{L}^2}{r^2} \ , \tag{1.30}$$

where the angular part of the operator acts on spherical harmonics as follows

$$\hat{L}^2 Y_{lm}(\theta,\phi) = l(l+1) Y_{lm}(\theta,\phi) \ . \tag{1.31}$$

We insert the expansion in partial waves (1.27) in Eq. (1.26) and then we multiply it with $Y^*_{lm}(\theta,\phi)$. By using the orthogonality of spherical harmonics (1.29) one obtains the following equations for the radial components

$$\frac{d^2 f_l(r)}{dr^2} \ = \ \left\{ \frac{l(l+1)}{r^2} + \frac{2\mu}{\hbar^2} \left[V_0(r) - E \right] \right\} f_l(r) \ . \tag{1.32}$$

This system of decoupled equations can be also written in terms of the dimensionless radius $\rho = \kappa r$, depending on the momentum $\kappa = \sqrt{2\mu E}/\hbar$, as follows

$$\left[-\frac{d^2}{d\rho^2} + \frac{V_l(r)}{E} - 1 \right] f_l(r) = 0 \tag{1.33}$$

where we introduced the angular momentum-dependent potential

$$\frac{V_l(r)}{E} = \frac{l(l+1)}{\rho^2} + \frac{V_0(r)}{E} \ . \tag{1.34}$$

Since the nuclear interaction V_N is of a finite range, one has $V_N(r) = 0$ beyond some radius. Therefore at large distances only the spherical Coulomb interaction is active and the ratio between the interaction potential and emission energy can be expressed as follows

$$\frac{V_0(r)}{E} \rightarrow \frac{Z_1 Z_2 e^2}{rE} = \frac{\chi}{\rho} \ , \tag{1.35}$$

where Z_k are the charges of the emitted fragments. where we introduced the Coulomb parameter (twice the Sommerfeld parameter)

$$\chi \ = \ 2 \frac{Z_1 Z_2 e^2}{\hbar v} \ , \tag{1.36}$$

with the asymptotic velocity defined as

$$v \ = \ \sqrt{\frac{2E}{\mu}} = \frac{\hbar \kappa}{\mu} \ . \tag{1.37}$$

The independent solutions of the Coulomb equation

$$\left[-\frac{d^2}{d\rho^2} + \frac{l(l+1)}{\rho^2} + \frac{\chi}{\rho} - 1 \right] f_l(r) = 0 \ , \tag{1.38}$$

are the standard regular and irregular Coulomb waves [30]. They are real functions of ρ. The regular solution $F_l(\chi,\rho)$ vanishes at the origin and increases as a function of the distance inside the Coulomb barrier, while the irregular solution $G_l(\chi,\rho)$ diverges at the origin but decreases with distance inside the Coulomb barrier.

At large distances both solutions oscillate, i. e. their asymptotic behaviour is given by

$$\begin{aligned} f_l(\chi,\rho) = \quad & F_l(\chi,\rho) \rightarrow_{\rho\rightarrow\infty} sin(\rho - \frac{1}{2} l\pi + \sigma_l) \ , \\ & G_l(\chi,\rho) \rightarrow_{\rho\rightarrow\infty} cos(\rho - \frac{1}{2} l\pi + \sigma_l) \ . \end{aligned} \tag{1.39}$$

where σ_l is the Coulomb phase shift

$$\sigma_l = arg\ \Gamma(l+1+i\frac{\chi}{2}) - \frac{1}{2}\chi ln\ 2\rho \ , \tag{1.40}$$

with Γ being the Euler Gamma-function. In the above definition we also included the term depending upon the logarithm of the reduced radius.

If one of the emitted fragments is neutral, like for instance the neutron, then $\sigma_l = 0$ and the above spherical waves are proportional with spherical Bessel functions

$$\begin{aligned} f_l(\rho) &= \rho j_l(\rho) \rightarrow_{\rho\rightarrow\infty} sin(\rho - \frac{1}{2}l\pi) \\ &= \rho n_l(\rho) \rightarrow_{\rho\rightarrow\infty} cos(\rho - \frac{1}{2}l\pi) \ . \end{aligned} \tag{1.41}$$

The outgoing/ingoing Coulomb-Hankel waves are defined in terms of the above Coulomb functions as follows

$$H_l^{(\pm)}(\chi,\rho) = G_l(\chi,\rho) \pm iF_l(\chi,\rho) \rightarrow_{\rho\rightarrow\infty} exp[\pm i(\rho - \frac{1}{2}l\pi + \sigma_l)] \ . \tag{1.42}$$

These waves become usual Hankel functions for neutral particles, i.e.

$$\rho h_l^{(\pm)}(\rho) = \rho[n_l(\rho) + ij_l(\rho)] = exp[\pm i(\rho - \frac{1}{2}l\pi)] \ . \tag{1.43}$$

Spherical fermion emitters

In case of fermion (proton or neutron) emission from spherical nuclei the central potential entering Schrödinger equation (1.26) contains also the spin-orbit part, i.e.

$$V_0(r,\mathbf{s}) = V_0(r) + V_{so}(r)\mathbf{l}.\sigma \ , \tag{1.44}$$

where $V_0(r)$ is the central nuclear plus Coulomb potential and $\sigma = 2\mathbf{s}$. The wave function is expanded

$$\Psi(\mathbf{r},\mathbf{s}) = \sum_l \frac{f_{lj}(r)}{r}\mathcal{Y}_{jm}^{(l)}(\hat{r},\mathbf{s}) \ , \tag{1.45}$$

in terms spin-orbital harmonics

$$\mathcal{Y}_{jm}^{(l)}(\hat{r},\mathbf{s}) = \Big[Y_l(\hat{r}) \otimes \chi_{\frac{1}{2}}(\mathbf{s})\Big]_{jm} \equiv \sum_{m_1+m_2=m} \langle lm_1;\frac{1}{2}m_2|mj\rangle Y_{lm_1}(\hat{r})\chi_{\frac{1}{2}m_2}(\mathbf{s}) \ , \tag{1.46}$$

where the bracket symbol denotes Clebsch-Gordan recoupling coefficients corresponding to the angular momentum addition $\mathbf{j} = \mathbf{l} + \mathbf{s}$. By using the same manipulations as in the previous case one obtains the system of equations for radial components

$$\left[-\frac{d^2}{d\rho^2} + \frac{l(l+1)}{\rho^2} + \frac{V_0(r) + V_{so}(r)\langle\mathbf{l}.\sigma\rangle}{E} - 1\right] f_{lj} = 0 \ , \tag{1.47}$$

where

$$\langle\mathbf{l}.\sigma\rangle = j(j+1) - l(l+1) - \frac{3}{4} \ . \tag{1.48}$$

At large distances the system contains only Coulomb interaction (1.35).

B. S-matrix

Scattering states

In the following we will investigate the so-called scattering states, i.e. real solutions of the Schrödinger equation with positive energy. The formalism presented below is common for boson and fermion cases. In order to simplify notations we will use boson channel notation l. For the fermion emission this index should be replaced by $l \rightarrow (lj)$.

In the external region, where the nuclear interaction vanishes, the solution is a combination of the Coulomb functions. The standard form that one adopts is

$$\begin{aligned} f_l^{(ext)}(E,r) &\sim G_l(\chi,\rho)\sin\delta_l(E) + F_l(\chi,\rho)\cos\delta_l(E) \\ &= \frac{i}{2}e^{-i\delta_l(E)}\left[H_l^{(-)}(\chi,\rho) - \mathcal{S}_l(E)H_l^{(+)}(\chi,\rho)\right] \ . \end{aligned} \tag{1.49}$$

Notice that this form is valid for spherical emitters, where in each spherical channel, corresponding to a given angular momentum l, there is an incoming wave $H_l^{(-)}$. Later on, in Section devoted to the R-matrix method, we will give a more general expression corresponding to deformed emitters. We will show below that the phase shift is a real number, as it should be so that the S-matrix, defined by

$$\mathcal{S}_l(E) = e^{2i\delta_l(E)} \ , \tag{1.50}$$

satisfies the unitarity condition

$$\mathcal{S}_l(E)\mathcal{S}_l^\dagger(E) = 1 \ . \tag{1.51}$$

To evaluate the phase shift and therefore the S-matrix one requires the continuity of the external and internal wavefunctions and of the corresponding derivatives at the point $r = R$. The internal wave function should be regular in origin

$$f_l^{(int)} \rightarrow_{r\rightarrow 0} r^{l+1} \ . \tag{1.52}$$

This is achieved through the matching of the internal and external logarithmic derivatives of the wavefunction $f_l(r)$, i.e.

$$\beta_l^{(int)}(R) \equiv \frac{1}{f_l^{(int)}(R)}\frac{df_l^{(int)}(R)}{dr} = \beta_l^{(ext)}(R) \equiv \frac{1}{f_l^{(ext)}(R)}\frac{df_l^{(ext)}(R)}{dr} \ . \tag{1.53}$$

From Eq. (1.49), writing the trigonometric functions in terms of exponentials, one gets

$$\mathcal{S}_l(E) = e^{2i\overline{\delta}_l(E,R)}\frac{\beta_l^{(int)}(E,R) - D_l(E,R) + iP_l(E,R)}{\beta_l^{(int)}(E,R) - D_l(E,R) - iP_l(E,R)} \ . \tag{1.54}$$

where we have defined

$$\begin{aligned}
D_l(E,R) &\equiv kR\frac{F_l'(\chi,\kappa R) + iG_l'(\chi,\kappa R)}{F_l^2(\chi,\kappa R) + G_l^2(\chi,\kappa R)} = i\kappa R\frac{\left[H_l^{(-)}(\chi,\kappa R)\right]'}{\left|H_l^{(+)}(\chi,\kappa R)\right|^2} \ , \\
P_l(E,R) &\equiv \frac{\kappa R}{F_l^2(\chi,\kappa R) + G_l^2(\chi,\kappa R)} = \frac{\kappa R}{\left|H_l^{(+)}(\chi,\kappa R)\right|^2} \ , \\
e^{2i\overline{\delta}_l(E,R)} &\equiv -\frac{F_l(\chi,\kappa R) + iG_l(\chi,\kappa R)}{F_l(\chi,\kappa R) - iG_l(\chi,\kappa R)} = \frac{H_l^{(-)}(\chi,\kappa R)}{H_l^{(+)}(\chi,\kappa R)} \ ,
\end{aligned} \tag{1.55}$$

with, e.g. $F_l'(\chi,\kappa R) \equiv dF_l(\chi,\rho)/d\rho|_{\rho=\kappa R}$. We have also used the property that the Wronskian for Coulomb functions is unity, i. e. $F_l'(\chi,\rho)G_l(\chi,\rho) - G_l'(\chi,\rho)F_l(\chi,\rho) = 1$ for all values of ρ_c [30]. One notices that $\overline{\delta}_l$ is real, since the Coulomb functions are real. Moreover, it vanishes inside the barrier for narrow resonant states due to very small values of the regular Coulomb function, i. e. in this region it is $e^{2i\overline{\delta}_l(E,R)} \approx 1$.

Resonances

Close to the resonant energy E_n one can expand the logarithmic derivative as follows

$$\beta_l^{(int)}(E,R) \approx \beta_l(E_n,R) + \beta_l'(E_n,R)(E - E_n) \ , \tag{1.56}$$

and the S-matrix becomes

$$\mathcal{S}_{nl}(E,R) = e^{2i\overline{\delta}_l(E,R)}\frac{E - E_n - \Delta_{nl}(E,R) - \frac{i}{2}\Gamma_{nl}(E,R)}{E - E_n - \Delta_{nl}(E,R) + \frac{i}{2}\Gamma_{nl}(E,R)} \tag{1.57}$$

where we introduced the energy shift and decay width as

$$\begin{aligned}
\Delta_{nl}(E,R) &\equiv \frac{D_l(E,R) - \beta_l(E_n,R)}{\beta_l'(E_n,R)} \ , \\
\Gamma_{nl}(E,R) &\equiv -\frac{2P_l(E,R)}{\beta_l'(E_n,R)} \ .
\end{aligned} \tag{1.58}$$

In order to estimate the derivative of the logarithmic derivative with respect to the energy we consider two internal solutions of Eq. (1.83), namely $f_1(r) \equiv f_l(E_1, r)$ and $f_2(r) \equiv f_l(E_2, r)$. Since they obey the Schrödinger equation one gets

$$f_2(r)\frac{d^2 f_1(r)}{dr^2} - f_1(r)\frac{d^2 f_2(r)}{dr^2} = \frac{2\mu}{\hbar^2}(E_2 - E_1) f_1(r) f_2(r) \ . \tag{1.59}$$

By integrating both sides from 0 to R, dividing by $f_1(R)f_2(R)$ and using the fact that the internal solution should be regular in origin, i.e. $f_l(E, r = 0)$=0, one obtains

$$\begin{aligned} \frac{R}{f_1(R)}\frac{df_1(R)}{dr} - \frac{R}{f_2(R)}\frac{df_2(R)}{dr} &= \beta(E_1, R) - \beta(E_2, R) \\ &= (E_2 - E_1)\frac{2\mu R}{\hbar^2 f_1(R) f_2(R)} \int_0^R f_1(r) f_2(r) dr \ . \end{aligned} \tag{1.60}$$

In the limit $E_2 \to E_1 = E$ and normalizing to unity the internal wave function one gets

$$-\frac{d}{dE}\beta_l(E, R) = \frac{2\mu R}{\hbar^2 f_l^2(E, R)} \equiv \gamma_l^{-2}(E, R) \ , \tag{1.61}$$

where we introduced the reduced width γ_l. Thus, the decay width in Eq. (1.58) acquires the standard form

$$\Gamma_{nl}(E, R) = 2P_l(E, R)\gamma_l^2(E_n, R) \ , \tag{1.62}$$

which is a real positive number. We will see later that the same factorisation of the decay width is also given by the R-matrix theory [7].

According to Eq. (1.57) the maximum value of the S-matrix occurs when the denominator is a minimun, i. e. for the energy $E = E_{nl}^{(0)}(E, R) = E_n + \Delta_l(E, R)$. In terms of this energy the S-matrix reads

$$\mathcal{S}_{nl}(E, R) \ = \ e^{2i\overline{\delta}_l(E,R)} \frac{E - E_{nl}^{(0)}(E, R) - \frac{i}{2}\Gamma_{nl}(E, R)}{E - E_{nl}^{(0)}(E, R) + \frac{i}{2}\Gamma_{nl}(E, R)} \tag{1.63}$$

Physically, this equation is interpreted as the S-matrix corresponding to a resonance with energy $E_{nl}^{(0)}(E, R)$ and width $\Gamma_{nl}(E, R)$.

So far we have been careful to show the dependence upon E and R of the parameters entering the S-matrix, i. e. $E_{nc}^{(0)}(E, R)$ and $\Gamma_{nl}(E, R)$. However it has to be stressed that the dependence upon R is artificial, since the theory should not depend upon the matching radius if this point is properly chosen, i. e. beyond the range of the nuclear force. The dependence upon the energy, based in the approximation (1.56), is a more serious point. Wigner realized that this dependence is irrelevant in the analysis of observable resonances, since in that case the width is so small that in the energy range of the resonance Γ can be considered a constant. In the rest of this Section we will only consider narrow resonance. That is the S-matrix have the form

$$\mathcal{S}_{nl}(E) = e^{2i\overline{\delta}_l}\frac{E - E_{nl}^{(0)} - \frac{i}{2}\Gamma_{nl}}{E - E_{nl}^{(0)} + \frac{i}{2}\Gamma_{nl}} = e^{2i\overline{\delta}_l}\left[1 - \frac{i\Gamma_{nl}}{E - E_{nl}^{(0)} + \frac{i}{2}\Gamma_{nl}}\right] \ . \tag{1.64}$$

where $E_{nl}^{(0)}$ and Γ_{nl} are real positive numbers.

It is important to keep in mind that Eq. (1.64) was obtained by assuming that Γ_{nl} is small and therefore it is only valid for narrow (and therefore isolated) resonances.

Poles of the S-matrix

From Eq. (1.64) one sees that the energies and widths of narrow resonances can be obtained by calculating the complex poles of the S-matrix. But this can be a very difficult task because Γ_l can be many orders of magnitude smaller than $E_l^{(0)}$ and the computation of the complex energy $E_l^{(0)} + i\Gamma_l/2$ would require a very high precision. We will come back to this problem in Subsection II C. But still one can compute the energy of the resonance as the pole of the S-matrix and then the width as the corresponding residues. To see this we first notice that the number $\overline{\delta}_l$ (called "hard sphere phase shift") represents the contribution of the continuum

background to the S-matrix and its value is negligible close to a narrow resonance. Therefore the residues of the S-matrix at the pole n is

$$Res[\mathcal{S}_{nl}(E)] = \lim_{E \to E_{nl}^{(0)} - \frac{i}{2}\Gamma_{nl}} (E - E_{nl}^{(0)} + \frac{i}{2}\Gamma_{nl})\mathcal{S}_{nl}(E) = -i\Gamma_{nl} \ , \tag{1.65}$$

which is an important result since it shows that if the resonance is isolated then the residues of the S-matrix is a pure imaginary number. On the contrary, for resonances that are not isolated the residua are generally complex quantities [31].

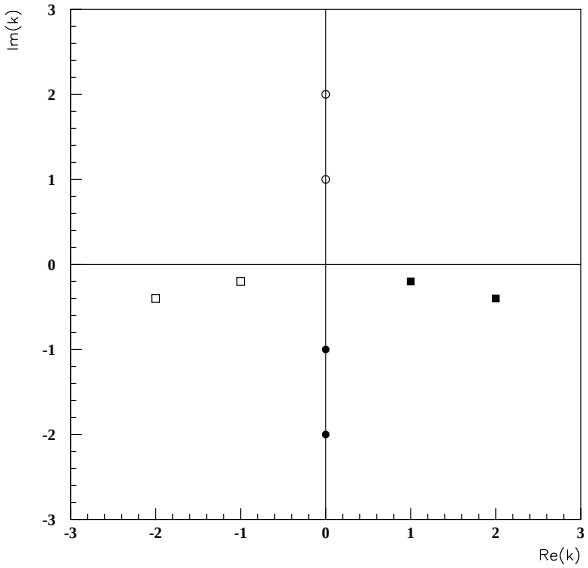

FIG. 2: *Poles of the S-matrix: bound states (dark circles), antibound states (open circles), decay states (dark squares), capture states (open squares).*

Let us mention that by exchanging between them $H_l^{(+)}$ and $H_l^{(-)}$ in Eq. (1.49) one obtains a symmetric pole. Thus, by writing

$$\kappa_{nl} = \kappa_{nl}^{(0)} - i\lambda_{nl} \ , \tag{1.66}$$

where $\lambda_{nl} = \Gamma_{nl}/2$ the poles of the S-matrix are [32, 33]:

(a) decay states (Gamow resonances) with $\kappa_{nl}^{(0)} > 0$, $\lambda_{nl} > 0$ (dark squares in Fig. 2);

(b) capture states with $\kappa_{nl}^{(0)} < 0$, $\lambda_{nl} > 0$. (open squares in Fig. 2).

Let us mention that for negative energies the S-matrix has only imaginary poles, corresponding in (1.43) to the following asymptotics

$$f_l(\rho) \to exp[\mp(\rho + \frac{1}{2}l\pi)] \ , \tag{1.67}$$

These are

(c) bound states, for which $\kappa_{nl}^{(0)}$=0 and $\lambda_{nl} < 0$ (dark circles in Fig. 2);

(d) antibound states with $\kappa_{nl}^{(0)}$=0, $\lambda_{nl} > 0$ (open circles in Fig. 2).

From Eq. (1.64) one also obtains

$$\delta_{nl} = arctan\frac{\Gamma_{nl}/2}{E_{nl}^{(0)} - E} \tag{1.68}$$

which shows that a resonance appears when the phase shift increases as it approaches the value $\delta_{nl} = \pi/2$ as a function of increasing energy assuming, also here, that the hard sphere phase shift is negligible. This criterion is often used to determine the energies of resonances.

Eq. (1.68) allows one to evaluate the decay width by using still another expression, namely

$$\Gamma_{nl} = -2 \left[\frac{\partial ctg\ \delta_{nl}}{\partial E} \right]^{-1}_{E=E^0_{nl}} . \tag{1.69}$$

Finally, it is worthwhile to mention that from Eq. (1.64) the cross section corresponding to the scattering of the particle at the energy of the resonance acquires the form

$$\sigma_{nl}(E) = (2l+1)\frac{\pi}{k^2} \frac{\Gamma^2_{nl}}{(E - E^{(0)}_{nl})^2 + (\Gamma_{nl}/2)^2} , \tag{1.70}$$

This formula was derived by G. Breit and E. P. Wigner [2] to explain the capture of slow neutrons. It is one of the most successful expressions ever written in quantum physics, as shown by its extensive use in the study of resonances ever since. It was by comparing with experiment that Wigner interpreted the number Γ as the width of the resonance. Since the imaginary part of the S-matrix pole is -Γ/2 (Eq. (1.64)), this interpretation coincided with the Gamow interpretation of the width.

C. Gamow states

The states with complex energies $E = E^{(0)}_l - \frac{i}{2}\Gamma_l$, corresponding to the poles of the type (a) and (b), are called Gamow outgoing/ingoing states. According to the representation of the S-matrix (1.63) the scattering state (1.49) is given by

$$f^{(ext)}_l(r) \sim \left(E - E^{(0)}_l + \frac{i}{2}\Gamma_l \right) H^{(\mp)}_l(\chi,\rho) - \left(E - E^{(0)}_l - \frac{i}{2}\Gamma_l \right) H^{(\pm)}_l(\chi,\rho) , \tag{1.71}$$

and the first term vanishes. Therefore they are eigenstates of the stationary system of equations (1.32) with the following asymptotics

$$f^{(ext)}_l(r) = N_l H^{(\pm)}_l(\chi,\rho) , \tag{1.72}$$

We can now formulate the complex eigenvalue problem for the Gamow states. The internal components of the relative wave function $f^{(int)}_l(r)$ should be regular in origin (1.52). The continuity of logarithmic derivatives for the internal and external wavefunction components (1.72) at some large radius R, where the interaction is given by the Coulomb interaction, can be fulfilled only for a discrete set of complex values of the wave number κ_{nl} (1.66), given by the above cases (a) and (b).

The angular momentum representation can be generalized for deformed nuclei, when both emitted fragments have structure and they can be left in some excited state. The dynamics of the decaying system is described by the following stationary Schrödinger equation

$$\mathbf{H}\Psi_{J_iM_i}(\mathbf{x_1},\mathbf{x_2},\mathbf{r}) = E\Psi_{J_iM_i}(\mathbf{x_1},\mathbf{x_2},\mathbf{r}) . \tag{1.73}$$

We consider that the Hamiltonian describing binary emission is given by the following general ansatz

$$\mathbf{H} = -\frac{\hbar^2}{2\mu}\Delta_r + \mathbf{H}_1(\mathbf{x_1}) + \mathbf{H}_2(\mathbf{x_2}) + V(\mathbf{x_1},\mathbf{x_2},\mathbf{r}) . \tag{1.74}$$

where $\mathbf{x}_k$ denote the internal coordinates of fragments and $\mathbf{r}$ the distance between them. We denote by V the inter-fragment potential and by $\mathbf{H}_k$ the Hamiltonians describing the internal motion of the emitted fragments, i.e.

$$\mathbf{H}_k\Phi_{J_kM_k}(\mathbf{x}_k) = E_k\Phi_{J_kM_k}(\mathbf{x}_k) , \quad k = 1,2 , \tag{1.75}$$

where E_k are the excitation energies of emitted fragments and $\Phi_{J_kM_k}(\mathbf{x}_k)$ their eigenstates, satisfying the orthonormality condition

$$\langle \Phi_{J_kM_k} | \Phi_{J'_kM'_k} \rangle = \delta_{J_kJ'_k}\delta_{M_kM'_k} . \tag{1.76}$$

The external solution can be written as a superposition of different outgoing channels $c \equiv (J_1, J_2, J_c, j_c)$, describing all possible binary splittings, i.e.

$$\Psi_{J_iM_i}(\mathbf{x_1},\mathbf{x_2},\mathbf{r}) = \sum_c \Psi^{(c)}_{J_iM_i}(\mathbf{x_1},\mathbf{x_2},\mathbf{r}) = \sum_c \frac{f_c(r)}{r}\mathcal{Y}^{(c)}_{J_iM_i}(\mathbf{x_1},\mathbf{x_2},\hat{r}) , \tag{1.77}$$

where, with $\hat{r} \equiv (\phi, \theta)$, we introduced the core-angular harmonics

$$\langle \mathbf{x_1}, \mathbf{x_2}, \hat{r}|c\rangle \equiv \mathcal{Y}^{(c)}_{J_i M_i}(\mathbf{x_1}, \mathbf{x_2}, \hat{r}) = \left\{ [\Phi_{J_1}(\mathbf{x}_1) \otimes \Phi_{J_2}(\mathbf{x}_2)]_{J_c} \otimes \mathcal{Y}_{j_c}(\hat{r}) \right\}_{J_i M_i} \ . \tag{1.78}$$

As usually, the symbol $[... \otimes ...]_{JM}$ denotes the angular momentum coupling. Thus, the total spin is decomposed in each channel as follows

$$\begin{aligned} \mathbf{J}_i &= \mathbf{J}_c + \mathbf{j}_c \\ \mathbf{J}_c &= \mathbf{J}_1 + \mathbf{J}_2 \ . \end{aligned} \tag{1.79}$$

These functions are also introduced within the R-matrix theory [5–7], were they are called surface functions. Obviously when one of the emitted fragments is structureless, like for instance in proton of α emission, one has $\Phi_{J_2}(\mathbf{x}_2) = 1$. The harmonics $\mathcal{Y}_{j_c m_c}(\hat{r})$ describe the angular relative motion and they coincide with usual spherical harmonics (1.28) in the case when both fragments are bosons. Here j_c is an integer number.

On the other hand they coincide with spin-orbital harmonics (1.46) for the fermion (proton or neutron) emission, where j_c is half integer.

Due to the orthonormality of their components, the core-angular harmonics are mutually orthonormal, i.e.

$$\langle c|c'\rangle = \langle \mathcal{Y}^{(c)}_{J_i M_i} | \mathcal{Y}^{(c')}_{J_i M_i} \rangle \ = \ \delta_{cc'} \ . \tag{1.80}$$

We split the potential into a spherical and a deformed component, i.e. $V = V_0 + V_d$. By projecting out a given channel c and taking into account the orthonormality condition (1.80) one obtains the coupled channels system of equations for the radial wavefunctions

$$\frac{d^2 f_c(r)}{dr^2} \ = \ \left\{ \frac{l_c(l_c+1)}{r^2} + \frac{2\mu}{\hbar^2}\left[V_0(r) - E_c\right] \right\} f_c(r) + \frac{2\mu}{\hbar^2} \sum_{c'} V_d^{(cc')}(r) f_{c'}(r) \ , \tag{1.81}$$

where the channel energy is defined as $E_c = E - E_1 - E_2$ and

$$V_d^{(cc')}(r) = \langle \mathcal{Y}^{(c)}_{J_i M_i} | V_d | \mathcal{Y}^{(c')}_{J_i M_i} \rangle \ . \tag{1.82}$$

At large distances only the spherical components are dominant and therefore the above system becomes decoupled

$$\left[-\frac{d^2}{d\rho_c^2} + \frac{l_c(l_c+1)}{\rho_c^2} + \frac{V_0(r)}{E_c} - 1 \right] f_c(r) = 0 \ , \tag{1.83}$$

in terms of the reduced radius for a given channel "c" $\rho_c = \kappa_c r$, where momentum is defined by $\kappa_c = \sqrt{2\mu E_c}/\hbar$. At large distances only the spherical Coulomb interaction (1.35) is active. In this region the system (1.83) has the form similar to (1.38) for each angular momentum of the channel c, i.e.

$$\left[-\frac{d^2}{d\rho_c^2} + \frac{l_c(l_c+1)}{\rho_c^2} + \frac{\chi_c}{\rho_c} - 1 \right] f_c(\chi_c, \rho_c) = 0 \ , \tag{1.84}$$

where the channel Coulomb parameter is given by

$$\chi_c \ = \ 2\frac{Z_1 Z_2 e^2}{\hbar v_c} \ . \tag{1.85}$$

with the asymptotic channel velocity defined as

$$v_c \ = \ \sqrt{\frac{2E_c}{\mu}} = \frac{\hbar \kappa_c}{\mu} \ . \tag{1.86}$$

The outgoing/ingoing solutions of Eq. (1.84) are the standard Coulomb-Hankel waves (1.42). Thus, the general solution is an eigenstate of the stationary system of equations (1.81) with the following asymptotics

$$f_c(r) \rightarrow_{r\to\infty} f_c^{(ext)}(r) \ , \tag{1.87}$$

where $f_c^{(ext)}(r)$ satisfies Eq. (1.84), i.e. it is a linear combination of (1.42). As in the spherical case, by denoting with $f_c^{(int)}(r)$ the internal components of the relative wave function regular in the origin, the continuity of the

logarithmic derivatives of the wavefunction components at some large radius R, where the interaction is given by (1.35), has the following form

$$\beta_c^{(int)}(R) \equiv \frac{1}{f_c^{(int)}(R)} \frac{df_c^{(int)}(R)}{dr} = \beta_c^{(ext)}(R) \equiv \frac{1}{f_c^{(ext)}(R)} \frac{df_c^{(ext)}(R)}{dr} \ . \tag{1.88}$$

It can be fulfilled only for a discrete set of complex values of the wave number κ_n for the above (a)-(d) cases. As in the spherical case, the cases (a) and (b) are respectivelly satisfied by the following asymptotics

$$f_c^{(ext)}(r) = N_c H_{l_c}^{(\pm)}(\chi_c, \rho_c) \ , \tag{1.89}$$

where N_c are the scattering amplitudes in the channel c.

Boson emission

Boson emission mainly occurs in the case of the binary cold fission, α and heavy cluster emission. Most of binary cold fission processes (1.20) refer to the initial ground state of an even-even nucleus with $J_i = 0$. The relative motion of emitted fragments is described by the standard angular harmonics $Y_{lm}(\hat{r})$. Various channels are defined by $c \equiv (J_1 J_2 l)$, where J_k are the spins of the fragments, while l is the relative angular momentum. Thus, one has $j_c = l$ in the definition of channel core-angular harmonics (1.78) of axially deformed fragments, i.e.

$$\mathcal{Y}_{J_1 J_2 l}(\mathbf{x_1}, \mathbf{x_2}, \hat{r}) = \{[\Phi_{J_1}(\mathbf{x}_1) \otimes \Phi_{J_2}(\mathbf{x}_2)]_l \otimes Y_l(\hat{r})\}_0 \ . \tag{1.90}$$

For the α-decay or heavy cluster emission

$$P(J_i M_i) \to D(J_f M_f) + C(l) \ , \tag{1.91}$$

connecting the parent (P) and daughter (D) deformed nuclei, the light fragment (C) is a structureless boson with $J_2 = 0$ and therefore one has $\Phi_{J_2}(\mathbf{x}_2) = 1$. The most general form of core-angular harmonics is given by

$$\mathcal{Y}^{(J_f l)}_{J_i M_i}(\mathbf{x}, \hat{r}) = \left[\Phi_{J_f}(\mathbf{x}) \otimes Y_l(\hat{r})\right]_{J_i M_i} \ . \tag{1.92}$$

If the initial spin is zero, like in α-transitions from ground to some excited state in the daughter nucleus, one obtains a simpler ansatz

$$\mathcal{Y}_J(\omega, \hat{r}) = [\Phi_J(\omega) \otimes Y_J(\hat{r})]_0 \ . \tag{1.93}$$

Fermion emission

As a typical example of fermion emission is proton emission from proton rich nuclei, but neutron/proton delayed emission from giant resonant states or beta delayed emission can also be considered in this class. All these processes can be described within the same formalism. Thus, let us consider a general fermion emission process

$$P(J_i M_i) \to D(J_f M_f) + p(lj) \ . \tag{1.94}$$

The wave function of the decaying system has the following form

$$\Psi_{J_i M_i}(, \mathbf{x}, \mathbf{r}, \mathbf{s}) = \sum_{J_f l j} \frac{f_{J_f l j}(r)}{r} \mathcal{Y}^{(J_f l j)}_{J_i M_i}(\mathbf{x}, \hat{r}, \mathbf{s}) \ . \tag{1.95}$$

where J_i (J_f) is the spin of the mother (daughter) nucleus but, as mentioned above, this index also labels all other quantum numbers, while (l, j) are the angular momentum and spin of the outgoing fermion. These angular momenta should satisfy the triangular relation, i. e.

$$|J_i - J_f| \le j \le |J_i + J_f| \ . \tag{1.96}$$

If the emitter is an odd-even nucleus and the daughter nucleus is left in its ground state one has $J_f = 0$ and the fermion carries the spin $j = J_i$.

In the expansion (1.95) we introduced the core-spin-orbit harmonics defined by the tensor

$$\mathcal{Y}^{(J_f l j)}_{J_i M_i}(\mathbf{x}, \hat{r}, \mathbf{s}) = \left[\Phi_{J_f}(\mathbf{x}) \otimes \mathcal{Y}^{(l\frac{1}{2})}_{j}(\hat{r}, \mathbf{s}) \right]_{J_i M_i} \ , \tag{1.97}$$

where the angular part, describing fermion motion, is

$$\mathcal{Y}^{(l\frac{1}{2})}_{jm}(\hat{r}, \mathbf{s}) = \left[Y_l(\hat{r}) \otimes \chi_{\frac{1}{2}}(\mathbf{s}) \right]_{jm} \ , \tag{1.98}$$

with $\chi_{\frac{1}{2}}(\mathbf{s})$ denoting the spin function.

D. Decay width

For Gamow states (a) the imaginary part of κ according to (1.25) is negative and the modulus of the outgoing wave increases at large distances. By considering Eqs. (1.24) and (1.25), one obtains that the matter density decreases according to

$$|\Phi(t, \mathbf{r})|^2 = |\Psi(\mathbf{r})|^2 \, e^{-\Gamma t/\hbar} \ , \tag{1.99}$$

which is nothing else than the well-known exponential decay law, giving the number of nuclei at a certain moment

$$N(t) = N(0) e^{-\lambda t} \ , \tag{1.100}$$

where the decay constant is defined by $\lambda = \Gamma/\hbar$. The half-life is defined as the interval of time after which the number if initial nuclei decreases to half with respect to the initial value, i.e.

$$T = \frac{\hbar ln\ 2}{\Gamma} = \frac{4.56\ 10^{-22}}{\Gamma} \ , \tag{1.101}$$

where Γ is in MeV and T in seconds.

The decay width can in principle be determined by solving the coupled channels system (1.81) with the matching conditions (1.88) in the complex energy plane. The evaluation of the poles of the S-matrix can be performed using the same procedure as the one used to evaluate bound states. The difference is that now one has to introduce the outgoing boundary condition given by Eq. (1.89). There are standard computer codes to do this, e. g. the codes of Refs. [34, 35]. These codes evaluate the energies corresponding to all poles of the S-matrix. The real energies define either the bound or the antibound states. The complex energies which are close to the real energy axis correspond to narrow resonances and therefore they accept the interpretation given above to such energies. That is, the real part is the position of the decaying resonance and minus twice the imaginary part is the corresponding width. However the value of the imaginary part is in observable emission proceses usually much smaller, in absolute value, than the corresponding real part and its calculation is a difficult numerical task. But even if this calculation is possible we want to stress that not always does the imaginary part of the energies correspond to the width of a resonance.

There is also an equivalent way to determine the width. Let us consider the stationary Schrödinger equation and its complex congugate

$$\begin{aligned} \left(E - \frac{i}{2}\Gamma \right) \Psi &= \left(-\frac{\hbar^2}{2\mu}\nabla^2 + V \right) \Psi \\ \left(E + \frac{i}{2}\Gamma \right) \Psi^* &= \left(-\frac{\hbar^2}{2\mu}\nabla^2 + V \right) \Psi^* \ . \end{aligned} \tag{1.102}$$

One multiplies to the left the first relation by Ψ^* and the second one by Ψ. By substracting the two equalities one obtains

$$\Gamma \Psi^* \Psi = \frac{\hbar^2}{2\mu i} \left(\Psi^* \nabla^2 \Psi - \Psi \nabla^2 \Psi^* \right) \ . \tag{1.103}$$

Here we considered that the potential operator V is Hermitian and therefore the corresponding difference vanishes. We then integrate this relation over internal variables $\mathbf{x}_1$, $\mathbf{x}_2$ and the relative coordinate $\mathbf{r}$ inside a

sphere with a large radius. By transforming the right hand side term into a surface integral one obtains the following expression of the decay width

$$\Gamma = \frac{\hbar \oint \mathcal{J}(\hat{r}) d\hat{r}}{\int \mathcal{P}(\mathbf{r}) d\mathbf{r}} \ . \tag{1.104}$$

Here we introduced the internal probability

$$\mathcal{P}(\mathbf{r}) = \int d\mathbf{x}_1 \int d\mathbf{x}_2 \left|\Psi\right|^2 \ , \tag{1.105}$$

and the probability flux

$$\mathcal{J}(\hat{r}) \ = \ \frac{\hbar}{2\mu i} \int d\mathbf{x}_1 \int d\mathbf{x}_2 \left(\Psi^* \nabla \Psi - \Psi \nabla \Psi^*\right) r^2 \ . \tag{1.106}$$

We consider that the wave function is normalised to unity inside the considered sphere. In this way we suppose that the two fragments exist with the unity probability inside this volume. This statement is in an aparent contradiction with the emission process leading to a decrease of the internal probability. Anyway, due to the very small value of the decay width compared with the emission energy one can use this condition, for a relative large time interval compared with the characteristic nuclear time [36].

On the surface of the sphere the gradient operator acts only on the radial direction $\nabla \to \mathbf{e}_r \frac{\partial}{\partial r}$, i.e.

$$\mathcal{J}(\hat{r}) \to \frac{\hbar}{2\mu i} \int d\mathbf{x}_1 \int d\mathbf{x}_2 \left(\Psi^* \frac{\partial \Psi}{\partial r} - \Psi \frac{\partial \Psi^*}{\partial r}\right) r^2 \ . \tag{1.107}$$

Thus, by using the channel expansion (1.77) and

$$\frac{\partial \Psi^{(c)}}{\partial r} \to i\kappa_c \Psi^{(c)} \ , \tag{1.108}$$

the angular distribution becomes

$$\Gamma(\hat{r}) = \hbar \mathcal{J}(\hat{r}) = \hbar \sum_{cc'} v_c \lim_{r\to\infty} r^2 \int d\mathbf{x}_1 \int d\mathbf{x}_2 \Psi^{(c)*} \Psi^{(c')} \ . \tag{1.109}$$

By using the orthogonality of the core-angular harmonics (1.80) the decay width, proportional with the total probability flux through the surface of this sphere, becomes

$$\Gamma = \oint \Gamma(\hat{r}) d\hat{r} = \hbar \sum_c v_c \lim_{r\to\infty} \oint r^2 d\hat{r} \int d\mathbf{x}_1 \int d\mathbf{x}_2 |\Psi_c|^2 = \sum_c \hbar v_c |N_c|^2 \equiv \sum_c \Gamma_c \ , \tag{1.110}$$

where we used the asymptotic relation (1.89) and the fact that the modulus of the outgoing Coulomb-Hankel wave function is unity, as seen from Eq. (1.42). Thus, the total decay width can be written as a sum of partial decay widths corresponding to the considered channels. The equality between internal and external radial wave functions together with Eq. (1.89), i.e.

$$f_c^{(int)}(E_c, R) = f_c^{(ext)}(E_c, R) = N_c H_{l_c}^{(+)}(\chi_c, \kappa_c R) \ , \tag{1.111}$$

determines the scattering amplitude

$$N_c = \frac{f_c^{(int)}(E_c, R)}{H_{l_c}^{(+)}(\chi_c, \kappa_c R)} \ . \tag{1.112}$$

Notice that N_c does not depend upon R, since both internal and external components satisfy the same Schrödinger equation. By inserting this value in the expression of the decay width (1.110) one obtains the following relation

$$\Gamma_c = \hbar v_c \left| \frac{f_c^{(int)}(E_c, R)}{H_{l_c}^{(+)}(\chi_c, \kappa_c R)} \right|^2 = 2P_{l_c}(E_c, R) \gamma_c^2(E_c, R) \ , \tag{1.113}$$

where χ_c is the Coulomb parameter corresponding to the resonant complex energy. Here we introduced the standard penetrability and reduced width squared [7]

$$\begin{aligned} P_{l_c}(E_c,R) &= \frac{\kappa_c R}{\left|H_{l_c}^{(+)}(\chi_c,\kappa_c R)\right|^2} = \frac{\kappa_c R}{F_{l_c}^2(\chi_c,\kappa_c R)+G_{l_c}^2(\chi_c,\kappa_c R)} \ , \\ \gamma_c^2(E_c,R) &= \frac{\hbar^2}{2\mu R}|f_c^{(int)}(E_c,R)|^2 \ . \end{aligned} \tag{1.114}$$

The form of the above decay width at the energy $E = E_c$, in terms of the penetrability and reduced width is the same as in Eqs. (1.62).

E. Decay rules

According to the factorisation of the decay width (1.113) and the above relation for the penetrability (1.114) the half life (1.101) is proportional with the modulus squared of the Coulomb-Hankel function inside the barrier. In this region it practically coincides with the irregular Coulomb function and has a very simple WKB ansatz, given in Appendix B by

$$\begin{aligned} H_l^{(+)}(\chi,\rho) &\approx (ctg\ \alpha)^{1/2}\ exp\left[\chi\left(\alpha - sin\ \alpha\ cos\ \alpha\right)\right] C_l \\ &= \left(\frac{1}{x}-1\right)^{-1/4}\ exp\left[\chi\left(arccos\sqrt{x}-\sqrt{x(1-x)}\right)\right] C_l \\ &\equiv H_0^{(+)}(\chi,\rho) C_l \end{aligned} \tag{1.115}$$

where, with the external turning point $R_b = Z_1 Z_2 e^2/E$ and barrier energy $V_0 = Z_1 Z_2 e^2/R$, we introduced the following notations

$$\begin{aligned} cos^2\ \alpha &= x = \frac{\rho}{\chi} = \frac{R}{R_b} = \frac{E}{V_0} \\ C_l &= exp\left[\frac{l(l+1)}{\chi}\sqrt{\frac{\chi}{\rho}-1}\right] \ . \end{aligned} \tag{1.116}$$

Thus, the logarithm of the half-life, corrected by the exponential centrifugal factor C_l defined by the second line of this relation, should be proportional with the Coulomb parameter, i.e.

$$log_{10} T_{red} = a_0 \chi + b_0 \ , \tag{1.117}$$

where we defined the reduced half life by

$$T_{red} = \frac{T_{1/2}}{C_l^2} = \frac{ln2}{v_l}\left|\frac{H_0^{(+)}(\chi,\rho)}{f_l^{(int)}(R)}\right|^2 \ . \tag{1.118}$$

This relation is also called Geiger-Nuttall law, discovered in 1911 for α-decay between ground states (where the angular momentum carried by the α-particle is $l = 0$) and written as follows

$$log_{10} T_{1/2} = a\frac{Z}{\sqrt{Q_\alpha}} + b \ , \tag{1.119}$$

where Z is the charge of the left daughter nucleus and Q_α the Q-value of the α-particle. As we pointed out the explanation of this law was given by G. Gamow in 1928 [1], in terms of quantum-mechanical penetration of the Coulomb barrier, given in the first line of (1.114). It is characterized by the Coulomb parameter, which is proportional to the ratio $Z/\sqrt{Q_\alpha}$.

A special situation occurs in the case of proton emission, when the angular momentum of the emitted proton in general is different from zero. The half lives systematics for known proton emitters [37, 38, 40] is given in Figure 3 (a). The picture becomes much simpler for the reduced half life in Figure 3 (b).

The Geiger-Nuttall law for proton emitters can be reproduced by the formula

$$\begin{aligned} log_{10}\ T_{red}^{(k)} &= a_k(\chi - 20) + b_k \ , \\ a_1 &= 1.31 \ , \quad b_1 = -2.44 \ , \quad Z < 68 \\ a_2 &= 1.25 \ , \quad b_2 = -4.71 \ , \quad Z > 68 \ , \end{aligned} \tag{1.120}$$

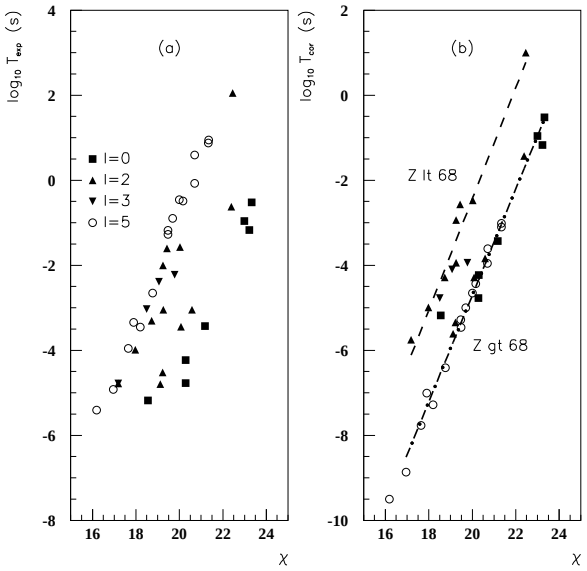

FIG. 3: *(a) Logarithm of half lives for proton emiters versus the Coulomb parameter (1.85). Different symbols denote angular momenta carried by the emitted proton. (b) Logarithm of reduced half lives (1.118) for proton emiters versus the Coulomb parameter.*

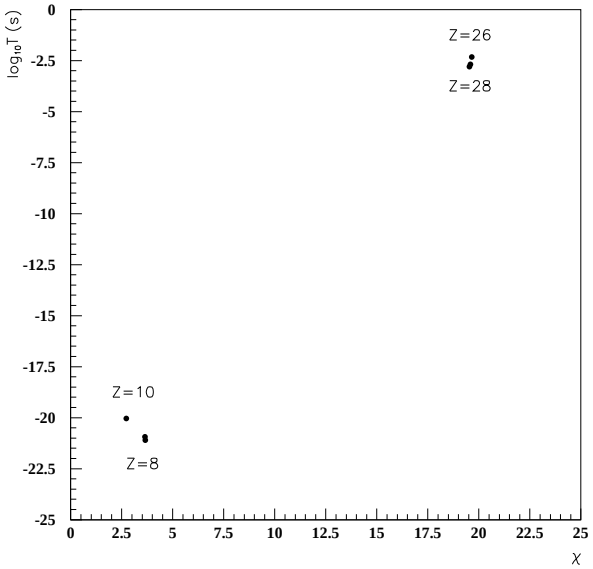

FIG. 4: *Logarithm of half lives for two proton emiters versus the Coulomb parameter (1.85). The charge of the mother nucleus is indicated.*

where $k = 1$ corresponds to the upper line in figure 3 (b). The standard errors are $\sigma_1 = 0.26$ and $\sigma_2 = 0.23$, corresponding to a mean factor less than two. Here we considered the geometrical radius, i.e. $R = 1.2(A_D^{1/3} + 1)$. The analysis in Ref. [40] showed that this behaviour can be explained only by an abrupt change in the nuclear structure of the emitters.

The two-proton emission was predicted in 1960 [17], but at the moment the experimetal material concerning consists in only few cases. In figure 4 it is shown the logarithm of the half life versus the Somerfeld parameter, by considering a di-proton emission.

The α-decays between ground states are characterized by a remarkable regularity, especially for transitions

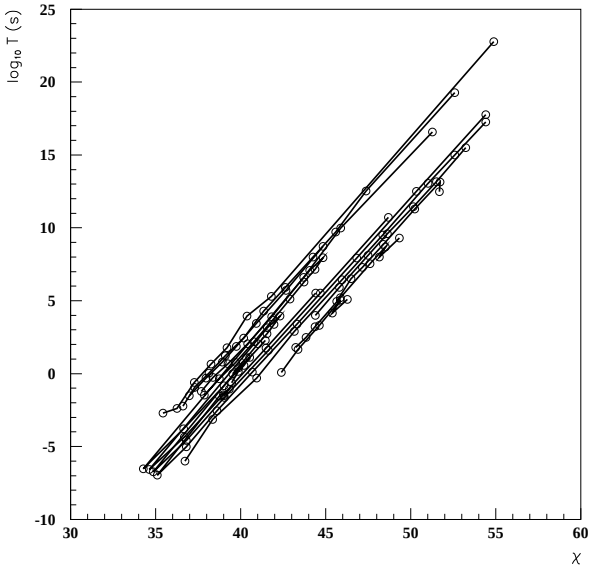

FIG. 5: *Logarithm of half lives for α-decays from even-even nuclei versus Coulomb parameter (1.85). Differents lines connect decays from nuclei with the same charge number.*

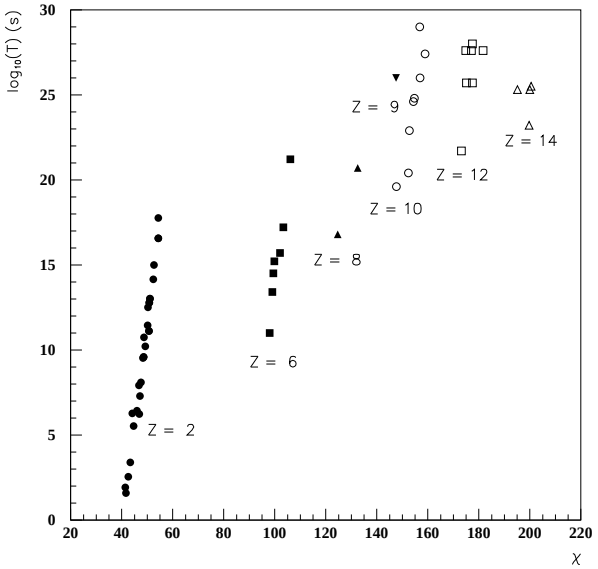

FIG. 6: *Logarithm of half lives for heavy cluster decays and the corresponding α-decays from the same mother nuclei versus Coulomb parameter (1.85). Differents symbols denote charge number of the emitted cluster.*

between ground states of even-even nuclei. The fact that α-transitions along various isotopic chains lie on separate lines, as stated by the Viola-Seaborg rule [41], i.e.

$$log_{10}T_{1/2} = \frac{a_1 Z + a_2}{\sqrt{Q_\alpha}} + b_1 Z + b_2 \ , \tag{1.121}$$

was connected with different α-particle reduced widths, multiplying the penetrability in (1.113). This feature is shown in Figure 5. Still in doing systematics along neutron chains there are important deviations with respect to this rule, as for instance in α-decay from odd mass nuclei, and this feature is strongly connected with nuclear structure details.

F. Double folding potential

As we already mentioned, we can describe within the stationary coupled channels formalism various emission processes, from proton emission to cold fission. We suppose that the emitted fragments are already born and their motion is fully described by a Schrödinger equation with some two-body potential, defined for all iter-fragment distances. Of course such a description is strictly valid only for particle (proton/neutron) emission, because it is possible to describe its dynamics by a selfconsistent mean field.

In the case when both emitted fragments are composite, like for instance in the α-decay, the potential picture is an idealisation. Anyway, the emitted fragments are already formed in the region around the geometrical touching point, i.e. at the nuclear surface and only here one can determine a two-body potential. In the overlapping region acts Pauli principle and the two fragments loose their identity. The equivalent potential becomes non-local and for a corect treatment it is necessary the antisymmetrisation of the wave function within the so-called Resonanting Group Method, as it is described in the review [42], devoted to the microscopic description of cluster emission. Unfortunatelly this method is adequate to describe only relative light systems, or heavy nuclei close to a double magic nucleus, at is is the α-decay from ^{212}Po.

On the other hand, a good way to simulate the Pauli principle is the introduction of a repulsive core. As many calculations showed, the shape of this potential is not important, the only role is to adjust the energy of the resonant state in the resulting pocket-like potential to the experimental Q-value. The reason for this is that only the external part of the potential is important in order to determine the asymptotics of the wave function and therefore the physical observables, like channel decay widths.

First we will consider that both emission fragments can be excited during the decay process. We will separate the rotational fragment degrees of freedom from other internal coordinates i.e. $\mathbf{x_k} = (\alpha_k, \omega_k)$, where ω_k are the Euler rotational coordinates. The most general Hamiltonian describing a binary emission process is given by

$$\mathbf{H} = -\frac{\hbar^2}{2\mu}\Delta_r + \mathbf{H}_1(\alpha_1) + \mathbf{H}_2(\alpha_2) + \mathbf{T}_1(\omega_1) + \mathbf{T}_2(\omega_2) + V(\alpha_1, \alpha_2, \omega_1, \omega_2, \mathbf{r}) \ , \tag{1.122}$$

where $\mathbf{H}_k(\alpha_k)$ are the Hamiltonians describing the internal dynamics, while $\mathbf{T}_k(\omega_k)$ the rotation of the fragments. This Hamiltonian describes a large variety of situations, i.e. proton/neutron emission, α-decay, heavy cluster emission and fission.

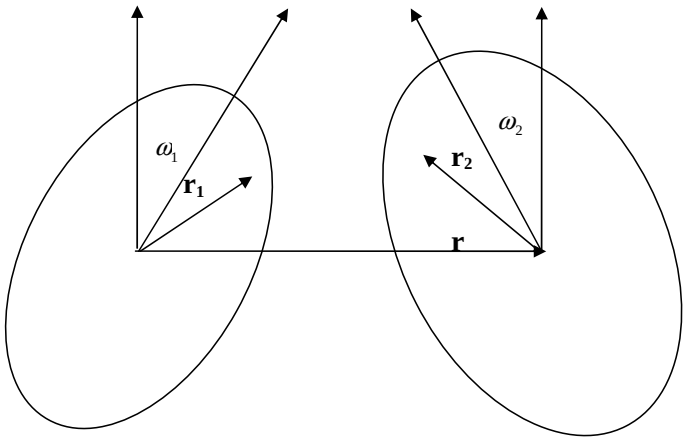

FIG. 7: *Geometry of the double folding interaction.*

The most general method to estimate the interaction between two massive fragments is given by the double folding procedure between the nuclear densities. This procedure is described in many text-books and review papers, e.g. [43] and consists in the following double integral

$$V(\alpha_1, \alpha_2, \omega_1, \omega_2, \mathbf{r}) = \int d\mathbf{r}_1 \int d\mathbf{r}_2 \rho_1(\alpha_1, \mathbf{r}_1)\rho_2(\alpha_2, \mathbf{r}_2)v(\mathbf{r}_{12}) \ , \quad \mathbf{r}_{12} \equiv \mathbf{r} + \mathbf{r}_2 - \mathbf{r}_1 \ , \tag{1.123}$$

where $\mathbf{r}_k$ is the radius giving the nucleon position inside the k-th nucleus, as seen in Fig. 7, with the density ρ_k and v is the nucleon-nucleon force. The most popular two-body interaction, used to describe heavy ion scattering is given by a superposition of Yukawa potentials, simulating the exchange of different mesons, called

also M3Y interaction [44]. It is given for the soft-Reid potential by the following relation

$$v(\mathbf{r}_{12}) = v_{00}(r_{12}) + \hat{J}_{00}\delta(\mathbf{r}_{12}) + v_{01}(r_{12})\tau_1.\tau_2 + \frac{e^2}{r_{12}} \ , \tag{1.124}$$

where the central and isospin parts have respectivelly the following expressions

$$\begin{aligned} v_{00}(r) &= \left[7444\frac{e^{-4r}}{4r} - 2134\frac{e^{-2.5r}}{2.5r}\right] \ MeV \\ v_{01}(r) &= \left[-4885.5\frac{e^{-4r}}{4r} + 1175.5\frac{e^{-2.5r}}{2.5r}\right] \ MeV \ . \end{aligned} \tag{1.125}$$

The second term in Eq. (1.124) approximates the single-nucleon exchange exchange effects through a zero-range pseudopotential with the strength $\hat{J} = -262 \ MeV \ fm^3$.

Let us consider for simplicity that both nuclei are axially symmetric, but the generalisation to the triaxial case is straightforward. The radial components of the nuclear densities are given by the standard multipole expansion, which can be written in both intrinsic and laboratory systems of coordinates as follows

$$\rho(\alpha_k, \mathbf{r_k}) = \sum_{\lambda} \rho_\lambda(\alpha_k, r_k) Y_{\lambda 0}(\hat{r}'_k) = \sum_{\lambda\mu} \rho_\lambda(\alpha_k, r_k) D^{\lambda}_{\mu 0}(\omega_k) Y_{\lambda\mu}(\hat{r_k}), \ k = 1, 2 \ . \tag{1.126}$$

We then expand the two-body interaction in Fourier components

$$v(\mathbf{r} + \mathbf{r}_2 - \mathbf{r}_1) = \int q^2 dq d\hat{q} \tilde{v}(q) e^{i\mathbf{qr}} e^{i\mathbf{qr}_1} e^{-i\mathbf{qr}_2} \ . \tag{1.127}$$

By using the multipole representation of the plane wave we obtain

$$V(\alpha_1, \alpha_2, \omega_1, \omega_2, \mathbf{r}) = V_0(\alpha_1, \alpha_2, r) + V_d(\alpha_1, \alpha_2, \omega_1, \omega_2, \mathbf{r}) \ , \tag{1.128}$$

where the deformed part of the potential is given by

$$V_d(\alpha_1, \alpha_2, \omega_1, \omega_2, \mathbf{r}) = \sum_{\lambda_1\lambda_2\lambda_3} V_{\lambda_1\lambda_2\lambda_3}(\alpha_1, \alpha_2, r) \left\{ \left[D^{\lambda_1}_0(\omega_1) \otimes D^{\lambda_2}_0(\omega_2) \right]_{\lambda_3} \otimes Y_{\lambda_3}(\hat{r}) \right\}_0 \ . \tag{1.129}$$

Here the term $(\lambda_1\lambda_2\lambda_3) = (000)$ is excluded from summation. The spherical part of the potential can be written as a particular case of the above double folding potential, i.e.

$$V_0(\alpha_1, \alpha_2, r) = \frac{1}{\sqrt{4\pi}} V_{000}(\alpha_1, \alpha_2, r) \ . \tag{1.130}$$

G. Numerical integration

In this subsection we will present the numerical integration procedure. The solution of the coupled channel equations should be regular at origin. This provides a set of N linear independent vector functions satisfying

$$\mathcal{R}_{ca}(r) \rightarrow_{r\rightarrow 0} \delta_{ca} r^{l_c+1} \ , \tag{1.131}$$

if the potential has a Woods-Saxon shape. The first index "c" of this radial wave function denotes the basis while the second one "a" the eigenvalue. In a matrix notation this relation can be written as follows

$$\begin{bmatrix} \mathcal{R}_{11} & \mathcal{R}_{21} & ... & \mathcal{R}_{N1} \\ \mathcal{R}_{12} & \mathcal{R}_{22} & ... & \mathcal{R}_{N2} \\ ... & ... & ... & ... \\ \mathcal{R}_{1N} & \mathcal{R}_{2N} & ... & \mathcal{R}_{NN} \end{bmatrix} \rightarrow_{r\rightarrow 0} \begin{bmatrix} r^{l_1+1} & 0 & ... & 0 \\ 0 & r^{l_2+1} & ... & 0 \\ 0 & 0 & ... & r^{l_N+1} \end{bmatrix} \ . \tag{1.132}$$

Each left hand side column is found by using a forward integration with the initial conditions in the corresponding right hand side column.

In case the interaction has a strong repulsive core in origin, then the condition at a certain radius r_0 inside the core is the following

$$\mathcal{R}_{ca}(r) \rightarrow_{r\rightarrow r_0} \delta_{ca}\epsilon \ , \tag{1.133}$$

where ϵ is an arbitrary small number.

It is necessary to integrate numerically only once the system of equations, because the fundamental system of solutions at the radius r is generated by a multiplication between the propagator matrix given by the Runge-Kutta methodand the matrix of initial conditions. If the interaction does not contain first derivative one can use the Numerov method.

In general the forward integration is stable until some point R where the nuclear potential vanishes and total potential reaches a maximum. The internal solution can be written as a superposition of these fundamental solutions

$$f_c^{(int)}(r) = \sum_a \mathcal{R}_{ca}(r) M_a \ . \tag{1.134}$$

In matrix notation the vector of solutions is given as the product of the internal matrix of fundamental solutions times the unknown coefficients, i.e. $\mathbf{f}^{(int)}(r) = \mathcal{R}(r)\mathbf{M}$.

Beyond R the forward integration procedure is not convenient because the regular increasing solution "contaminates" the irregular decreasing one. Nevertheless this integration can be performed from the point where the interaction becomes spherical. Here we define the $N \times N$ matrix of outgoing fundamental solutions (Gamow matrix) with the asymptotics

$$\mathcal{H}_{ca}^{(+)}(r) \equiv \mathcal{G}_{ca}(r) + i\mathcal{F}_{ca}(r) \rightarrow_{r\rightarrow\infty} \delta_{ca} H_{l_c}^{(+)}(\chi_c, \kappa_c r) \equiv \delta_{ca}[G_{l_c}(\chi_c, \kappa_c r) + iF_{l_c}(\chi_c, \kappa_c r)] \ , \tag{1.135}$$

which, as in (1.132), can be written in matrix notation

$$\begin{bmatrix} \mathcal{H}_{11}^{(+)} & \mathcal{H}_{21}^{(+)} & ... & \mathcal{H}_{N1}^{(+)} \\ \mathcal{H}_{12}^{(+)} & \mathcal{H}_{22}^{(+)} & ... & \mathcal{H}_{N2}^{(+)} \\ ... & ... & ... & ... \\ \mathcal{H}_{1N}^{(+)} & \mathcal{H}_{2N}^{(+)} & ... & \mathcal{H}_{NN}^{(+)} \end{bmatrix} \rightarrow_{r\rightarrow\infty} \begin{bmatrix} H_{l_1}^{(+)} & 0 & ... & 0 \\ 0 & H_{l_2}^{(+)} & ... & 0 \\ 0 & 0 & ... & H_{l_N}^{(+)} \end{bmatrix} \ . \tag{1.136}$$

The matrix $\mathcal{H}$ is found by backward integration starting from large distance. The c-th component of the external solution is built as a linear superposition of the column-vectors in $\mathcal{H}$, i. e.

$$f_c^{(ext)}(r) = \sum_a \mathcal{H}_{ca}^{(+)}(r) N_a \rightarrow_{r\rightarrow\infty} N_c H_{l_c}^{(+)}(\chi_c, \kappa_c r) \ , \tag{1.137}$$

or in matrix notation $\mathbf{f}^{(ext)}(r) = \mathcal{H}^{(+)}(r)\mathbf{N}$.

The matching constants are found using the continuity conditions. The corresponding system of equations is given by

$$\begin{aligned} f_c^{(int)}(R) &= f_c^{(ext)}(R) \ , \\ \frac{d}{dr} f_c^{(int)}(R) &= \frac{d}{dr} f_c^{(ext)}(R) \ . \end{aligned} \tag{1.138}$$

In order to find a non-trivial solution the following secular equation has to be fulfilled

$$det \begin{bmatrix} \mathcal{R}(R) & \mathcal{H}^{(+)}(R) \\ \frac{d}{dr}\mathcal{R}(R) & \frac{d}{dr}\mathcal{H}^{(+)}(R) \end{bmatrix} \approx det \begin{bmatrix} \mathcal{R}(R) & \mathcal{G}(R) \\ \frac{d}{dr}\mathcal{R}(R) & \frac{d}{dr}\mathcal{G}(R) \end{bmatrix} = 0 \ . \tag{1.139}$$

The solutions corresponding to the first determinant provide complex energies which are the S-matrix poles. They define the deformed Gamow decaying states. For a large Coulomb barrier the resonance is very narrow and therefore the regular Coulomb functions have vanishing values inside the barrier. Thus, the approximation of using real irregular Coulomb functions, as in (1.139), is very good.

The matching constants can be obtained by inverting (1.137) together with the first condition (1.138), i.e.

$$N_a = \sum_c \left[\mathcal{H}_{ac}^{(+)}(R)\right]^{-1} f_c^{(int)}(R) \ , \tag{1.140}$$

where the wave function is normalized in the internal region, i.e.

$$\int_0^R \sum_c |f_c(r)|^2 \, dr = 1 \ . \tag{1.141}$$

This normalisation constant, which is just the scattering amplitude, can be written in terms of the propagator operator as

$$N_c = \frac{1}{H_{l_c}^{(+)}(\kappa_c R)} \sum_{c'} \mathcal{K}_{cc'}(R) f_{c'}^{(int)}(R) \ , \tag{1.142}$$

where the propagator matrix describes the transition from the initial state $\mathcal{H}^{(+)}$ to the final solution $H^{(+)}$ as

$$\mathcal{K}_{cc'}(R) = H_{l_c}^{(+)}(\chi_c, \kappa_c R) \left[\mathcal{H}_{cc'}^{(+)}(R)\right]^{-1} = \delta_{cc'} + \Delta\mathcal{K}_{cc'}(R) \ . \tag{1.143}$$

It is defined in such a way that for a spherical Coulomb field becomes the unity matrix and, therefore, $\Delta\mathcal{K}_{cc'}(R) = 0$ in this case. It turns out that even for large quadrupole deformations, e. g. $\beta_2 = 0.4$, the correcting matrix is rather small, i.e. $max\left[\Delta\mathcal{K}_{cc'}(R)\right] < 0.1$. It is worthwhile to point out that this operator is the exact counterpart of the the so-called WKB Fröman matrix introduced in the theory of α-decay [9]. For a spherical potential obviously this matrix is diagonal and is given by the ratio between the integrated solution $\mathcal{H}_{cc}^{(+)}(R)$ the Gamow function $H_{l_c}^{(+)}$.

The relation (1.142) leads to a factorised form of the partial decay width which is similar to the spherical relation, i.e.

$$\Gamma_c = 2P_{l_c}(R) \left|\gamma_c^{(d)}(R)\right|^2 \ , \tag{1.144}$$

where the penetrability has the standard form for spherical emitters, i.e.

$$P_{l_c}(E_c, R) \ \equiv \ \frac{\kappa_c R}{F_{l_c}^2(\chi_c, \kappa_c R) + G_{l_c}^2(\chi_c, \kappa_c R)} = \frac{\kappa_c R}{\left|H_{l_c}^{(+)}(\chi_c, \kappa_c R)\right|^2} \ , \tag{1.145}$$

while the deformed reduced decay width is given by

$$\begin{aligned} \gamma_c^{(d)}(R) \ &= \ \sqrt{\frac{\hbar^2}{2\mu R}} s_c(R) \ , \\ s_c(R) \ &\equiv \ \sum_{c'} \mathcal{K}_{cc'}(R) f_{c'}^{(int)}(R) \ . \end{aligned} \tag{1.146}$$

It is also possible to have an alternative matrix factorisation of the following form

$$\Gamma_c = 2 \sum_{c'} \left|P_{cc'}^{1/2}(R) \gamma_{c'}(R)\right|^2 \ , \tag{1.147}$$

where now we introduced the matrix elements of the deformed penetrability

$$P_{cc'}^{1/2}(R) = P_{l_c}^{1/2}(E_c, R) \mathcal{K}_{cc'}(R) = \sqrt{\kappa_c R} \left[\mathcal{H}_{cc'}^{(+)}(R)\right]^{-1} \ , \tag{1.148}$$

but with the standard spherical reduced width

$$\gamma_c(R) \ = \ \sqrt{\frac{\hbar^2}{2\mu R}} f_c^{(int)}(R) \ . \tag{1.149}$$

For large radii, where the interaction becomes spherical, one obtains obviouly the diagonal relation (1.113) in both cases.

By inverting (1.140) one obtains the components of the wave function in terms of partial channels widths

$$f_c^{(int)}(r) = \sum_a \mathcal{H}_{ca}^{(+)}(r) \sqrt{\frac{\Gamma_a}{\hbar v_a}} \ . \tag{1.150}$$

Thus, in order to determine the radial components of the wave function it is necessary first of all to know all relevant partial decay widths. On the other hand the components obviously depend upon the concrete form of

the used potential, determining the fundamental matrix of Gamow solutions. For this reason instead to use the so-called hindrance factors, which are model dependent

$$HF_c = \left| \frac{f_0^{(int)}(r)}{f_c^{(int)}(r)} \right|^2 \ , \tag{1.151}$$

where by "0" we denoted the ground state channel, more appropriate are the intensity ratios

$$I_c = log_{10} \frac{\Gamma_0}{\Gamma_c} \ . \tag{1.152}$$

If the numerical integration is performed in the external region on the real axis this method gives reliable solutions for the irregular Coulomb matrix $\mathcal{G}$. Likewise the approximation $\mathcal{H}^{(+)}(R) \approx \mathcal{G}(R)$ is very good to estimate the scattering amplitudes (and therefore the decay widths) by using Eq. (1.142). On the other hand, the regular Coulomb matrix $\mathcal{F}$ is necessary only to obtain the very small imaginary part of the energy, that is the solutions of Eq. (1.139), which is minus twice the decay width. The difficult task of evaluating simultaneously the functions $\mathcal{F}$ and $\mathcal{G}$, can be accomplished by using the complex scaling method [45]. In this method the integration is performed in the complex radial plane, thus avoiding the drastic decrease of the regular solution.

Historically the first generally available computer code to evaluate Gamow states in spherical symmetric potentials, is the code GAMOW [34]. It computes all poles of the S-matrix, including wide resonances and antibound states. Later improved numerical techniques were used to evaluate those poles with high accuracy [35]. This was necessary since, as already mentioned, measurable half-lives correspond to imaginary parts of the energy which are, in absolute value, many orders of magnitude smaller than the corresponding real part.

H. Diagonalisation method

In emission processes the Coulomb barrier is much higher than the energy of the emitted fragments. As a result, the ratio between the irregular and regular Coulomb waves at the matching radius $r = R$ is

$$\frac{G_l(\chi, kR)}{F_l(\chi, kR)} > 10^{10} \ . \tag{1.153}$$

The resonant state in the internal region $[0, R]$ is practically real and it behaves like a bound state due to the exponential decreasing character of the irregular Coulomb wave for $r > R$. This property implies that one can obtain the wavefunction in the internal region by using a ho representation. To do this in our coupled channels case we rewrite the coupled system of equations (1.81) in the following form

$$\begin{aligned} H_{l_c}^{(\beta_0)} f_c(r) &\equiv -\frac{\hbar\omega}{2\beta_0} \left[\frac{d^2}{r^2} - \frac{l_c(l_c+1)}{r^2} \right] f_c(r) \\ &= \left[E - E_c - V_0(r) \right] f_c(r) - \sum_{c'} V_d^{(cc')}(r) f_{c'}(r) \ , \end{aligned} \tag{1.154}$$

where we introduced the harmonic oscillator parameter

$$\beta_0 = \frac{\mu\omega}{\hbar} \ . \tag{1.155}$$

Expanding the internal radial wave function in this basis one gets

$$f_c^{(int)}(r) = \sum_n^{n_{max}} d_{nc} \overline{\mathcal{R}}_{nl_c}^{(\beta)}(r) \ , \tag{1.156}$$

where the new harmonic oscillator parameter β gives the best fit of the spherical part of the interaction $V_0(r)$ with an harmonic oscillator potential. The eigenvalue system of equations is readily obtained from (1.154) and the harmonic oscillator equation

$$H_l^{(\beta_0)} \overline{\mathcal{R}}_{nl}^{(\beta_0)}(r) = -\frac{\hbar\omega}{2\beta_0} \left[\frac{d^2}{r^2} - \frac{l(l+1)}{r^2} \right] \overline{\mathcal{R}}_{nl}^{(\beta_0)}(r) = \hbar\omega \left(2n + l + \frac{3}{2} - \frac{\beta_0 r^2}{2} \right) \overline{\mathcal{R}}_{nl}^{(\beta_0)}(r) \ . \tag{1.157}$$

which has the analytical solution

$$\overline{\mathcal{R}}_{nl}^{(\beta_0)}(r) \equiv \langle r|\beta_0 nl\rangle = r\mathcal{R}_{nl}^{(\beta_0)}(r) = (-)^n \left[\frac{2\beta_0^{l+3/2} n!}{\Gamma(n+l+3/2)}\right]^{1/2} r^{l+1} e^{-\frac{\beta_0 r^2}{2}} L_n^{l+1/2}(\beta_0 r^2) \ , \tag{1.158}$$

where $\mathcal{R}_{nl}^{(\beta_0)}(r)$ is the standard radial ho wave function, described in Appendix D, depending upon the Laguerre polinomial $L_n^{\alpha}(x)$. When using these functions as a representation we will make ample use of the orthonormality condition that they obey, which reads

$$\langle \beta_0 nl|\beta_0 n'l\rangle = \int_0^{\infty} \overline{\mathcal{R}}_{nl}^{(\beta_0)}(r)\overline{\mathcal{R}}_{n'l}^{(\beta_0)}(r)dr = \delta_{nn'} \ . \tag{1.159}$$

One finally gets

$$\sum_{n'c'} H_{nc,n'c'}^{(\beta)} d_{n'c'} = E d_{nc} \ , \tag{1.160}$$

where the Hamiltonian matrix is

$$\begin{aligned} H_{nc,n'c'}^{(\beta)} &= \left\{\left[f\hbar\omega\left(2n+l_c+\frac{3}{2}\right)+E_c\right]\delta_{nn'} + \left[\langle \beta nl_c|V_0(r)|\beta n'l_c\rangle - \frac{f\hbar\omega}{2}\langle \beta nl_c|\beta r^2|\beta n'l_c\rangle\right]\right\}\delta_{cc'} \\ &+ \langle \beta nl_c|V_d^{(cc')}(r)|\beta n'l_{c'}\rangle \ . \end{aligned} \tag{1.161}$$

The new parameter $\beta = f\beta_0$ is choosen to minimize the contribution of the difference between the spherical and harmonic oscillator potential.

On concludes that any emission process is characterized by two parameters

1) the harmonic oscillator parameter β, defining the size of the internal part of the interaction and

2) the Colomb parameter χ (1.85), giving the ratio between the barrier and Q-value.

These two parameters are aparently independent. The Q-value, which characterizes the stong interacting part of the process enters in χ together with the electromagnetic charges. Therefore between them it should be a connection and we will discuss this point later.

As a rule the dimension of the algebraic system of equations (1.160) is by one order of magnitude larger than the dimension of the differential system (1.154), but this drawback is compensated by the convenience of having a standard eigenvalue problem. A good approximation of the matching constant, and therefore of the decay width, is given by (1.140) using the irregular Coulomb matrix $\mathcal{G}$ defined by (1.135).

I. Two potential method

The initial potential can be splitted into two parts with respect to a radius r_B, i. e. [46, 47].

$$V(r) = U(r) + W(r) \ . \tag{1.162}$$

The first part describe the proton motion in a bound potential

$$\begin{aligned} U(r) &= V(r) \ , \quad r \le r_B \ , \\ &= V_B \equiv V(r_B) \ , \quad r > r_B \ , \end{aligned} \tag{1.163}$$

while the second one describes the transition to the continuum

$$\begin{aligned} W(r) &= 0 \ , \quad r < r_B \ , \\ &= V(r) - V_B \ , \quad r \ge r_B \ . \end{aligned} \tag{1.164}$$

In Fig. 8 we plotted by the solid line a simple potential, describing the main features of the emission process, namely

$$\begin{aligned} V(r) &= \left(\frac{C}{r_B} - v_0\right)\frac{r^2}{r_B^2} + v_0 \ , \quad r \le r_B \\ &= \frac{C}{r} \ , \quad r > r_B \ , \end{aligned} \tag{1.165}$$

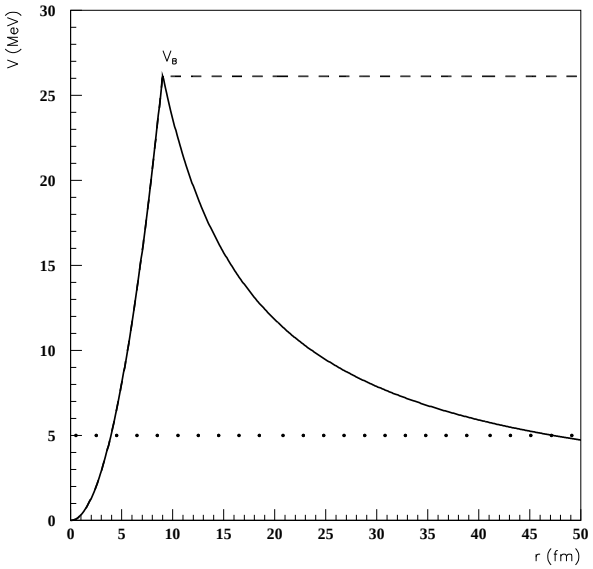

FIG. 8: *The α-core potential (1.165) with $v_0 = 0$ (solid line) and its barrier value (dashed line). The potential W(R) is the difference between the solid and dottted lines. Q-value is denoted by a dotted line.*

where $C = Z_1 Z_2 e^2$ and v_0 is the depth fixing the eigenvalue to the experimental Q-value. The difference between this potential and the maximal value (dashed line) is the "transition operator" W(r) triggering the emission. Indeed, the initial wave function satisfy the Schrödinger equation

$$\mathbf{H}_0 \Phi_0 = (T + U)\, \Phi_0 = E_0 \Phi_0 \ . \tag{1.166}$$

The perturbation W changes the proton state from its initial to its final value. Since $W(r)$ does not vanish at infinity one solves the problem in a shifted potential $\tilde{W}(r) = W(r) + V_B$. The partial decay is given by the distorted wave formula [48], i.e.

$$\Gamma_l = \frac{4\mu}{\hbar^2 k} \left| \int_{r_B}^{\infty} \phi_l(r) W(r) \chi_l(r) dr \right|^2 \ , \tag{1.167}$$

where $\phi_l(r)$ is the radial part of Φ_0 and $\chi_l(r)$ is the regular wave function of the Hamiltonian $T + \tilde{W}$. This method was used to describe α-decays between ground states [49, 50] and the anisotropic α-particle emission in odd-mass nuclei [51].

J. Semiclassical approach

The semiclassical, or Wentzell-Kramers-Brillouin (WKB), approach can be applied for the whole interval, not only inside the Coulomb barrier. The decay width in the spherical case can be derived by using the Gurwitz and Kälbermann procedure [46], namely

$$\begin{aligned} \Gamma_{WKB} &= \lambda_0 F \frac{\hbar^2}{4\mu} P \\ P &\equiv exp\left[-2 \int_{r_2}^{r_3} k(r) dr \right] \ , \end{aligned} \tag{1.168}$$

where λ_0 is the fragment preformation probability and F is the normalisation factor given by the integration over the internal interval, i.e.

$$F^{-1} = \int_{r_1}^{r_2} \frac{dr}{k(r)} cos^2 \left[\int_{r_1}^{r} k(r') dr' - \frac{\pi}{4} \right] \ , \tag{1.169}$$

We denoted by $k(r)$ the wave number

$$k(r) = \sqrt{\frac{2\mu}{\hbar^2}|E - V(r)|} \ . \tag{1.170}$$

The radii $r_1 < r_2 < r_3$ are the classical turning points, given as solutions of the equation $k(r) = 0$ and E is the energy of the emitted proton (Q-value). For high lying strongly oscillating states cos^2 term can be replaced by $\frac{1}{2}$. Then

$$F^{-1} \approx \int_{r_1}^{r_2} \frac{dr}{2k(r)} = \frac{\hbar T}{4\mu} \ , \tag{1.171}$$

where T is the classical period of motion inside the barrier. In this way the preexponential factor in (1.168) becomes proportional to $\nu = \hbar/T$, which is called assault frequency.

As we already mentioned, all phenomenological descritions suppose that the fragment dynamics is described by an inter-fragment potential, defined for all distances and the wave function has the factorized cluster-like form (1.77) in terms of core-angular harmonics (1.78). From this point of view all phenomenological approaches can be considered as "cluster models".

The simplest α-cluster model was applied in Ref. [52] and concerned the α-core dynamics described the potential in Fig. 9

$$\begin{aligned} V(r) &= -V_N + \frac{C}{R} \ , \quad r < R_0 \\ &= \frac{C}{r} \ , \quad r \geq R \ , \end{aligned} \tag{1.172}$$

with $C = 2(Z-2)e^2$.

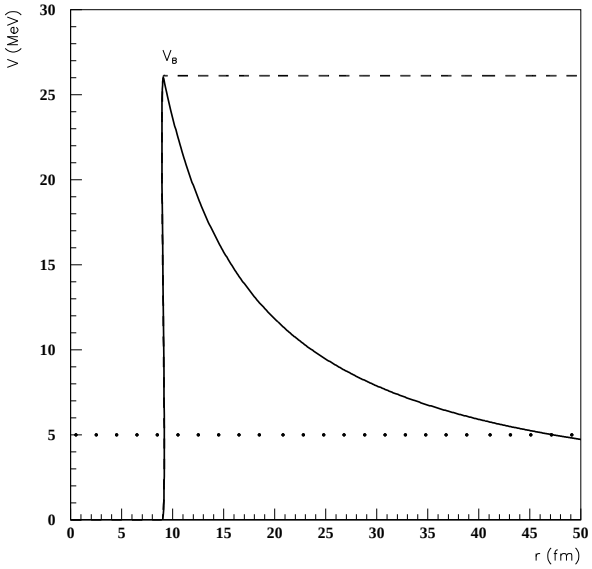

FIG. 9: *The α-core potential (1.172) with $V_N = 0$ (solid line) and its barrier value (dashed line). Q-value is denoted by a dotted line.*

The decay width, according to (1.168), becomes

$$\Gamma = \lambda_0 \frac{\hbar K}{2\mu R} exp\left[-2\int_R^{C/Q} k(r)dr\right] \ , \tag{1.173}$$

where K and k are the wavenumbers in the internal and barrier regions, respectivelly

$$\begin{aligned} K &= \left[\frac{2\mu}{\hbar}\left(Q+V_N-\frac{C}{R}\right)\right]^{1/2} \\ k(r) &= \left[\frac{2\mu}{\hbar}\left(\frac{C}{r}-Q\right)\right]^{1/2} . \end{aligned} \tag{1.174}$$

It turned out that it is more profitable to fix V_N and to change the radius R for each individual decay in order to produce a resonant state at the Q-value, which satisfies the Bohr-Sommerfeld condition with $L=0$, i.e.

$$\int_0^R dr\sqrt{\frac{2\mu}{\hbar^2}\left(Q+V_N-\frac{C}{R}\right)} = R\sqrt{\frac{2\mu}{\hbar^2}\left(Q+V_N-\frac{C}{R}\right)} = (G+1)\frac{\pi}{2} . \tag{1.175}$$

This relation determines the radius R. The penetration integral can be performed analitically, i.e.

$$2\int_R^{C/Q} k(r)dr = 2\sqrt{\frac{2\mu}{\hbar^2}}\frac{C}{\sqrt{Q}}\left[\frac{\pi}{2} - arcsin\ x - x\sqrt{1-x^2}\right] , \tag{1.176}$$

where $x=\sqrt{RQ/C}$. By using the following set of parameters

$$\lambda_0 = 1 , \quad V_N = 135.6\ MeV , \quad G = 22\ (N \le 126) , \quad G = 24\ (N > 126),$$

it was possible to obtain an agreement within a factor of two for most even-even α-emiters.

We mention in this context that this problem was for the first time solved in Ref. [53]. Later on a simple method to solve Schrödinger equation with complex energies in a similar square well was developed in Ref. [54].

K. Fragmentation Theory (FT)

Fragmentation theory (FT) [55, 56] is able to compute the probability of a binary splitting from a given parent nucleus in terms of mass and charge assymetry coordinates, respectively defined as

$$\eta = \frac{A_1 - A_2}{A} , \quad \eta_Z = \frac{Z_1 - Z_2}{Z} . \tag{1.177}$$

Potential energy surface (PES), as a function of these variables and relative distance between centers $V(\eta,\eta_Z,R)$, can be estimated by using various methods. One of the most popular approaches is to consider the liquid drop model plus shell-model corrections, given by the Two Center Schell Model (TSCM) [57–60]. This potential can be inserted in a Schrödinger-like equation, by using a kinetic term with respect to the mass coordinate η. The solutions of this equation describe the probability to create different combinations of fragments.

One of the most successfull applications of the FT is the Preformed Cluster Model (PCM) [61, 62]. Here one computes the preformation amplitude to create the mass splitting (A_1, A_2) with a given charge asymmetry η_Z and at a fixed radius R, by solving the following Schrödinger equation

$$\left[-\frac{\hbar^2}{2\sqrt{B_{\eta\eta}}}\frac{\partial}{\partial\eta}\frac{1}{\sqrt{B_{\eta\eta}}}\frac{\partial}{\partial\eta} + V(\eta,\eta_Z,R)\right]\psi^{(n)}_{R\eta_Z}(\eta) = E^{(n)}_{R\eta_Z}\psi^{(n)}_{R\eta_Z}(\eta) . \tag{1.178}$$

The probability to find a pair in a mass asymmetry space is given by

$$P_0(A_1) = |\psi^{(0)}_{R\eta_Z}(A_1)|^2\sqrt{B_{\eta\eta}}\frac{2}{A} . \tag{1.179}$$

By solving Eq. (1.178) one makes a simplification concerning the radius R, by considering the touching configuration of emitted fragments. The potential $V(\eta,\eta_Z,R)$ has a typical parabolic-like minimum with respect to the charge asymmetry coordinate η_Z and the calculations are performed in this "charge equilibrium" point. The remaining potential $V(\eta,R)$ has several minima corresponding to different splittings. For instance in Ref. [61] the potential for ^{222}Ra at the touching configuration has minima corresponding to

^{4}He, ^{10}Be, ^{14}C ^{48,50}Ca, ^{70}Ni, ^{88}Kr.

The quantum numbers $n = 0, 1, 2, ...$ correspond to vibrational states in this potential. By considering the ground state with $n = 0$ it is assumed that the process has a non-dissipative character. The mass parameter $B_{\eta\eta}$ was estimated within the classical model of Kröger and Scheid [63]. The radial potential is given by the nuclear V_N plus Coulomb V_C components, by considering the normalisation at infinity, i.e. by substracting the binding energies of fragments

$$V(\eta, r) = V_N(R) + V_C(R) + \frac{Z_1 Z_2 e^2}{R} - B(A_1, Z_1) - B(A_2, Z_2) \ . \tag{1.180}$$

As a nuclear interaction V_N it was used the proximity potential [64].

The total decay width is given by the following product

$$\Gamma = P_0(A_1)\hbar\nu P \ , \tag{1.181}$$

where the assault frequency

$$\nu = \frac{v}{R_0} = \sqrt{\frac{2E_2}{\mu R_0^2}} \ , \tag{1.182}$$

is defined in terms of the parent radius R_0 and the kinetic energy of the mitted cluster E_2. The penetrability P is considered as the WKB integral

$$P = \int_{R_1}^{R_2} \left[-\frac{2}{\hbar}\sqrt{2\mu(V(R) - Q)} \right] \ . \tag{1.183}$$

FT/PCM was successfully applied to describe α-decay, cluster radioactivity and cold fission [65, 66].

III. MICROSCOPIC DESCRIPTION

The R-matrix theory [6, 7] makes a step forward with respect to the Gamow theory [1], by expressing the decay width as a product between the particle preformation probability and the penetration through the barrier [10–12, 67–69]. This relation is similar to the phenomenological one (1.113), but the role of the wave function at the matching point $f_c(R)/R$ is played by the preformation amplitude, already introduced by Eq. (1.186) and defined as the overlap of the initial wave function and the product between the daughter and α-particle wave functions. This approach takes into account the nuclear structure details, by expressing the cluster wave function in terms of two protons and two neutrons moving in some mean field and interacting with each other via two-body residual forces [11, 68]. Due to the antisymmetrisation effects between the α-particle and daughter wave functions the interaction becomes non-local in the internal region [42, 70]. It was shown that the usual shell-model space using N=6-8 major shells underestimates the experimental decay width by several orders of magnitude [72, 73], due to the exponential decrease of bound single particle wave functions [74]. An answer to the problem would be the inclusion of the sp narrow resonances lying in continuum [75–77], the so called Gamow states. In spite of the fact that the true asymptotic behaviour of the wave functions is achieved, the value of the half life is still not reproduced [78]. Only the background components in continuum can describe the right order of magnitude of experimental decay widths [79–82]. The inclusion of the background contribution becomes important because an important part of the α-clustering process proceeds through such states.

The problem of considering the continuum part of the spectrum in microscopic calculations is rather involved, but very important especially for drip-line nuclei [83]. The idea to replace the integration over the real spectrum in continuum by sp Gamow resonances plus an integration along a contour in the complex plane including these resonances was considered by T. Berggren in Ref. [32]. The calculation is very much simplified if one considers that in some physical processes only the narrow resonances are relevant and the integration, giving the background, can be neglected [84, 85]. This was shown to be an adequate approach for instance in giant resonances [31] and in the nucleon decay processes [86]. To estimate the decay width the states in continuum can be taken into account effectively by including an α-cluster component [87] or by considering a sp basis with a larger harmonic oscillator (ho) parameter for states in continuum [82].

The α-decaying state can be described as a sp resonance, namely by using the matching between logarithmic derivatives of the preformation amplitude and external Coulomb function. The derivative of the α-particle preformation factor, estimated within the shell model is almost constant along any neutron chain and therefore is not consistent with the decreasing behaviour of Q-values along such chains [88, 89]. The slope of the preformation amplitude can be corrected by changing the ho parameter of sp components. These components are connected

with an α-cluster term, not predicted by the standard shell model [87]. Indeed, the even-odd pair staggering of binding energies found along the α-lines with $N - Z$=const, can be explained in terms of a "pairing" in the isospin space between proton and neutron pairs, considered as bosons [91, 92]. The generalisation of this approach in terms many-body Greens's functions was performed in Ref. [93]. This suggest that α-particles are already preformed at least in the low density region of the nuclear surface and they can indeed explain the above inconsistency.

A. Spectroscopic factor

The phenomenological double folding procedure to estimate inter-fragment potential supposes that the two fragments are already born. Therefore the wave function describing the cluster emission process $P \to D + C$, where P (D) is the parent (daughter) nucleus, has a cluster-like ansatz, i.e. it is a superposition of different mutually orthogonal channel components, similar with that given by Eq. 1.77

$$\Psi_{J_i M_i}(\mathbf{x}_P, \mathbf{r}) \to \sum_c \mathcal{F}_c(r) \mathcal{Y}^{(c)}_{J_i M_i}(\mathbf{x}_D, \mathbf{x}_C, \hat{r}) \ , \tag{1.184}$$

where $\mathbf{x}$ indicates the internal coordinate. We did not write the equality sign because in general the wave function of the initial configuration, given by the left hand side, does not contain a 100% cluster-like representation, as it is written by the right hand side.

Indeed, the ratio between the computed half-life, by using the phenomenologic double folding potential, and the experimental value is less than unity and is called phenomenologic spectroscopic factor

$$S = \frac{T_{phen}}{T_{exp}} \ . \tag{1.185}$$

This is due to the fact that is reality the emitted fragments do not exist during the decay process, but they are born with certain probability. In deriving the expression of the decay width (1.110) we divided the outgoing flux to the volume integral of the wave function squared over the internal volume, by considering its value unity. Actually this volume integral gives the creation probability of emitted fragments.

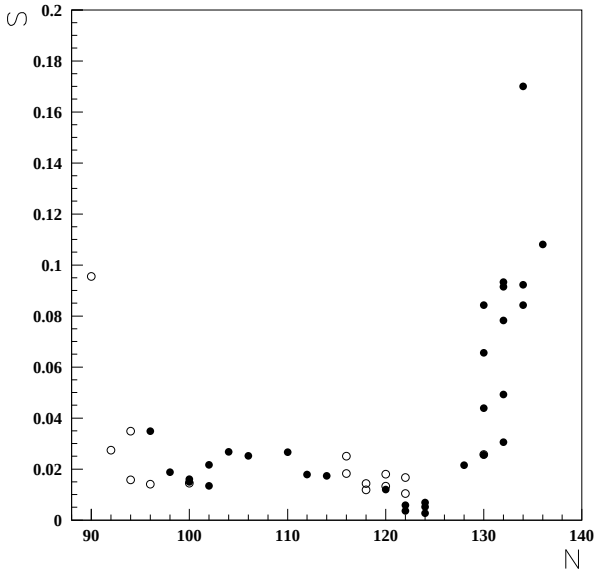

FIG. 10: *Phenomenological spectroscopic factor versus the neutron number*

The amplitude that the cluster-like ansatz is contained in the initial wave function (1.184) is the overlap between the initial wave function and the product between the internal wave functions of the emitted fragments, i. e.

$$\mathcal{F}_c(r) = \langle \mathcal{Y}^{(c)}_{J_i M_i} | \Psi_{J_i M_i} \rangle \ . \tag{1.186}$$

We distinguish two important cases.

Particle emission

For a proton emission from an odd-even emitter, connecting deformed nuclei in their ground states, the channel is given by spin projection, i.e. $c \equiv K$. Let us denote by $a^{\dagger}_{\pi K}$ the *particle* creation operator. The initial wave function in the pairing approach is a superposition of different proton *quasiparticle* excitations of the parent Bardeen-Cooper-Schriffer (BCS) vacuum $\alpha^{\dagger}_{\pi K}|BCS_{\pi P}\rangle$. Since

$$a^{\dagger}_{\pi K}|BCS_{\pi D}\rangle = \left[u^{(D)}_{\pi K}\alpha^{\dagger}_{\pi K} + v^{(D)}_{\pi K}\alpha_{\pi\overline{K}}\right]|BCS_{\pi D}\rangle \ . \tag{1.187}$$

the preformation amplitude becomes

$$\mathcal{F}_K \equiv \langle BCS_{\pi D}|c_{\pi K}\alpha^{\dagger}_{\pi K}|BCS_{\pi P}\rangle = u^{(D)}_{\pi K}\langle BCS_{\pi D}|BCS_{\pi P}\rangle \approx u^{(D)}_{\pi K} \ . \tag{1.188}$$

where the last approximation is due to the blocking effect of the odd proton. It is important to point out that in proton emission the spectroscopic amplitude $\mathcal{F}_K$ is a constant, corresponding to the BCS amplitude around the Fermi surface, i.e. $u_K \sim \sqrt{0.5}$. It multiplies the scattering amplitude N_K.

Cluster emission

The situation changes for cluster emission. The preformation amplitude (1.186) is a function of the radius between emitted fragments and it plays the role of the "internal" wave function. It should satisfy the matching condition with respect to the corresponding "external" channel radial component at certain radius R, i.e.

$$\begin{aligned} \mathcal{F}_c(R) &= \frac{f_c(R)}{R} \\ \mathcal{F}'_c(R) &= \left[\frac{f_c(r)}{r}\right]'_{r=R} \ . \end{aligned} \tag{1.189}$$

In the second part, devoted to microscopic approaches we will analyze in detail the properties of the preformation amplitude. Here we give only some preliminary details.

Let us illustrate how to estimate the overlap integral (1.186) in the case of α-decays involving transitions between ground states. The exact estimate we will perform in the next part devoted to microscopic approaches. The main idea is to find an α-like four body operator connecting daughter with parent nuclei, i.e.

$$|\Psi_P\rangle = P^{\dagger}_{\alpha}|\Psi_D\rangle \ . \tag{1.190}$$

If both parent and daughter are deformed nuclei, described within the pairing approach, than one has the following representation

$$\begin{aligned} P^{\dagger}_{\alpha} &= P^{\dagger}_{\pi}P^{\dagger}_{\nu} \ , \\ P^{\dagger}_{\tau} &= \sum_{K>0} X_{\tau K}a^{\dagger}_{\tau K}a^{\dagger}_{\pi\overline{K}} \ , \end{aligned} \tag{1.191}$$

where the expanssion coefficients are given by

$$X_{\tau K} = \langle BCS_{\tau P}|a^{\dagger}_{\tau K}a^{\dagger}_{\tau\overline{K}}|BCS_{\tau D}\rangle \approx u^{(D)}_{\tau K}v^{(D)}_{\tau K} \ . \tag{1.192}$$

Thus the overlap integral becomes

$$\mathcal{F}_{\alpha}(\mathbf{r}) = \langle\Psi_D\Psi_{\alpha}|P^{\dagger}_{\alpha}|\Psi_D\rangle = \sum_{KK'>0} X_{\pi K}X_{\nu K'}\langle\Psi_{\alpha}|a^{\dagger}_{\pi K}a^{\dagger}_{\pi\overline{K}}a^{\dagger}_{\nu K'}a^{\dagger}_{\nu\overline{K'}}|0\rangle \ , \tag{1.193}$$

where Ψ_{α} is the α-particle wave function, written as a product of three Gaussians in relative proton-neutron coordinates [67–69]. This four-body overlap can be computed by using the standard recoupling of two proton and two neutron single particle states, given by $a^{\dagger}$ operators, from absolute to the relative and center of mass coordinates [82].

In the case of cluster emission one obtains a similar representation [94]. For instance in ^{14}C emission a good approximation of the parent wave function, at distances where Pauli principle is less important, is given by

$$|\Psi_P\rangle \approx P^\dagger_{\alpha_1} P^\dagger_{\alpha_2} P^\dagger_{\alpha_3} P^\dagger_\nu |\Psi_D\rangle \ , \tag{1.194}$$

and the preformation factor is given by a similar expression, i.e.

$$\mathcal{F}_{^{14}C}(\mathbf{r}) = \langle \Psi_D \Psi_{^{14}C} | P^\dagger_{\alpha_1} P^\dagger_{\alpha_2} P^\dagger_{\alpha_3} P^\dagger_\nu |\Psi_D\rangle \ , \tag{1.195}$$

where $\Psi_{^{14}C}$ is the ^{14}C wave function, written as a product of several Gaussians in relative coordinates. One defines the microscopic spectroscopic factor by the following integral

$$S_{gs} = \sum_c \int_0^\infty |r\mathcal{F}_c(r)|^2 dr \ . \tag{1.196}$$

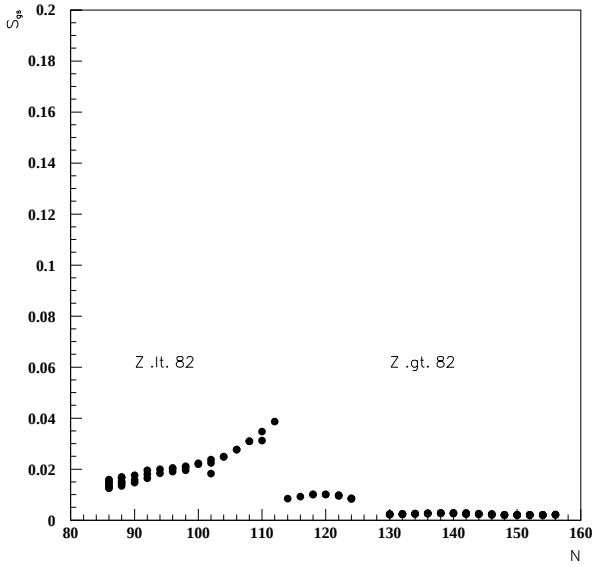

FIG. 11: *Microscopic spectroscopic factor versus the neutron number*

It gives the order of magnitude of the cluster content inside the parent wave function. In principle it shoud have the same order of magnitude with the spcetroscopic factor defined by Eq. (1.185). Actually they are quite different and the ratio S/S_{gs} defines the amount of the additional clustering with respect to the microscopic estimate, given by the preformation amplitude (1.186). For cluster emission the order of magnitude for the microscopic spectroscopic factor is given by [95]

$$S_{bulk} = S_\alpha^{(a-1)/3} \ , \tag{1.197}$$

where a is the cluster mass and $S_\alpha \approx 10^{-2}$ is the α-decay microscopic spectroscopic factor (1.196).

B. Resonating Group Method (RGM)

The Resonating Group Method (RGM) is the most general many-body approach to evaluate scattering processes involving composite objects, like for instance α-scattering on nuclei. Outgoing Gamow-like solutions can be extracted in a standard way, in order to evaluate decay widths of the emission process. RGM is closely related to the Generator Coordinate Method (GCM) by an unitary transformation between the corresponding basis vectors and operators[96].

First of all we will give basic relation concerning RGM [70, 71]. The wave function of the system is given by

$$\Psi(\mathbf{R}_{12}, \mathbf{x}_1, \mathbf{x}_2) = \mathcal{A}\left[u(\mathbf{R}_{12})\Phi_1(\mathbf{x}_1)\Phi_2(\mathbf{x}_2)\right] \ , \tag{1.198}$$

where $\mathbf{R}_{12}$ is the distance between the cm of the two fragments, Φ_k the shell model wave functions of the fragments. By introducing the basis states in the coordinate representation, corresponding to the separation distance $\mathbf{R}$ between fragments

$$\langle \mathbf{r}_1, ..., \mathbf{r}_N | \mathbf{R} \rangle = \mathcal{A} \left[\delta(\mathbf{R} - \mathbf{R}_{12}) \Phi_1 \Phi_2 \right] \ , \tag{1.199}$$

the wave function (1.198) can be written as follows

$$|\Psi\rangle = \int d\mathbf{R} u(\mathbf{R}) |\mathbf{R}\rangle \ . \tag{1.200}$$

By projecting out from the stationary Schrödinger equation

$$\mathbf{H}|\Psi\rangle = E|\Psi\rangle \ , \tag{1.201}$$

a given components of the basis (1.199) one obtains the RGM integral equation

$$\int d\mathbf{R}' \left[H(\mathbf{R}, \mathbf{R}') - EN(\mathbf{R}, \mathbf{R}') \right] u(\mathbf{R}') = 0 \ , \tag{1.202}$$

where the coresponding kernels are given by

$$\begin{aligned} N(\mathbf{R}, \mathbf{R}') &\equiv \langle \mathbf{R} | \mathbf{R}' \rangle = \delta(\mathbf{R} - \mathbf{R}') - K(\mathbf{R}, \mathbf{R}') \\ H(\mathbf{R}, \mathbf{R}') &\equiv \langle \mathbf{R} | (\mathbf{H} - E_1 - E_2) | \mathbf{R}' \rangle \ . \end{aligned} \tag{1.203}$$

The RGM equation (1.202) has a similar form with the CGM equation [96], by replacing delta function with a Gaussian distribution in the basis state (1.199), i.e.

$$\langle \mathbf{r}_1, ..., \mathbf{r}_N | \mathbf{S} \rangle = \mathcal{A} \left[\Gamma(\mathbf{S} - \mathbf{R}_{12}) \Phi_1 \Phi_2 \right] \ , \tag{1.204}$$

where

$$\Gamma(\mathbf{S}, \mathbf{R}_{12}) \ = \ \left(\frac{\pi}{\beta} \right)^{3/2} exp \left[-(\mathbf{S} - \mathbf{R}_{12})^2 / (2\beta^2) \right] \ , \tag{1.205}$$

so that (1.200) becomes

$$|\Psi^{CGM}\rangle = \int d\mathbf{S} u^{CGM}(\mathbf{S}) |\mathbf{S}\rangle \ . \tag{1.206}$$

The CGM basis (1.204) has practical advantages due to the finite Gaussian distribution of the kernel (1.205). The RGM equation (1.202) can be symbolically written as follows

$$\left[\hat{H} - E(1 - \hat{K}) \right] |u\rangle = 0 \ . \tag{1.207}$$

By excluding the vanishing eigenvalues $\lambda_n = 0$ of the metric matrix

$$\left(1 - \hat{K} \right) |\psi_n\rangle = \lambda_n |\psi_n\rangle \ , \tag{1.208}$$

one obtains an equivalent standard Schrödinger equation, i.e.

$$\left(\hat{H}_\Omega - E \right) |\Omega\rangle = 0 \ , \tag{1.209}$$

where we introduced a new basis vector

$$|\Omega\rangle \equiv \left(1 - \hat{K} \right)^{\frac{1}{2}} |u\rangle \ , \tag{1.210}$$

and the transformed operator in this new basis is given by

$$\hat{H}_\Omega \equiv \left(1 - \hat{K} \right)^{\frac{1}{2}} \hat{H} \left(1 - \hat{K} \right)^{-\frac{1}{2}} \ . \tag{1.211}$$

This procedure is equivalent to the diagonalisation in a non-orthogonal basis, described in Appendix H. The advantage to work with the new basis vectors (1.210) is that they are properly normalized, i.e.

$$\langle \Omega_E | \Omega_{E'} \rangle = \delta(E - E') \ . \tag{1.212}$$

This property leds to the idea to replace in the matrix element defining the decay width, the wave function $U(\mathbf{R})$ by the properly normalized function $\Omega(\mathbf{R})$ [70]. In this way in order to keep constant the product

$$U(\mathbf{R})\mathcal{F}(R) = \Omega(\mathbf{R})\mathcal{G}(R) \ , \tag{1.213}$$

one has to replace the preformation amplitude $\mathcal{F}(R)$ (1.246) by a new one, defined as follows

$$\mathcal{G}(R) = \left(1 - \hat{K}\right)^{-\frac{1}{2}} \mathcal{F}(R) \ . \tag{1.214}$$

Anyway, the overlap kernel $1 - \hat{K}$ strongly depends upon the radius inside the nuclear volume [70], where the exchange effects are important. For this reason here is more appropriate to speak about α-coorelations than about an α-particle. For distances beyond the geometrical touching point, where Pauli effects diminish, the exchange kernel $\hat{K}$ practically vanishes and‘the two amplitudes coincide $\mathcal{G} \approx \mathcal{F}$.

C. R-matrix approach

In the R-matrix theory one also divides the space into an internal and an external region at a radius R. The fundamental ingredient of the theory is the logarithmic derivative of the internal wave function at R, i. e. $\beta_c^{(int)}(E, R)$. In the standard version of the R-matrix theory [5–7] these quantities are taken as free parameters because the microscopical evaluation of the internal solution was considered impossible in the processes thought to be of interest at that time. Nowadays one can perform that calculation in various processes. Thus, concerning for instance proton emission, in Ref. [90] the quantities β were evaluated by using a diagonalisation procedure in a spherical harmonic oscillator basis. On the other hand the preformation amplitude (1.246) in the internal region can be estimated for α and other cluster decays. Due to the fact that R-matrix theory played a central role in the microscopic theory of the α-decay and heavy custer emission we will present it in detail.

Spherical emitters

Let us first present the R-matrix theory for spherical boson emitters, like even-even α-emitters. Here the channel index is identified with the angular momentum of the relative motion $c = l$. Within the R-matrix theory one expands the internal wave function by using a *different basis* $u_l(r)$ with respect to the standard diagonalisation basis, defined only for the internal region $r \in [0, R]$. This basis is obtained by imposing the boundary condition

$$\beta_l^{(int)}(E, R) = \left[\frac{r}{f_{nl}(r)} \frac{df_{nl}(r)}{dr} \right]_{r=R} \ . \tag{1.215}$$

for all values of n.

The system of functions $f_{nl}(r)$ is orthonormal in the *finite interval* $[0, R]$, i.e.

$$\int_0^R f_{nl}^*(r) f_{n'l} dr = \delta_{nn'} \ . \tag{1.216}$$

which differs from the orthonormality condition on the infinite interval of Eq. (1.159). In this basis the internal wave function reads

$$f_l^{(int)}(E, r) = \sum_n a_n(E) f_{nl}(r) \ . \tag{1.217}$$

The difference between this expansion and the corresponding one in a harmonic oscillator basis is very small inside the nuclear volume.

By using again Eq. (1.60) for two wave functions with energies E and E_n one readily obtains the expansion coefficient as

$$a_n(E) = \int_0^R f_{nl}^*(r) f_l^{(int)}(E, r) dr = \frac{\hbar^2}{2\mu R} \frac{f_{nl}(R)}{E_n - E} \left[R \frac{df_l^{(int)}(E, R)}{dr} - f_l^{(int)}(E, R) \beta_l^{(int)}(E_n, R) \right] \ . \tag{1.218}$$

Then the internal wave function can be expressed as follows

$$f_l^{(int)}(E,r) = \mathcal{G}(r,R)\left[R\frac{df_l^{(int)}(E,R)}{dr} - f_l^{(int)}(E,R)\beta_l^{(int)}(E_n,R)\right] , \tag{1.219}$$

in terms of the Green's function

$$\mathcal{G}(r,R) = \frac{\gamma_{nl}(r)\gamma_{nl}(R)}{E_n - E} , \tag{1.220}$$

where $\gamma_{nl}(R)$ is the reduced width (1.61). This relation allows us to express the logarithmic derivative of the internal wave function at the radius R

$$\left[\frac{R}{f_l^{(int)}(E,R)}\frac{df_l^{(int)}(E,R)}{dr} - \beta_l^{(int)}(E_n,R)\right]^{-1} = \sum_n \frac{\gamma_{nl}^2(R)}{E_n - E} \equiv \mathcal{R}(R) , \tag{1.221}$$

where $\mathcal{R}$ denotes the R-matrix, which it turns out to be the Green's function for equal arguments $\mathcal{G}(R,R)$.

The external logarithmic derivative is given in term of the Coulomb-Hankel function

$$\beta_l^{(ext)}(E,R) \equiv \frac{\kappa R}{H_l^{(+)}(\chi,\kappa R)}\frac{dH_l^{(+)}(\chi,\kappa R)}{d\rho} \equiv S_l(E,R) + iP_l(E,R) . \tag{1.222}$$

where we introduced the so-called shift factor [7] and penetrability (1.55) in terms of regular and irregular Coulomb functions as follows

$$\begin{aligned} S_l(E,R) &\equiv \kappa R\frac{F_l'(\chi,\kappa R)F_l(\chi,\kappa R) + G_l'(\chi,\kappa R)G_l(\chi,\kappa R)}{F_l^2(\chi,\kappa R) + G_l^2(\chi,\kappa R)} , \\ P_l(E,R) &\equiv \frac{\kappa R}{F_l^2(\chi,\kappa R) + G_l^2(\chi,\kappa R)} . \end{aligned} \tag{1.223}$$

If the energy is close to an eigenvalue E_n one obtains from (1.221)

$$\left[\frac{r}{f_l^{(int)}(E,r)}\frac{df_l^{(int)}(E,r)}{dr}\right]_{r=R} \approx \beta_l^{(int)}(E_n,R) - \gamma_{nl}^{-2}(R)(E - E_n) , \tag{1.224}$$

which we already used in Eq. (1.56). By using the equality between the internal and external logarithmic derivative, as given by Eq. (1.222), the S-matrix becomes

$$\mathcal{S}_l \approx \overline{\mathcal{S}}_l(E)\left[1 - \frac{i\Gamma_{nl}(E,R)}{E - E_n - \Delta_{nl}(E,R) + \frac{i}{2}\Gamma_{nl}(E,R)}\right] , \tag{1.225}$$

where $\overline{\mathcal{S}}_l$ is the background contribution (1.55) and the width is given by (1.62). The energy shift is defined by

$$\Delta_{nl}(E,R) = -[S_l(E,R) - \beta_l^{(int)}(E,R)]\gamma_{nl}^2(R) . \tag{1.226}$$

At the pole of the S-matrix one gets the resonant energy $E_r = E^{(0)} - \frac{i}{2}\Gamma_r$ which should therefore satisfy the equation

$$E_r - E_n - \Delta_{nl}(E_r,R) + \frac{i}{2}\Gamma_{nl}(E_r,R) = 0 , \tag{1.227}$$

which is a nonlinear equation for the real ($E^{(0)}$) and imaginary (Γ_r) part of the energy of the Gamow state.

This procedure ensures the independence of the decay width upon the matching radius and restores the properties of the resonant states at large distances only if the dynamics is described by a potential defined for external, as well as internal regions, like is the case in proton emission. If the internal wave function is computed independently from the potential describing the extenal wave function, as is the case of the preformation amplitude, then this condition is not anymore fulfilled. this point will be discussed later.

Deformed emitters

Next we will describe the generalization of the R-matrix formalism to deformed nuclei [7]. The internal parent wave function can be expanded in term of some eigenstates

$$\Psi^{(P)} = \sum_n a_n \Psi_n^{(P)} \ , \tag{1.228}$$

where

$$\begin{aligned} \mathbf{H}\Psi_n^{(P)} &= E_n \Psi_n^{(P)} \\ \langle \Psi_n^{(P)} | \Psi_{n'}^{(P)} \rangle &= \delta_{nn'} \ . \end{aligned} \tag{1.229}$$

The coefficients a_n in Eq. (1.228) are given by

$$a_n = \langle \Psi_n^{(P)} | \Psi^{(P)} \rangle \ . \tag{1.230}$$

The parent wave function and its n-th component have a channel representation in terms of core-angular harmonics similar to Eq. (1.77), i.e.

$$\begin{aligned} \Psi^{(P)} &\to \ \sum_c \frac{f_c^{(int)}(R)}{R} \mathcal{Y}^{(c)} \\ \Psi_n^{(P)} &\to \ \sum_c \frac{f_{nc}(R)}{R} \mathcal{Y}^{(c)} \ . \end{aligned} \tag{1.231}$$

Thus, the radial components can be projected out by using the core-angular hamonics (1.78) and they can be identified with the preformation amplitude (1.246), i.e

$$\begin{aligned} \frac{f_c^{(int)}(R)}{R} &\to \ \mathcal{F}_c(R) = \langle \mathcal{Y}^{(c)} | \Psi^{(P)} \rangle \\ \frac{f_{nc}(R)}{R} &\to \ \mathcal{F}_{nc}(R) = \langle \mathcal{Y}^{(c)} | \Psi_n^{(P)} \rangle \ . \end{aligned} \tag{1.232}$$

For each channel one introduces the reduced width and its gradient

$$\begin{aligned} \gamma_{nc}(R_c) &= \sqrt{\frac{\hbar^2}{2\mu_c R_c}} f_{nc}(R_c) \\ \delta_{nc}(R_c) &= \sqrt{\frac{\hbar^2 R_c}{2\mu_c}} \left[\frac{df_{nc}(r)}{dr} \right]_{r=R_c} \ . \end{aligned} \tag{1.233}$$

One has similar definitions for $\gamma_c(R_c)$, $\delta_c(R_c)$ involving parent function $\Psi^{(P)}$. The usual condition in within the R-matrix theory is that the logarithmic derivative of the internal wavefunction component

$$\frac{\delta_{nc}(R_c)}{\gamma_{nc}(R_c)} = \beta_c^{(int)}(R_c) \ , \tag{1.234}$$

has the same value for all eigenstates n. The generalisation of the R-function (1.221) to the deformed case is straightforward. By using Schrödinger equation for two different energies

$$\mathbf{H}\Psi_1 = E_1 \Psi_1 \ , \quad \mathbf{H}\Psi_2 = E_2 \Psi_2 \ , \tag{1.235}$$

we multiply each equality at left with the other wave function conjugate, substract the equalities and integrate over the coordinates of the fragments and the internal volume. For a Hermitian potential one obtains the Green's theorem, i.e.

$$\begin{aligned} (E_2 - E_1) \int \Psi_1^* \Psi_2 d\mathbf{r} &= \frac{\hbar^2}{2\mu_c} \int_S (\Psi_2^* \nabla_S \Psi_1 - \Psi_1 \nabla_S \Psi_2^*) \, dS \\ &= \sum_c (\gamma_{2c}^* \delta_{1c} - \gamma_{1c} \delta_{2c}^*) \ , \end{aligned} \tag{1.236}$$

where the integration over the surface S we understand as an integration over fragment coordinates and relative angular variable. From (1.230), with $\Psi_1 \to \Psi^{(P)}(E, r)$ and $\Psi_2 \to \Psi_n^{(P)}(r)$, one obtains the expression of the expansion coefficients similar to Eq. (1.218), i.e.

$$a_n = \sum_c \frac{\gamma_{nc}}{E_n - E} \left[\delta_c(E) - \gamma_c(E) \beta_c^{(int)}(E_n) \right] \ , \tag{1.237}$$

where we used the expansions (1.232) and the orthogonality of core-angular harmonics. We also evidenced the energy as the argument in the above relation, except the functions with the lower index "n", which implicitely have as argument E_n. The wave function is given by

$$\Psi^{(P)}(E,r)=\sum_c\left[\sum_n\frac{\Psi_n^{(P)}(r)\gamma_{nc}(R_c)}{E_n-E}\right]\left[\delta_c(E,R_c)-\gamma_c(E,R_c)\beta_c^{(int)}(E_n,R_c)\right]\ , \tag{1.238}$$

where the function within the first brackets plays the role of the Green's function. We evidenced here the radial argument, because this relation expresses the wave function in any point r in terms of the values and derivaties at the channel surface R_c. By multiplying to left with the core-angular harmonics $\mathcal{Y}^{(c')}$ and integrating one obtains the channel reduced width

$$\gamma_{c'}(E)=\sum_c\mathcal{R}_{c'c}\left[\delta_c(E)-\gamma_c(E)\beta_c^{(int)}(E_n)\right]\ , \tag{1.239}$$

where the R-matrix is defined as follows [7]

$$\mathcal{R}_{cc'}=\sum_n\frac{\gamma_{nc'}\gamma_{nc}}{E_n-E}\ . \tag{1.240}$$

The above relation (1.239) is the analog of Eq. (1.221). One obtains the S-matrix in the one-level approximation by using the equality between internal and external logarithmic derivatives with the channel angular momentum l_c in (1.223), i.e

$$\mathcal{S}_{cc'}\approx\overline{\mathcal{S}}_{cc'}(E)\left[\delta_{cc'}-\frac{i\Gamma_{nc}^{1/2}(E,R)\Gamma_{nc'}^{1/2}(E,R)}{E-E_n-\Delta_n(E,R)+\frac{i}{2}\Gamma_n(E,R)}\right]\ , \tag{1.241}$$

where the total width and energy shift are

$$\begin{aligned}\Gamma_n(E,R)&=\sum_c\Gamma_{nc}(E,R)\ ,\\ \Delta_n(E,R)&=\sum_c\Delta_{nc}(E,R)\ ,\end{aligned} \tag{1.242}$$

with the partial quantities defined as follows

$$\begin{aligned}\Gamma_{nc}(E,R)&\equiv 2P_{l_c}(E,R)\gamma_{nc}^2(R)\ ,\\ \Delta_{nc}(E,R)&\equiv -[S_{l_c}(E,R)-\beta_c^{(int)}(E,R)]\gamma_{nc}^2(R)\ .\end{aligned} \tag{1.243}$$

The above expression of the S-matrix (1.241) is the generalisation of the spherical version, given by Eq. (1.64). The channel reduced width has the already known expression in (1.233). We introduced the partial channel shift and penetrability as a generalisation of (1.222) and (1.223)

$$\frac{\kappa R}{H_{l_c}^{(+)}(\chi,\kappa R)}\frac{dH_{l_c}^{(+)}(\chi,\kappa R)}{d\rho}\equiv S_{l_c}(E,R)+iP_{l_c}(E,R)\ . \tag{1.244}$$

As we already mentioned, in order to make the theory selfconsistent it is necessary that the product between the reduced width and penetrability in the decay width (1.243) should not depend upon the matching radius R. This is not at all a trivial operation.

In order to obtain the complex resonant energy, $E_r=E^{(0)}-\frac{i}{2}\Gamma_r$ one finds the pole of the S-matrix (1.241), i.e.

$$E_r-E_n-\Delta_n(E_r,R)+\frac{i}{2}\Gamma_n(E_r,R)=0\ , \tag{1.245}$$

By inserting the energy dependence (1.244), one obtains a nonlinear equation, giving the real $E^{(0)}$ and imaginary part Γ_r of the Gamow state energy.

D. Preformation amplitude of the α-decay

In the following we will consider the so-called α-like microscopic theories, based on the concept of the preformation probability of the light partner. This concept can be applied to the emission of particles, like protons and neutrons, or light clusters like α-particles, ^{8}Be, or ^{12,14}C and ^{16}O. The main building blocks are single particle (sp) wave functions, computed as eigenstates of the nuclear plus Coulomb mean field. For heavier clusters emission, like for instance cold fission, the α-like description becomes not tractable and the so called fission-like theories are anymore suitabe. In such theories the building block shold be also sp states, but estimated as eigenstates in the two-center representation of the mean field as for instance in Ref. [59] and the references therein.

The α-particle preformation amplitude is given as an overlap integral over the internal coordinates of the daughter nucleus and the emitted cluster [10, 11]

$$\mathcal{F}(\mathbf{R}_\alpha) = \langle \alpha D|P\rangle = \int d\mathbf{x}_\alpha d\mathbf{x}_D \left[\psi_\alpha^{(\beta_\alpha)}(\mathbf{x}_\alpha)\Psi^{(D)}(\mathbf{x}_D)\right]^* \Psi^{(P)}(\mathbf{x}_P) \ , \tag{1.246}$$

where by $\mathbf{x}$ we denoted the internal coordinates of the fragments. Therefore the final result should depend upon the relative radius between emitted fragments. We neglected the antisymmetrisation effects, because we are interested in distanced beyond the geometrical touching point, where Pauli principle diminishes. Taking into accout Eq. (1.190) the integration over daughter coordinates $\mathbf{x}_D$ can be carried out and the overlap integral becomes

$$\mathcal{F}_\alpha(\mathbf{R}_\alpha) = \int d\mathbf{x}_\alpha \psi_\alpha^*(\mathbf{x}_\alpha)\Psi_\alpha \ . \tag{1.247}$$

In order to understand the structure of the α-particle function let us transform the product of two proton and two neutron Gaussians to the center of mass (cm) system

$$\begin{aligned} e^{-\beta_\alpha r_1^2/2}e^{-\beta_\alpha r_2^2/2}e^{-\beta_\alpha r_3^2/2}e^{-\beta_\alpha r_4^2/2} &= e^{-\beta_\alpha(r_\pi^2+r_\nu^2+r_\alpha^2)/2}e^{-\beta_\alpha R_\alpha^2/2} \\ &\sim \psi_{rel}^{(\beta_\alpha)}(r_\pi, r_\nu, r_\alpha)\psi_{cm}^{(\beta_\alpha)}(R_\alpha) \ , \end{aligned} \tag{1.248}$$

where we have labelled by 1, 2 the proton and by 3, 4 the neutron coordinates. The relative and cm normalized wave functions are respectivelly given by

$$\begin{aligned} \psi_{rel}^{(\beta_\alpha)}(r_\pi, r_\nu, r_\alpha) &= \phi_{00}^{(\beta_\alpha)}(r_\pi)\phi_{00}^{(\beta_\alpha)}(r_\nu)\phi_{00}^{(\beta_\alpha)}(r_\alpha) \ , \\ \psi_{cm}^{(\beta_\alpha)}(R_\alpha) &= \phi_{00}^{(\beta_\alpha)}(R_\alpha) \ . \end{aligned} \tag{1.249}$$

Here $\phi_{nl}^{(\beta_\alpha)}$ is the radial ho wave function with the parameter $\beta_\alpha \approx 0.5 fm^{-2}$ [68]. These wave functions are written in terms of the relative and cm Moshinsky coordinates

$$\begin{pmatrix} \mathbf{r}_\pi \\ \mathbf{R}_\pi \end{pmatrix} = \frac{\mathbf{r}_1 \mp \mathbf{r}_2}{\sqrt{2}}, \quad \begin{pmatrix} \mathbf{r}_\nu \\ \mathbf{R}_\nu \end{pmatrix} = \frac{\mathbf{r}_3 \mp \mathbf{r}_4}{\sqrt{2}}, \quad \begin{pmatrix} \mathbf{r}_\alpha \\ \mathbf{R}_\alpha \end{pmatrix} = \frac{\mathbf{R}_\pi \mp \mathbf{R}_\nu}{\sqrt{2}} \ , \tag{1.250}$$

Therefore the internal α-particle wave function is written as follows

$$\psi_\alpha^{(\beta_\alpha)}(\mathbf{x}_\alpha) = \psi_{rel}^{(\beta_\alpha)}(r_\pi, r_\nu, r_\alpha)\chi_{00}^{(\pi)}(s_1, s_2)\chi_{00}^{(\nu)}(s_3, s_4) \ , \tag{1.251}$$

where we introduced spin singlet wave function

$$\chi_{00}^{(\tau)} = \left[\chi_{\frac{1}{2}}^{(\tau)} \otimes \chi_{\frac{1}{2}}^{(\tau)}\right]_{00} \ . \tag{1.252}$$

The absolute and relative volume elements are connected by the following relation

$$d\mathbf{r}_1 d\mathbf{r}_2 d\mathbf{r}_3 d\mathbf{r}_4 = 8 d\mathbf{r}_\pi d\mathbf{r}_\nu d\mathbf{r}_\alpha d\mathbf{R}_\alpha \equiv d\mathbf{x}_\alpha d\mathbf{R}_\alpha \ . \tag{1.253}$$

In the decay width

$$\Gamma = \sum_L \hbar v |N_L|^2 \ , \tag{1.254}$$

the main ingredients are the scattering amplitudes N_L, which are the coefficients of the outgoing Coulomb-Hankel waves $H_L^{(+)}$. We have shown that, by introducing the so-called external fundamental system of solutions, the scattering amplitudes are fully determined in terms of te internal wave function components, i.e.

$$N_L = \sum_{L'} \left[\mathcal{H}^{(+)}(R)\right]^{-1}_{LL'} f_{L'}^{(int)}(R) \ . \tag{1.255}$$

Partial decay widths in Eq. (1.254) contain components which should not depend upon the matching radius R. In other wordth each scattering amplitude in (1.255) should be a constant. In a phenomenological theory this condition is automatically fulfilled due to the fact that internal and external components satisfy the same equations. This becomes more clear for spherical emitters, where the scattering amplitude is the ratio between internal and external solution

$$N_L = \frac{f_L^{(int)}(R)}{H_L^{(+)}(\chi, \kappa R)} \ . \tag{1.256}$$

In a microscopic theory this statement is *a priori* not true and the check of the condition, called also *plateau condition*

$$\frac{\partial N_L}{\partial R} = 0 \ , \tag{1.257}$$

is a test of selfconsistency. To achieve it is a difficult task, but we should to understand how this goal can be achieved.

In spite of the fact that the two ho representation is able to describe the absolute values of the decay width, the shell model estimate of the α-particle preformation factor is not consistent with the decreasing behaviour of Q-values along any neutron chain [88, 89]. We consider α-decay by treating the decaying state as a resonance, namely by using the matching between logarithmic derivatives of the preformation amplitude and Coulomb function. It turns out that this condition is not satisfied along any neutron or α chain if one uses the standard shell model estimate for the preformation factor. On the other hand it is possible to correct the slope of the preformation amplitude by changing the ho parameter of single particle components [97]. Recently a similar idea was used in Ref. [98]. We will show that in order to fulfil the so-called plateau condition (1.257) it is necessary to consider the the ho parameter as being a function of the Coulomb parameter.

As we already pointed out the decay width is directly connected with the Q-value, computed as

$$E_\alpha = B(Z-2, N-2, \beta) + B(2,2,0) - B(Z,N,\beta) \ , \tag{1.258}$$

where $B(Z,N,\beta)$ is the binding energy, depending upon the charge, neutron numbers and quadrupole deformation parameter. This quantity is given by the Weizsäker type relation, like for instance in Ref. [99]

$$\begin{aligned} B(Z,N,\beta) \ &= \ a_{vol}A - a_{surf}A^{2/3} - a_{Coul}Z^2A^{-1/3} - E_{sym}(A,I) - a_{pair}A^{-1/2} \\ &\quad + E_{def}(Z,N,\beta) + E_{shell}(\beta) \ . \end{aligned} \tag{1.259}$$

Along any α-line with $I = N - Z$=const the Coulomb term has a much stronger variation versus Z (quadratic) than the other ones. Therefore the Q-value, depends linearly upon the charge number and the shell model dependence practically disapears.

It turns out that the expression of the decay width (1.254) for deformed emitters can be simplified. First of all let us point out that the major effect is given by the quadrupole deformation of the barrier [80, 100]. The monopole component of the internal wave function has the dominant role and the decay width can be approximated by

$$\Gamma(R) = \Gamma_0(R) D(R) \ , \tag{1.260}$$

where $\Gamma_0(R)$ is the standard spherical decay width

$$\Gamma_0(R) = \hbar v \left[\frac{f_0^{(int)}(R)}{G_0(\chi, \kappa R)}\right]^2 \ , \tag{1.261}$$

and the deformation function $D(R)$ is given in terms of the propagator matrix $\mathcal{K}_{cc'}(R)$. As usually by $G_0(\chi, kR)$ we denoted the monopole irregular Coulomb function, depending upon the reduced matching radius κR and the Coulomb parameter

$$\chi = 2\frac{Z_1 Z_2 e^2}{\hbar v} \ . \tag{1.262}$$

Thus, the decay width contains a ratio between the internal and external solutions. It does not depend upon the matching radius R within the local potential approach, because the internal and external wave functions satisfy the same equation and therefore are proportional. This is the so-called "plateau condition".

The situation becomes different when the value of the internal wave function $f_0^{(int)}(R)$ is given by an independent *microscopic approach*. It is replaced by the preformation amplitude (1.246). We expand sp wave functions in the ho basis, i.e.

$$\psi_{j_\tau m}(\mathbf{r}, s) = \sum_{n=0}^{n_{max}} c_{nj_\tau} \mathcal{R}_{nl}(\beta_0 r^2) \left[Y_l(\hat{r}) \otimes \chi_{\frac{1}{2}}(s) \right]_{j_\tau m} , \tau = \pi, \nu. \tag{1.263}$$

The radial ho wave function is defined in terms of the Laguerre polinomial. The sp parameter β_0 is connected with the standard ho parameter by using a scaling factor f_0 as follows

$$\beta_0 = f_0 \beta_N = f_0 \frac{M_N \omega}{\hbar} \approx \frac{f_0}{A^{1/3}} , \tag{1.264}$$

where A is the mass number. The preformation amplitude (1.246) can be written in terms of Laguerre polinomials as follows

$$\mathcal{F}_0(\beta_0, n_{max}, P_{min}; R) = e^{-4\beta_0 R^2/2} \sum_N W_N(\beta_0, n_{max}, P_{min}) \mathcal{N}_{N0}(4\beta_0) L_N^{1/2}(4\beta_0 R^2) , \tag{1.265}$$

We stress on the fact that the exponential term is similar to the cm α-particle wave function, but it depends upon the single particle ho parameter β_0. The expansion coefficients are given in terms of recoupling Talmi-Moshinsky brackets. The W-coefficients in the aboe expanssion depend upon the pairing density products $P_\tau = (j + 1/2)^{1/2} u_{\tau j} v_{\tau j}$. We consider only those values larger than the minimal value P_{min}, taken as a parameter.

The most important ingredient, governing the penetrability of the α-particle through the barrier, is the Coulomb parameter χ. The irregular Coulomb function $G_0(\chi, kR)$ depends exponentially on it

$$\begin{aligned} G_0(\chi, kR) &= (ctg\ \alpha)^{1/2}\ e^{\chi(\alpha - sin\ \alpha\ cos\ \alpha)}, \\ \cos^2\ \alpha &= \frac{kR}{\chi} = \frac{R}{R_0} , \quad R_0 = \frac{Z_1 Z_2 e^2}{E_\alpha} . \end{aligned} \tag{1.266}$$

The decay width has also an exponential dependence upon the quadrupole deformation. As it was shown in Ref. [102] the function $D(R)$ in Eq. (1.260) practically does not depend upon the radius. The largest correction gives a factor of three for heavy nuclei and a factor of five in superheavy ones.

The preformation amplitude, given by Eq. (1.265), is very collective and therefore the transitions between ground states are not sensitive to the mean field parameters. Thus, in our analysis we used the universal parametrisation of the Woods-Saxon potential [101] and we considered the gap parameter estimated by $\Delta_\tau = 12/\sqrt{A}$ [103], where A is the mass number of the mother nucleus. The quadrupole deformation parameters in the Fröman matrix are taken from Ref. [104].

The preformation factor is very sensitive with respect to the maximal sp radial quantum number n_{max}, the sp ho parameter β_0 and the amount of spherical configurations taken in the BCS calculation, given by $P_{min} = min\{P_\tau\}$. It turns out that beyond $n_{max} = 9$ the results saturate if one considers in the BCS basis sp states with $P \geq P_{min} = 0.02$. We improved the description of the continuum by choosing a sp scale parameter $f_0 < 1$ in Eq. (1.264). This parameter is not independent from P_{min}. It turns out that the common choice of f_0 and P_{min} ensures not only the right order of magnitude for the decay width, but also the above mentioned continuity of the derivative.

The logarithm of the decay width can be approximated by the following linear ansatz

$$log_{10} \left[\frac{\Gamma(R)}{\Gamma_{exp}} \right] = \gamma_0 + \gamma_1 R . \tag{1.267}$$

In the ideal case the coefficients should vanish, i.e. $\gamma_0 = \gamma_1 = 0$, in order to have a proper description of the decay width. The sensitivity of these parameters versus the Q-value is shown in figure 12. The plateau condition (1.257) can also be written as follows

$$\gamma_1(\chi) = 0 , \tag{1.268}$$

for given parameters $n_{max}, \beta_0, P_{min}$.

We analysed α-decay chains from even-even nuclei with $N > 126$, given in the Table I.

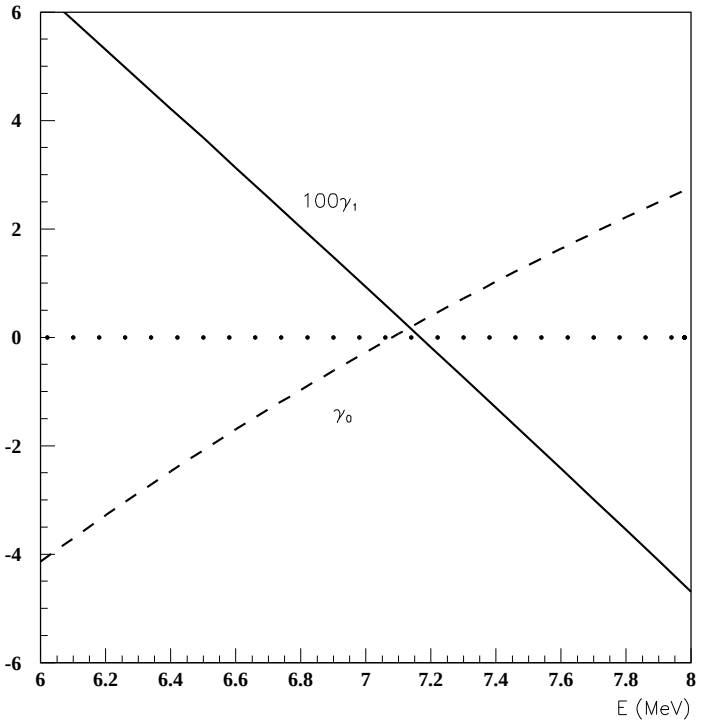

FIG. 12: *The slope parameter* $100\gamma_1$ *(solid line) and the ratio parameter* γ_0 *(dashed line) in (1.267) versus the* α*-particle energy for* $^{200}Rn \rightarrow^{196} Po + \alpha$.

TABLE I: *Even-even* α*-decay chains in the region* $Z > 82,\ N > 126$. *In the first column of each table is given the isospin projection* $I = N - Z$. *In the next columns are given the initial neutron and proton numbers, the number of states/chain and the reference.*

I	N_1	Z_1	No	Ref.
38	130	92	1	[27]
40	130	90	2	[27]
42	130	88	3	[27]
44	130	86	6	[27]
46	132	86	8	[27]
48	134	86	12	[27]
50	136	86	9	[27]
52	142	90	7	[27]
54	146	92	5	[27]
56	150	94	4	[27]
58	154	94	2	[27]
60	172	112	3	[105]

It turns out that the values $n_{max} = 9$, f_0=0.8 and P_{min}=0.025 give the best fit concerning the parameters γ_0 and γ_1. From Fig. 13 (a) we see that the quantity $\gamma_0 \approx log_{10}(\Gamma/\Gamma_{exp})$ has a variation of one order of magnitude around $\gamma_0 = 0$, but the description of the slope γ_1, given in Fig. 13 (b), is by far not satisfactory. The reason for the variation of the slope parameter γ_1 is the relative strong dependence of the Coulomb parameter χ upon the neutron number along α-chains. In Fig. 13 (c) we give the values of this parameter for the even-even chains, which is in an obvious correlation with the slope parameter γ_1. Therefore the derivative of the microscopic preformation amplitude changes along α-chains much slower in comparison with that of the

TABLE II: *Even-even α-decay chains in the region $Z > 82,\ 82 < N < 126$. The quantities are the same as in Table I.*

I	N_1	Z_1	No	Ref.
28	114	86	1	[27]
30	116	86	2	[27]
32	118	86	3	[27]
34	120	86	3	[27]
36	122	86	2	[27]
38	124	86	1	[27]

Coulomb function. As we pointed out the term given by the shell correction desapears in the Q-value (except the magic numbers) and it remains a linear in Z dependence. Thus, indeed the most important effect is given by the Coulomb repulsion. In order to stress on this dependence we performed the same analysis in the region $Z > 82,\ 82 < N < 126$, given in the Table II.

In Figs. 14 (a),(b) we plotted the parameters $\gamma_0,\ \gamma_1$ depending upon the neutron number. We used the same parameters, i.e. $n_{max} = 9$, f_0=0.8, P_{min}=0.025. One can see that indeed their values are very close to zero. The decay widths are reproduced within a factor of two. We point out the small decrease of parameters along considered α-chains is correlated with a similar behaviour of the Coulomb parameter χ in Fig. 14 (c).

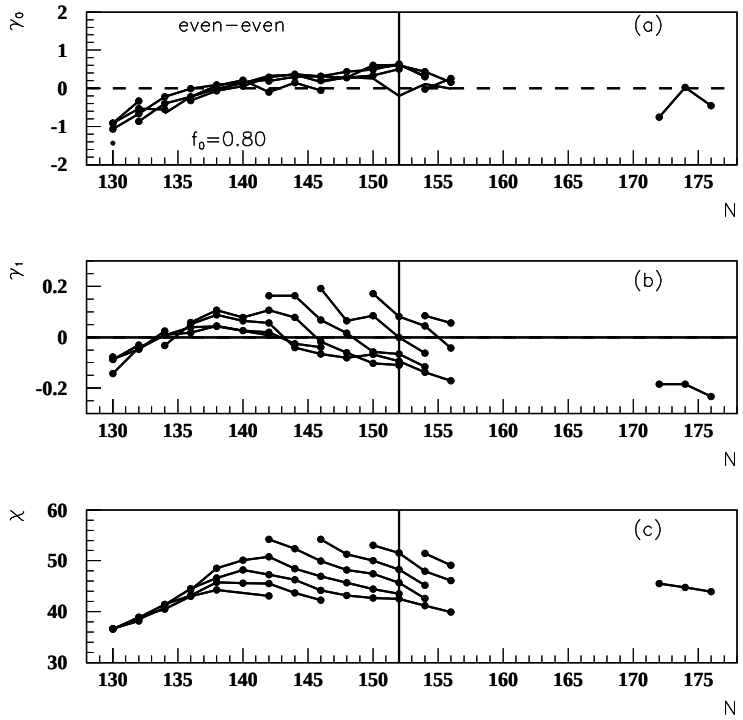

FIG. 13: (a) The ratio parameter γ_0, defined by Eq. (1.267), versus the neutron number for $f_0 = 0.8,\ P_{min} = 0.025$ and different even-even α-chains in Table I. (b) The slope parameter γ_1, defined by Eq. (1.267), versus the neutron number. (c) The Coulomb parameter χ, defined by Eq. (1.262), versus the neutron number.

Our estimate shows that the linear correlation coefficient between γ_1 and χ is larger than 0.7. This allows us to introduce a supplementary, but universal, correcting procedure for the preformation factor. Thus, let us define a variable size parameter f by a similar to (1.264) relation, namely

$$\beta = f\beta_N\ . \tag{1.269}$$

The parameter χ enters in the exponent of the Coulomb function (1.266). This fact suggests a similar correction of the preformation factor, i.e.

$$\overline{\mathcal{F}}_0(\beta,\beta_m,n_{max},P_{min};R)=e^{-4\beta R^2/2}\sum_N W_N(\beta_m,n_{max},P_{min})\mathcal{N}_{N0}(4\beta_m)L_{N0}^{(1/2)}(4\beta_m R^2)\ . \tag{1.270}$$

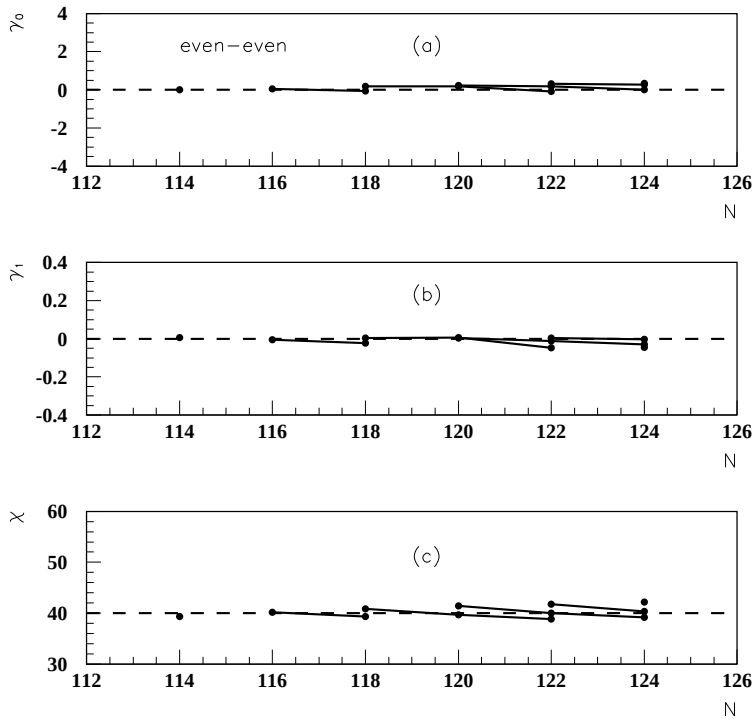

FIG. 14: (a) The ratio parameter γ_0, defined by Eq. (1.267), versus the neutron number for $f_0=0.8$, $P_{min}=0.025$ and different even-even α-chains in Table II. (b) The slope parameter γ_1, defined by Eq. (1.267), versus the neutron number. (c) The Coulomb parameter χ, defined by Eq. (1.262), versus the neutron number.

We suppose a linear dependence of the size parameter f upon the Coulomb parameter

$$\beta-\beta_m=(f-f_m)\beta_N=f_1(\chi-\chi_m)\beta_N\ . \tag{1.271}$$

The above relation (1.270) can be written as follows

$$\begin{aligned}\overline{\mathcal{F}}_0(\beta,\beta_m,n_{max},P_{min};R) &= e^{-4(\beta-\beta_m)R^2/2}\quad \mathcal{F}_0(\beta_m,n_{max},P_{min};R)\\ &= \mathcal{F}_0(\beta-\beta_m,0,0;R)\mathcal{F}_0(\beta_m,n_{max},P_{min};R)\ ,\end{aligned} \tag{1.272}$$

i.e. the usual preformation amplitude is multiplied by a cluster preformation amplitude with $n_{max}=0$. Thus, one has to multiply the right hand side of the expansion (1.265) by this factor.

In our calculations we used the parameters $f_m=0.83$, $\chi_m=55$. For the proportionality coefficient in Eq. (1.271) the regression analysis gives the value $f_1=8.0\ 10^{-4}$. The situation in the superheavy chain can be described by assuming a quadratic dependence of the coefficient f_1 upon the number of clusters $N_\alpha=(N-N_0)/2$ with $N_0=126$, namely

$$f_1\to f_1+f_2N_\alpha^2\ . \tag{1.273}$$

A quadratic in N_α dependence of the Q-value was also empirically found in Ref. [91]. The final results are given in Figs. 15 (a), (b). We considered a correcting term with $f_2=1.28\ 10^{-6}$. The improvement of the slope parameter is obvious. The mean value of this parameter and its standard deviation for even-even chains is $\gamma_1=-0.001\pm\ 0.034$.

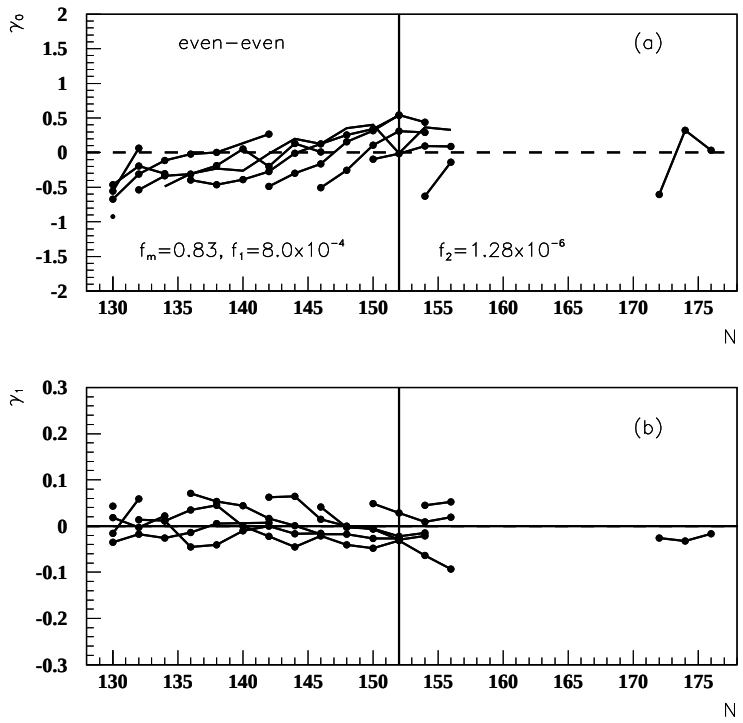

FIG. 15: (a) The parameter γ_0 versus the neutron number for different even-even α-chains in Table I. The preformation parameters are $f_m = 0.83,\ f_1 = 8.0\ 10^{-4},\ f_2 = 1.28\ 10^{-6}$, $P_{min} = 0.025$. (b) The same as in (a), but for the slope parameter γ_1.

The quadratic dependence in Eq. (1.273) can be also interpreted in terms of the total number of interacting clustering pairs, namely $N_\alpha^2 \approx 2N_\alpha(N_\alpha - 1)/2$ [91]. Thus, our analysis based on the logarithmic derivative continuity, shows very clearly that the effect of the α-clusterisation becomes much stronger for superheavy nuclei. We mention here that the effect of proton-neutron correlations on the α-decay rate was also evidenced by using the experimental double difference of binding energies [106]. The even-odd pair staggering of binding energies along α-lines was interpreted in Ref. [92] as an α-condensate of proton and neutron boson pairs, similar to the usual pairing condensate among protons or neutrons.

The microscopic spectroscopic factor S_{gs} is plotted in Fig. 11 versus the neutron number. In the regin with $Z < 82$ the values are comparable with those given by the phenomenological spectroscopic factor S given by Eq. (1.185), as can be seen in Fig. 10. This means that the α-clustering in this region can be fully described within the pairing model. On the other hand in the region $Z > 82$ the values of the microscopic epctroscopic factor S_{gs} are smaller. From Fig. 10 one cleary see that here the ratio $S/S_{gs} >> 1$ and indeed an additional α-clustering is necessary.

Appendix A
Single particle mean field

The single particle deformed potential in the intrinsic system, defined by the major axes of the nuclear ellipsoid, has the following general form

$$V(\mathbf{r},\mathbf{s}) = V_0(\mathbf{r}) + V_{so}(\mathbf{r},\mathbf{s}) \ , \tag{A.1}$$

where we denote by $\mathbf{r}$ intrinsic coordinates and V_0 is the central part of the interaction, containing the nuclear and proton Coulomb interaction

$$V_0(\mathbf{r}) = V_N(\mathbf{r}) + V_C(\mathbf{r}) \ . \tag{A.2}$$

Nuclear potential

The nuclear part of the interaction is given by

$$V_N(\mathbf{r}) = -V_N^{(0)} f(\mathbf{r}, r_{0c}, a_c) \ , \tag{A.3}$$

with a Woods-Saxon formfactor defined as the Fermi distribution

$$f(\mathbf{r}, r_0, a) \ = \ \frac{1}{1 + exp\left[\frac{r-R(\hat{r})}{a}\right]} \ , \tag{A.4}$$

where $\hat{r} \equiv (\theta, \phi)$ and the radius $R(\hat{r})$ of the nuclear surface is given by

$$R(\hat{r}) = cR_0 \left[1 + \sum_{\lambda\geq 2\mu} \beta_{\lambda\mu} Y_{\lambda\mu}(\hat{r})\right] \ , \quad R_0 = r_0 A_d^{1/3} \ . \tag{A.5}$$

The constant c is determined by the volume conservation condition

$$c^{-3} \ = \ \int \left[1 + \sum_{\lambda\mu} \beta_{\lambda\mu} Y_{\lambda\mu}(\hat{r})\right]^3 \frac{d\hat{r}}{4\pi} \ . \tag{A.6}$$

The most important quadrupole

$$\beta_{20} \ = \ \beta_2 cos\gamma \ , \quad \beta_{2\pm 2} = \beta_2 \frac{sin\gamma}{\sqrt{2}} \ , \tag{A.7}$$

and hexadecapole deformation parameters

$$\beta_{40} \ = \ \frac{1}{6}\beta_4 \left(5cos^2\gamma + 1\right) \ , \quad \beta_{4\pm 2} = \frac{\sqrt{30}}{12}\beta_4 sin2\gamma \ , \quad \beta_{4\pm 4} = \frac{\sqrt{70}}{12}\beta_4 sin^2\gamma \ . \tag{A.8}$$

The expansion of the nuclear potential

$$V_N(\mathbf{r}) \ = \ V_N(r) + \sum_{\lambda>0,\mu} V_{N,\lambda\mu}(r) Y_{\lambda\mu}(\hat{r}) \ , \tag{A.9}$$

where

$$V_{N,\lambda\mu}(r) \ \equiv \ -V_N^{(0)} f_{\lambda\mu}(r) \ , \tag{A.10}$$

contains the multipoles of the Fermi distribution defined by following expansion

$$f(r, \hat{r}, r_0, a) \ = \ \sum_{\lambda\mu} f_{\lambda\mu}(r, r_0, a) Y_{\lambda\mu}(\hat{r}) \ . \tag{A.11}$$

The coefficients are given by the inverse transformation

$$f_{\lambda\mu}(r, r_0, a) \ = \ \int Y^*_{\lambda\mu}(\hat{r}) f(\mathbf{r}, r_0, a) d\hat{r} \ . \tag{A.12}$$

The axially spherical symmetry corresponds to vanishing angles $\gamma = 0$ and therefore one has $\mu = 0$. All above relations become simpler by doing the replacement

$$d\hat{r} \ = \ 2\pi dt \ , \quad t \equiv cos\ \theta \ . \tag{A.13}$$

Coulomb potential

The Coulomb potential between a distributed charge $Z_D e$, inside the deformed surface (A.5), and a proton charge e is given by

$$V_C(\mathbf{r}) = \int \frac{\rho(\mathbf{r}')}{|\mathbf{r}-\mathbf{r}'|} d\mathbf{r}' \ , \tag{A.14}$$

where the charge density is

$$\rho(\mathbf{r}') = Z_D e^2 N f(\mathbf{r}', r_{0c}, a_c) \ . \tag{A.15}$$

The inverse of the normalisation constant

$$N^{-1} = \int f(\mathbf{r}', r_{0c}, a_c) d\mathbf{r}' = \sqrt{4\pi} \int_0^\infty f_{00}(r') r'^2 dr' \ , \tag{A.16}$$

is rather close to the geometric volume $4\pi R_{0c}^3/3$. By using an expansion of the density in multipoles

$$\rho(\mathbf{r}') = Z_D e^2 \sum_{\lambda\mu} \rho_{\lambda\mu}(r') Y_{\lambda\mu}(\hat{r}') \ , \tag{A.17}$$

and the well-known relation

$$\frac{1}{|\mathbf{r}-\mathbf{r}'|} = \sum_{\lambda\mu} \frac{4\pi}{2l+1} \frac{r_<^l}{r_>^{l+1}} Y_{\lambda\mu}(\hat{r}) Y^*_{\lambda\mu}(\hat{r}') \ , \tag{A.18}$$

where $r_< = min(r, r'),\ r_> = max(r, r')$, the multipole expansion of the Coulomb potential becomes

$$V_C(\mathbf{r}) = \sum_{\lambda\mu} \left[Z_D e^2 \frac{4\pi}{2\lambda+1} \int_0^\infty \rho_{\lambda\mu}(r') \frac{r_<^\lambda}{r_>^{\lambda+1}} r'^2 dr' \right] Y_{\lambda\mu}(\hat{r}) \equiv \sum_{\lambda\mu} V_{C\lambda\mu}(r) Y_{\lambda\mu}(\hat{r}) \ . \tag{A.19}$$

At large distances $r >> R(\hat{r}')$, where the density has vanishing values, one obtains

$$V_C(\mathbf{r}) \approx e \sum_{\lambda\mu} \frac{1}{r^{\lambda+1}} \left[Z_D e \frac{4\pi}{2\lambda+1} \int_0^\infty \rho_{\lambda\mu}(r') r'^{\lambda+2} dr' \right] Y_{\lambda\mu}(\hat{r}) \equiv e \sum_{\lambda\mu} \frac{Q_{\lambda\mu}}{r^{\lambda+1}} Y_{\lambda\mu}(\hat{r}), \tag{A.20}$$

where $Q_{\lambda\mu}$ denotes the intrinsic multipole moment.

Notice that the role of the difusivity a_c in the density distribution is rather week. The replacement of the Fermi distribution by a sharp one

$$\rho(\mathbf{r}, r_{0c}, 0) = \frac{3 Z_D e^2}{4\pi R_{oc}^3} \Theta[R(\hat{r}) - r] \ , \tag{A.21}$$

gives an error less that 5% in the internal region and practically leads to the same results for large distances. In particular the Coulomb potential of an uniformly charged sphere is given by

$$V_C(r) = \begin{array}{c} \frac{Z_D e^2}{2R_{0c}} \left(3 - \frac{r^2}{R_{0c}^2}\right) \ , \quad r \le R_{0c} \\ \\ \frac{Z_D e^2}{r} \ , \quad r > R_{0c} \end{array} \ . \tag{A.22}$$

Spin-orbit potential

Spherical symmetric interaction is obtained when $\beta_2 = \beta_4 = 0$ in Eq. (A.7). In this case the spin-orbit potential is given by the ansatz

$$V_{so}(r,\mathbf{s}) = -V_{so}^{(0)}\frac{1}{r}\frac{df(r,r_{0so},a_{so})}{dr}\ \mathbf{l}.\sigma \equiv V_{so}(r)\mathbf{l}.\sigma\ , \quad \sigma = 2\mathbf{s}\ , \tag{A.22}$$

where

$$V_{so}^{(0)} \equiv -\Lambda\left(\frac{\hbar c}{2Mc^2}\right)^2 \overline{V}_{so}^{(0)}\ . \tag{A.23}$$

The spherical spin-orbit interaction can be written in an invariant form by using the momentum operator $\hat{\mathbf{k}} = -i\nabla$

$$\frac{1}{r}\frac{df(r)}{dr}\mathbf{l}.\sigma\ =\ \frac{1}{r}\frac{df(r)}{dr}[\mathbf{r}\times\hat{\mathbf{k}}].\sigma = \frac{df(r)}{dr}\frac{\mathbf{r}}{r}.[\hat{\mathbf{k}}\times\sigma]\ , \tag{A.24}$$

or, by using ciclic permutation

$$\frac{1}{r}\frac{df(r)}{dr}\mathbf{l}.\sigma\ =\ \nabla f(\mathbf{r}).[-\mathbf{i}\nabla\times\sigma]\ . \tag{A.25}$$

Therefore the deformed spin-orbit interaction and its multipole expansion is given by

$$V_{so}(\mathbf{r},\mathbf{s}) = -V_{so}^{(0)}\nabla f(\mathbf{r},r_{0so},a_{so}).[-\mathbf{i}\nabla\times\sigma]\ ,= -V_{so}^{(0)}\sum_{\lambda\mu}\nabla[f_{\lambda\mu}(r,r_{0so},a_{so})Y_{\lambda\mu}].[-i\nabla\times\sigma]\ . \tag{A.26}$$

The gradient theorem allows one to write

$$\nabla\left[f(r)Y_{\lambda\mu}(\hat{r})\right]\ =\ \partial_{\lambda-1}f(r)\mathbf{Y}_{\lambda\mu}^{(\lambda-1)}(\hat{r}) + \partial_{\lambda+1}f(r)\mathbf{Y}_{\lambda\mu}^{(\lambda+1)}(\hat{r})\ , \tag{A.27}$$

where we introduced the vectorial harmonics

$$\mathbf{Y}_{\lambda\mu}^{(\lambda\pm1)}(\hat{r}) = [Y_{\lambda\pm1}(\hat{r})\mathbf{e}]_{\lambda\mu}\ , \tag{A.28}$$

With the differential operators written as

$$\partial_{\lambda-1} \equiv \sqrt{\frac{\lambda}{2\lambda+1}}\left(\frac{d}{dr}+\frac{\lambda+1}{r}\right)\ , \quad \partial_{\lambda+1} \equiv -\sqrt{\frac{\lambda+1}{2\lambda+1}}\left(\frac{d}{dr}-\frac{\lambda}{r}\right)\ . \tag{A.29}$$

and with

$$\mathbf{Y}_{\lambda\mu}^{(\lambda\pm1)}(\hat{r}).\mathbf{A} = [Y_{\lambda\pm1}(\hat{r})\mathbf{A}]_{\lambda\mu}\ , \tag{A.30}$$

where $\mathbf{A}$ is a vector, one obtains the multipole component of the spin-orbit interaction

$$\nabla[f_{\lambda\mu}(r)Y_{\lambda\mu}(\hat{r})].[-i\nabla\times\sigma]\ =\ \left[\partial_{\lambda-1}f_{\lambda\mu}(r)T_{\lambda\mu}^{(\lambda-1)}(\hat{r},\sigma) + \partial_{\lambda+1}f_{\lambda\mu}(r)T_{\lambda\mu}^{(\lambda+1)}(\hat{r},\sigma)\right]\ , \tag{A.31}$$

in terms of the following differential spin-orbit operators

$$T_{\lambda\mu}^{(\lambda\pm1)}(\hat{r},\sigma)\ \equiv\ [Y_{\lambda\pm1}(\hat{r})(-i\nabla\times\sigma)]_{\lambda\mu}\ . \tag{A.32}$$

Thus, the expanssion in multipoles of the spin-orbit potential is given by

$$V_{so}(\mathbf{r},\mathbf{s})\ =\ V_{so}(r)\mathbf{l}.\sigma + \sum_{\lambda>0,\mu}\left[V_{so,\lambda\mu}^{(\lambda+1)}(r)T_{\lambda\mu}^{(\lambda+1)}(\hat{r},\sigma) + V_{so,\lambda\mu}^{(\lambda-1)}(r)T_{\lambda\mu}^{(\lambda-1)}(\hat{r},\sigma)\right]\ , \tag{A.33}$$

where

$$V_{so,\lambda\mu}^{(\lambda\pm1)}(r)\ \equiv\ -V_{so}^{(0)}\partial_{\lambda\pm1}f_{\lambda\mu}(r,r_{0so},a_{so})\ . \tag{A.34}$$

The so-called universal parameters [107, 108] for both proton and neutron mean fields are given respectivelly by

$$V_N^{(0)} = \overline{V}_{so}^{(0)} = 49.6 \left(1 + \chi_\tau \frac{N-Z}{N+Z}\right) \quad (MeV), \quad \chi_{p,n} = \pm 0.86 \ , \tag{A.35}$$

where

$$r_{0c}(p) = 1.275 \ (fm), \quad r_{0c}(n) = 1.347 \ (fm) \ ,$$

$$r_{0so}(p) = 1.320 \ (fm), \quad r_{0so}(n) = 1.310 \ (fm) \ ,$$

$$a_c(p) = 0.70 \ (fm), \quad a_{so}(n) = 0.70 \ (fm) \ ,$$

$$\Lambda_p = 36.0 \ (MeV), \quad \Lambda_n = 35.0 \ (MeV) \ .$$

Appendix B
WKB for Coulomb functions

The WKB solution for the radial equation

$$\left[-\frac{d^2}{d\rho^2}+\frac{V_l(\rho)}{E}-1\right]f_l(r)=0$$
$$\frac{V_l(\rho)}{E}=\frac{l(l+1)}{\rho^2}+\frac{\rho}{\chi}\ , \tag{B.0}$$

where the Coulomb parameter χ is defined by (1.85), has the following form

$$\begin{aligned} H_l^{(\pm)}(\rho) &= \left(\frac{V_l}{E}-1\right)^{-1/4} exp\left[\pm\int_\rho^{\rho_3}\left(\frac{V_l}{E}-1\right)^{1/2}d\rho\right]\ , \quad \frac{V_l}{E}>1 \\ &= \left(1-\frac{V_l}{E}\right)^{-1/4} exp\left[\pm\int_\rho^{\rho_3}\left(1-\frac{V_l}{E}\right)^{1/2}d\rho\right]\ , \quad \frac{V_l}{E}<1\ , \end{aligned} \tag{B.0}$$

where we dropped the argument χ. We defined the turning points as the solutions $\rho_1<\rho_2<\rho_3$ of the equation

$$\frac{V_l(\rho)}{E}-1=0\ . \tag{B.1}$$

The WKB solution approximation is valid if the condition

$$\left|\frac{d}{d\rho}\left|\frac{V_l}{E}-1\right|^{-1/2}\right|<<1\ , \tag{B.2}$$

is fulfilled. In particular for V_l^C is the Coulomb plus centrifugal term. Apart from small regions around these points one obtains good analytical WKB estimates in the case of large Coulomb barriers. Let us concentrate upon the decay (outgoing) solution $H^{(+)}(\rho)$.

A) For the *internal region*

$$cos^2\ \alpha\equiv\frac{\rho}{\chi}=\frac{E}{V_0}<1\ , \tag{B.3}$$

One has the following solution

$$\begin{aligned} H_l^{(+)}(\rho) &\approx (ctg\ \alpha)^{1/2}\, exp\left[\chi\left(\alpha-sin\ \alpha\ cos\ \alpha\right)\right] C_l \\ C_l &\equiv exp\left[\frac{l(l+1)}{\chi}\sqrt{\frac{\chi}{\rho}-1}\right]\ , \end{aligned} \tag{B.3}$$

under the condition

$$2\chi sin^3\ \alpha\ cos\ \alpha>>1\ . \tag{B.4}$$

Inside a large Coulomb barrier the outgoing Coulomb wave practically coincides with the irregular function

$$H_l^{(+)}(\rho)\ \approx\ G_l(\rho)\ , \quad \frac{E}{V_0(\rho)}<<1\ . \tag{B.5}$$

B) For the *external region*

$$ch^2\ a\equiv\frac{\rho}{\chi}=\frac{E}{V_0}>1\ , \tag{B.6}$$

one obtains the following oscillating solution

$$H_l^{(+)}(\rho)\ \rightarrow\ _{\rho\rightarrow\infty} exp\left[i\chi\left(sh\ a\ ch\ a-a\right)+i\frac{\pi}{4}\right] exp\left[-i\frac{l(l+1)}{\chi}\right]\ , \tag{B.7}$$

which can be written as follows

$$H_l^{(+)}(\rho) \;=\; cos\;(\phi_0 - \phi_l) + i\;sin\;(\phi_0 - \phi_l)\;, \tag{B.8}$$

in terms of the phases, defined respectivelly by

$$\phi_0 = \chi\,(sh\;a\;ch\;a - a) + \frac{\pi}{4}\;, \quad \phi_l = \frac{l(l+1)}{\chi}\;. \tag{B.9}$$

The WKB condition is similar, i.e.

$$2\chi sh^3\;a\;ch\;a >> 1\;. \tag{B.10}$$

The WKB approximation for most decay processes gives very close values with respect to the exact Coulomb function.

Appendix C
Rotations

In order to avoid any confusion connected with conventions we we will give here the Wigner rotation functions used in this review. For this, we consider the wave function $|JM\rangle$ with angular momentum J and projection M in the laboratory system of coordinates. One can "rotate" this wave function in the intrinsic system of coordinates according to

$$\hat{R}(\omega)|JM\rangle = \sum_{M'} |JM'\rangle\langle JM'|\hat{R}(\omega)|JM\rangle \ . \tag{C.1}$$

By introducing the coordinate representation of the wave function

$$\psi_{JM}(\mathbf{r}) = \langle \mathbf{r}|JM\rangle \ , \tag{C.2}$$

and by denoting the rotation (Wigner) matrix in the Rose convention

$$D^J_{M'M}(\omega) \equiv \langle JM'|\hat{R}(\omega)|JM\rangle \ , \tag{C.3}$$

one obtains that

$$\hat{R}(\omega)\psi_{JM}(\mathbf{r}) = \sum_{M'} D^J_{M'M}(\omega)\psi_{JM'}(\mathbf{r}) = \psi_{JM}(\mathbf{r'}) \ . \tag{C.4}$$

The most important properties of the rotation matrix are

$$\sum_M D^J_{MM_1}(\omega)D^{J*}_{MM_2}(\omega) \ = \ \sum_M D^J_{M_1M}(\omega)D^{J*}_{M_2M}(\omega) = \delta_{M_1M_2} \ , \tag{C.5}$$

$$\sum_K D^J_{MK}(\omega)D^J_{KM'}(\omega') \ = \ D^J_{MM'}(\omega\omega') \ . \tag{C.6}$$

$$D^{J*}_{MM'}(\omega) \ = \ (-)^{M-M'} D^J_{-M-M'}(\omega) \ , \tag{C.7}$$

$$D^J_{MM'}(\omega^{-1}) \ = \ D^{J*}_{M'M}(\omega) \ . \tag{C.8}$$

By using the first relation one can invert the rotation (C.4)

$$\hat{R}(\omega^{-1})\psi_{JM}(\mathbf{r'}) = \sum_{M'} D^{J*}_{MM'}(\omega)\psi_{JM'}(\mathbf{r'}) = \psi_{JM}(\mathbf{r}) \ . \tag{C.9}$$

one gets the well known factorisation in terms of Euler angles $\omega = (\phi, \theta, \psi)$

$$D^J_{MK}(\phi,\theta,\psi) = e^{-iM\phi} d^J_{MK}(\theta) e^{-iK\psi} \ . \tag{C.10}$$

The rotation matrix

$$\mathcal{D}^J_{MK}(\omega) = \sqrt{\frac{2J+1}{8\pi^2}} D^J_{MK}(\omega) \ . \tag{C.11}$$

is normalized to unity

$$\int \mathcal{D}^{J*}_{MK}(\omega)\mathcal{D}^{J'}_{M'K'}(\omega)d\omega = \delta_{JJ'}\delta_{MM'}\delta_{KK'} \ . \tag{C.12}$$

In the Rose representation the eigenfunction of the angular momentum squared is given by $\mathcal{D}^{J*}_{MK}(\omega)$. Denoting the laboratory third axis z and the intinsic similar axis ζ one has

$$\mathbf{J}^2\mathcal{D}^{J*}_{MK}(\omega) \ = \ J(J+1)\mathcal{D}^{J*}_{MK}(\omega) \ , \tag{C.13}$$

$$\mathbf{J}_z\mathcal{D}^{J*}_{MK}(\omega) \ = \ M\mathcal{D}^{J*}_{MK}(\omega) \ , \tag{C.14}$$

$$\mathbf{J}_\zeta\mathcal{D}^{J*}_{MK}(\omega) \ = \ K\mathcal{D}^{J*}_{MK}(\omega) \ . \tag{C.15}$$

Some particular values of projections are important

$$D^l_{m0}(\phi,\theta,\psi) \;=\; \sqrt{\frac{4\pi}{2l+1}}Y^*_{lm}(\theta,\phi)\ , \tag{C.16}$$

$$D^l_{0m}(\phi,\theta,\psi) \;=\; (-)^m\sqrt{\frac{4\pi}{2l+1}}Y^*_{lm}(\theta,\psi)\ , \tag{C.17}$$

$$D^l_{00}(0,\theta,0) \;=\; P_l(cos\ \theta)\ . \tag{C.18}$$

The product of two rotation D-functions can be expressed in terms of the sum over single D-functions as

$$D^{J_1}_{M_1K_1}(\omega)D^{J_2}_{M_2K_2}(\omega) = \sum_{J=|J_1-J_2|}^{J_1+J_2}\langle J_1M_1;J_2M_2|JM\rangle\langle J_1K_1;J_2K_2|JK\rangle D^J_{MK}(\omega)\ , \tag{C.19}$$

For the orbital harmonics Y_{lm} this relation gives

$$Y^*_{lm}(\hat r)Y_{l'm'}(\hat r) \;=\; (-)^m\sum_{L=|l-l'|}^{l+l'}\frac{\hat l\hat l'}{\sqrt{4\pi}\hat L}\langle l,0;l'0|L,0\rangle\langle l,-m;l'm'|LM\rangle Y_{LM}(\hat r)\ . \tag{C.20}$$

The spin-orbital harmonics

$$\mathcal{Y}^{(ls)}_{jm}(\hat r,\mathbf{s}) \equiv \langle\hat r,\mathbf{s}|ljm\rangle\ , \tag{C.21}$$

defined as

$$\mathcal{Y}^{(ls)}_{jm}(\hat r,\mathbf{s}) = \left[i^lY_l(\hat r)\otimes\chi_s(\mathbf{s})\right]_{jm} = \sum_{m_1+m_2=m}\langle lm_1;sm_2|jm\rangle i^lY_{lm_1}(\hat r)\chi_{sm_2}(\mathbf{s})\ . \tag{C.22}$$

describe the angular behaviour of a fermion in the static nuclear field. By considering the orthonormality of spin functions

$$\chi^\dagger_{s,m}\chi_{s,m'} = \delta_{mm'}\ , \tag{C.23}$$

one obtains a relation similar to (C.20)

$$\mathcal{Y}^{(ls)\dagger}_{jm}(\hat r,\mathbf{s})\mathcal{Y}^{(l's)}_{j'm'}(\hat r,\mathbf{s}) \;=\; (-)^{m+\frac{1+l'-l}{2}}\sum_{L=|l-l'|}^{l+l'}\frac{\hat j\hat j'}{\sqrt{4\pi}\hat L}\langle j,s;j',-s|L,0\rangle\langle l,-m;l'm'|LM\rangle Y_{LM}(\hat r)\ . \tag{C.24}$$

Appendix D
Spherical oscillator

The Schrödinger equation for the ho potential

$$\hbar\omega\left[-\frac{\Delta^2}{2\beta}+\frac{\beta r^2}{2}\right]\phi^{(\beta)}_{nlm}(\mathbf{r})=E_N\phi^{(\beta)}_{nlm}(\mathbf{r})\ , \tag{D.1}$$

where we introduced the ho parameter

$$\beta=\frac{M\omega}{\hbar}\ , \tag{D.2}$$

has the eigenstates given by

$$\begin{aligned}\phi^{(\beta)}_{nlm}(\mathbf{r}) &= \mathcal{R}^{(\beta)}_{nl}(r)Y_{lm}(\hat{r})\ ,\\ \mathcal{R}^{(\beta)}_{nl}(r) &= (-)^n\left[\frac{2\beta^{l+3/2}n!}{\Gamma(n+l+3/2)}\right]^{1/2}r^l e^{-\frac{\beta r^2}{2}}L_n^{l+1/2}(\beta r^2)\ ,\end{aligned} \tag{D.2}$$

where L_n^α denotes the Lagguere polinomial. The radial ho wave function satisfies the following equation

$$\hbar\omega\left[-\frac{1}{2\beta}\left(\frac{1}{r}\frac{d^2}{dr^2}r+\frac{l(l+1)}{r^2}\right)+\frac{\beta r^2}{2}\right]\mathcal{R}^{(\beta)}_{nl}(r)=E_N\mathcal{R}^{(\beta)}_{nl}(r)\ . \tag{D.3}$$

The eigenvalues are

$$E_N=\hbar\omega\left(N+\frac{3}{2}\right)\ ,\quad N=2n+l\ . \tag{D.4}$$

The sum of two ho potentials can be recoupled into the relative and cm terms as follows

$$\frac{1}{2}m\omega^2r_1^2+\frac{1}{2}m\omega^2r_2^2=\frac{1}{2}\hbar\omega\beta\left(r^2+R^2\right)\ , \tag{D.5}$$

where

$$\mathbf{r}=\frac{\mathbf{r}_1-\mathbf{r}_2}{\sqrt{2}}\ ,\quad \mathbf{R}=\frac{\mathbf{r}_1+\mathbf{r}_2}{\sqrt{2}}\ . \tag{D.6}$$

The Talmi-Moshinsky transformation transforms the product of the ho wave function into the product between the relative and cm functions

$$\left[\phi^{(\beta_1)}_{n_1l_1}(\mathbf{r}_1)\phi^{(\beta)}_{n_2l_2}(\mathbf{r}_2)\right]_{\lambda\mu}=\sum_{nlNL}\langle nlNL;\lambda|n_1l_1n_2l_2;\lambda\rangle\left[\phi^{(\beta)}_{nl}(\mathbf{r})\phi^{(\beta)}_{NL}(\mathbf{R})\right]_{\lambda\mu}\ . \tag{D.7}$$

The spherical ho wave functions are defined as

$$\begin{aligned}\varphi^{(\beta)}_{nljm}(\mathbf{x}) &\equiv \langle\mathbf{x}|\beta nljm\rangle=[\phi^{(\beta)}_{nl}(\mathbf{r})i^l\chi_{\frac{1}{2}}(s)]_{jm}\ ,\\ \phi^{(\beta)}_{nlm}(\mathbf{r}) &\equiv \langle\mathbf{r}|\beta nlm\rangle=\mathcal{R}^{(\beta)}_{nl}(r)Y_{lm}(\hat{r})\ ,\end{aligned} \tag{D.7}$$

where

$$\mathcal{R}^{(\beta)}_{nl}(r)\equiv\langle r|\beta nl\rangle \tag{D.8}$$

are the radial spherical ho functions.

[1] G. Gamow, Z. Phys. **51**, 204 (1928).
[2] G. Breit and E.P. Wigner, Phys. Rev **49**, 519 (1936).
[3] G. Breit, *Theory of resonant reactions and allied topics*, (Springer-Verlag, Berlin, 1959).
[4] P. L. Kapur and R. Peirls, Proc. Roy. Soc. A**166**, 277 (1938).
[5] T. Teichmann and E. P. Wigner, Phys. Rev. **87**, 123 (1952).
[6] R.G. Thomas, Prog. Theor. Phys. **12**, 253 (1954).
[7] A.M. Lane and R.G. Thomas, Rev. Mod. Phys. **30**, 257 (1958).
[8] H. Feshbach, Ann. Phys. (NY) **5**, 357 (1958).
[9] P.P. Fröman, Mat. Fys. Skr. Dan. Vid. Selsk. **1**, no. 3 (1957).
[10] H.J. Mang, Phys. Rev. **119**, 1069 (1960).
[11] A. Săndulescu, Nucl. Phys. A **37**, 332 (1962).
[12] V. G. Soloviev, Phys. Lett. **1**, 202 (1962).
[13] A. Săndulescu, D.N. Poenaru, and W. Greiner, Fiz. Elem. Chastits At Yadra **11**, 1334 (1980); Sov. J. Part. Nucl. **11**, 528 (1980)
[14] H.J. Rose and G.A. Jones, Nature (London) **307**, 245 (1984).
[15] K.P. Jackson, *et. al.*, Phys. Lett. B**33**, 281 (1970).
[16] P.J. Woods and C.N. Davids, Ann. Rev. Nucl. Part. Sci. **47**, 541 (1997).
[17] V.I. Goldansky, Nucl. Phys. **19**, 482 (1960).
[18] R.A. Kryger, *et. al.* Phys. Rev. Lett **74**, 860 (1995).
[19] L.V. Grigorenko, R.C. Johnson, I.G. Mukha, I.J. Thomson, and M.V. Zhukov, Phys. Rev. C **64**, 054002 (2001).
[20] J.C.D. Milton and J.S. Fraser, Can. J. Phys. **40** 1626 (1962).
[21] C. Guet, M. Ashgar, P. Perrin, and C. Signarbieux, Nucl. Instrum. Methods **150** 189 (1978).
[22] J.H. Hamilton, *et al.*, J. Phys. G **20** L85 (1984).
[23] G.M. Ter-Akopian, *et al.*, Phys. Rev. Lett. **73** (1994) 1477.
[24] S.L. Glashow, Nucl. Phys. **22**, 579 (1961).
[25] S. Weinberg, Phys. Rev. Lett. **22**, 1264 (1967).
[26] A. Salam, *Elementary Particle Theory: Relativistic Groups and Analyticity (Proc. 8th Nobel Symp.)*, Ed. N. Svartholm (Almqvist and Wiksell, Stocknolm, 1968) p. 367.
[27] B. Buck, A. C. Merchand and S. M. Perez, Atomic Data and Nuclear Data Tables **54** (1993) 53
[28] H. -J. Unger, Nucl. Phys. **A104**, 564 (1967).
[29] O. Civitarese and M. Gadella, Phys. Rep. **396**, 41 (2004).
[30] M. Abramowitz and I. A. Stegun, eds., *Handbook of Mathematical Functions*, (Dover Publications Inc., New York, 1983).
[31] T. Vertse, R.J. Liotta, and E. Maglione, Nucl. Phys. A **584**, 13 (1995).
[32] T. Berggren, Nucl. Phys. A **109**, 265 (1968).
[33] T. Berggren, Phys. Lett. B **73**, 389 (1978).
[34] T. Vertse, K.F. Pál, and A. Balogh, Comput. Phys. Commun. **27**, 309 (1982).
[35] L. Ixaru, M. Rizea, and T. Vertse, Comput. Phys. Commun. **85**, 217 (1995).
[36] J.R. Taylor, *Scattering Theory* (Willey, New York, 1972).
[37] A.A. Sonzogni, Nucl. Data Sheets **95**, 1 (2002).
[38] D.S. Delion, R.J. Liotta, and R. Wyss, Phys. Rep. **424**, 113 (2006).
[39] D.S. Delion, S. Peltonen, and J. Suhonen, Phys. Rev. C **73**, 014315 (2006).
[40] D.S. Delion, R.J. Liotta, and R. Wyss, Phys. Rev. Lett. **96**, 072501 (2006).
[41] V.E. Viola and G.T. Seaborg, J. Inorg. Nucl. Chem. **28**, 741 (1966).
[42] R.G. Lovas, R.J. Liotta, A. Insolia, K. Varga, D.S. Delion, Phys. Rep. **294**, 265 (1998).
[43] F. Carstoiu and R.J. Lombard, Ann. Phys. (N.Y.) **217** (1992) 279.
[44] G. Bertsch, J. Borysowicz, H. McManus, and W.G. Love, Nucl. Phys. A **284** (1977) 399.
[45] B. Gyarmati and T. Vertse, Nucl. Phys. A **160**, 523 (1971).
[46] S.A. Gurvitz and G. Kalbermann, Phys. Rev. Lett. **59**, 262 (1987).
[47] S.A. Gurvitz, Phys. Rev. A **38**, 1747 (1988).
[48] G.R. Satchler, *Direct Nuclear Reactions* (Clarendon Press, Oxford, 1983).
[49] D.F. Jackson and M. Rhoades-Brown, Ann Phys. **105**, 151 (1977).
[50] T. Berggren and P. Olanders, Nucl. Phys. A **473**, 189 (1987).
[51] T. Berggren, Phys. Rev. C **50**, 2494 (1994).
[52] B. Buck, A.C. Merchand, and S.M. Perez, J. Phys. G **17**, 1223 (1991).
[53] M.A. Preston, Phys. Rev. **71**, 865 (1947); Phys. Rev. **75**, 90 (1949).
[54] M. Pierronne and L. Marquez, Z. Phys. A **286**, 19 (1978).
[55] J.A. Maruhn and W. Greiner, Phys. Rev. Lett. **32**, 548 (1974).
[56] R.K. Gupta, W. Scheid, and W. Greiner, Phys. Rev. Lett. **35**, 353 (1975).
[57] J. Maruhn and W. Greiner, Z. Phys. **251**, 431 (1972).
[58] W. Greiner, J.Y. Park, and W. Scheid, *Nuclear molecules* (World Scientific, Singapore, 1994).
[59] M. Mirea, Phys. Rev. C **54**, 302 (1996).

[60] R.A. Gherghescu, Phys. Rev. C **67**, 014309 (2003).
[61] S.S. Malik and R.K. Gupta, Phys. Rev. C **39**, 1992 (1989).
[62] R.K. Gupta, S. Singh, R.K. Puri, A. Săndulescu, W. Greiner, and W. Scheid, J. Phys. G **18**, 1533 (1992).
[63] H. Kröger and W. Scheid, J. Phys, G **6**, 85 (1980).
[64] J. Blocki, J. Randrup, W.J. Swiatecki, and C.F. Tsang, Ann. Phys. (NY) **105**, 427 (1977).
[65] R.K. Gupta, D. Bir, M. Balasubramaniam, and W. Scheid, J. Phys. G **26**, 1373 (2000).
[66] R.K. Gupta,S. Dhaulta, R. Kumar, and M. Balasubramaniam, Phys. Rev. C **68**, 034321 (2003).
[67] H.J. Mang and J.O. Rasmussen, Mat. Fys. Skr. Dan. Vid. Selsk. **2**, no. 3 (1962).
[68] H.J. Mang, Ann. Rev. Nucl. Sci. **14**, 1 (1964)
[69] J.K. Poggenburg, H.J. Mang, and J.O. Rasmussen, Phys. Rev. **181**, 1697 (1969).
[70] T. Fliessbach, Z. Phys. A **272** (1975) 39.
[71] T. Fliessbach and H. Walliser, Nucl. Phys. A **377**, 84 (1982).
[72] I. Tonozuka and A. Arima, Nucl. Phys. **A323**, 45 (1979).
[73] T. Fliessbach, H.J. Mang and J.O. Rasmussen, Phys. Rev. **C13** (1976) 1318
[74] T. Fliessbach and S. Okabe, Z. Phys. A **320**, 289 (1985).
[75] F. A. Janouch and R. Liotta, Phys. Rev. C **27** (1983) 896
[76] G. Dodig-Crnkovic, F. A. Janouch and R. J. Liotta, Phys. Scr. **37** (1988) 523;
[77] S.M. Lenzi, O. Dragun, E.E. Maqueda, R.J. Liotta and T. Vertse, Phys. Rev. C **48**, 1463 (1993).
[78] D.S. Delion and J. Suhonen, Phys. Rev. C **61**, 024304 (2000).
[79] A. Insolia, P. Curutchet, R. J. Liotta and D. S. Delion, Phys. Rev. C **44**, 545 (1991).
[80] D. S. Delion, A. Insolia and R. J. Liotta, Phys. Rev C **46** (1992) 884; Phys. Rev C **46** (1992) 1346
[81] D.S. Delion, A. Insolia and R.J. Liotta, Phys. Rev. C **49**, 3024 (1994).
[82] D.S. Delion, A. Insolia, R.J. Liotta, Phys. Rev. C **54**, 292 (1996).
[83] J. Dobaczewski, W. Nazarewicz, T.R. Werner, J.F. Berger, C.R. Chinn and J. Decharge, Phys. Rev. C **53**, 2809 (1996).
[84] T. Vertse, P. Curuchet, O. Civitarese, L.S. Ferreira, and R.J. Liotta, Phys. Rev. C **37**, 876 (1988).
[85] P. Curuchet, T. Vertse and R.J. Liotta, Phys. Rev. C **39**, 1020 (1989).
[86] E. Maglione, L.S. Ferreira, and R.J. Liotta Phys. Rev. Lett. **81**, 583 (1998).
[87] K. Varga, R. G. Lovas and R. J. Liotta, Nucl. Phys. A **550**, 421 (1992).
[88] J.O. Rasmussen, Phys. Rev. **113**, 1593 (1959).
[89] Y.A. Akovali, Nucl. Data Sheets **84**, 1 (1998).
[90] A.T. Kruppa, and W. Nazarewicz, Phys. Rev. C **69**, 054311 (2004).
[91] G. Dussel, E. Caurier, and A.P. Zuker, At. Data Nucl. Data Tables, **39**, 205 (1988).
[92] Y.K. Gambhir, P. Ring, and P. Schuck. Phys. Rev. Lett. **51**, 1235 (1983).
[93] G.G. Dussel, A.J. Fendrik, and C. Pomar, Phys. Rev. C **34**, 1969 (1986); G.G. Dussel and. Fendrik, Phys. Rev. C **34**, 1097 (1986).
[94] D.S. Delion, A. Insolia, and R.J. Liotta, Phys. Rev. Lett. **78** (1997) 4549.
[95] R. Blendowske, T. Fliessbach, and H. Walliser, Z. Phys. A **339**, 121 (1991).
[96] F. Canto and D.M. Brink, Nucl. Phys. A **279**, 85 (1977).
[97] D.S. Delion, A. Săndulescu, J. Phys. G **28**, 617 (2002).
[98] P. Schuck, A. Tohsaki, H. Horiuchi, and G. Röpke, *The Nuclear Many Body Problem 2001* Eds. W. Nazarewicz and D. Vretenar (Kluwer Academic Publishers, 2002) p. 271.
[99] L. Spanier and S.A.E. Johansson, At. Data Nucl. Data Tab. **39**, 259 (1988).
[100] D.S. Delion and R.J. Liotta, Phys. Rev. C **58**, 2073 (1998).
[101] J. Dudek, Z. Szymanski, and T. Werner, Phys. Rev. C **23**, 920 (1981).
[102] D.S. Delion, A. Săndulescu, and W. Greiner, Phys. Rev. C **69**, 044318 (2004).
[103] A.Bohr and B. Mottelson, *Nuclear structure* (Benjamin, New York, 1975).
[104] P. Möller, R.J. Nix, W.D. Myers, and W. Swiatecki, At. Data Nucl. Data Tables **66**, 131 (1995).
[105] Yu. Ts. Oganessian, *et. al.*, Phys. Rev. C **62**, 041604 (2000).
[106] K. Kaneko and M. Hasegawa, Phys. Rev. C **67**, 041306(R) (2003).
[107] J. Dudek, Z. Szymanski, T. Werner, A. Faessler, and C. Lima, Phys. Rev. C **26**, 1712 (1982).
[108] S. Cwiok, J. Dudek, W. Nazarewicz, J.Skalski, and T. Werner, Comput. Phys. Commun. **46**, 379 (1987).